Dopaquinone as a Common Intermediate in the Biogenesis of Tyrosine-Derived Quinone Cofactors

By

Robyn H. Moore

Submitted to the Department of Chemistry and the Faculty of the Graduate School of the University of Kansas in partial fulfillment of the requirements for the degree of Doctor of Philosophy.

Committee Members:

_____
Minae Mure (Chair)

_____
Richard L. Schowen

_____
Richard S. Givens

_____
Paul R. Hanson

_____
Emily E. Scott

Date defended: _____

This Dissertation Committee for Robyn H. Moore certifies that this is the approved version of the following dissertation:

Dopaquinone as a Common Intermediate in the Biogenesis of Tyrosine-Derived Quinone Cofactors

Committee:

_____
Minae Mure (Chair)

_____
Richard L. Schowen

_____
Richard S. Givens

_____
Paul R. Hanson

_____
Emily E. Scott

Abstract

Robyn Haley Moore

Department of Chemistry, University of Kansas

Copper amine oxidases (CAOs) are ubiquitously expressed in nature but vary with regard to their substrate specificity and their role in various organisms.[8-11] In bacteria, CAOs serve to break down amines to supply the sole source of carbon or nitrogen.[9,13] In plants, the H_2O_2 formed in CAO catalysis is proposed to play a role in cell wall formation and wound healing.[16] In higher organisms, the role of amine oxidases is more complex. Three CAOs have been identified in a variety of tissues in the human body and have potential roles in regulating the level of biogenic amines, reducing inflammation, and cell signaling.[17-21] Lysyl oxidase (LOX), another copper-containing amine oxidase, is known to play a role in stabilizing the extracellular matrix by forming cross-links in collagen and elastin.[22,23] It has been shown to play a role in metastatic breast cancer along with other cancers in humans.[24]

The biogenesis of the topaquinone (TPQ) cofactor of copper amine oxidase (CAO) is a self-catalyzed process that requires copper and molecular oxygen. A putative dopaquinone (DPQ) intermediate has been proposed to react with a copper-associated water molecule, through a 1,4-addition mechanism, to form the reduced form of TPQ (TPQ_{red}). An oxidation reaction by O_2 yields the mature TPQ (TPQ_{ox}). Site-directed mutagenesis was used to incorporate a lysine residue into the active site of a phenethylamine oxidase from *Arthrobacter globiformis* (AGAO) producing D298K-AGAO. The X-ray crystal structure of the mature form of D298K-AGAO revealed the formation of a covalent linkage between the ε-amino side chain of Lys298 and the C2 position of the proposed DPQ intermediate. The quinone formed was proposed to be an iminoquinone tautomer (LTI) of lysine tyrosylquinone (LTQ), the organic cofactor of lysyl oxidase (LOX). UV/vis and resonance Raman spectroscopic studies of the time course of the formation of LTI at pH 6.8 detected an LTQ-like intermediate in the early phase of the reaction, which slowly converts to LTI. The LTI form of the tautomer is stabilized by hydrogen bonding interactions with the conserved tyrosine residue (Tyr284) in the active site. The results of this study strongly support the proposal that DPQ is an intermediate, not only in TPQ biogenesis, but also in the biogenesis of LTQ in LOX. This study also indicates that DPQ, in the biogenesis of TPQ, is mobile and can leave the copper site to react with Lys298.

A study of the pH-dependency on the rate of formation of the LTQ-like cofactor in D298K-AGAO showed that the protonation states of two residues influence the rate. The residue with a pK_a of 7.93 ± 0.10 is deprotonated when the rate of the reaction was the fastest and we propose that it is the precursor tyrosine (Y382), while the residue with a pK_a of ~ 9.62 ± 0.13 is protonated when the rate of the reaction was the fastest and is proposed to be Tyr284. Tyr284 is most likely in hydrogen bonding interaction with DPQ to facilitate the 1,4-addition of K298 side

chain. TPQ was not detected at pH range studied (6.8 to 9.5) for D298K-AGAO biogenesis. Although the mutation at D298 is not expected to alter the environment around the active site copper, 1,4-addition of K298 side chain to DPQ has out competed the 1,4-addition of a copper-associated water molecule. A 370 nm species was observed in the initial seconds of the biogenesis reaction. This species is most likely a charge-transfer species formed between the active site copper and a Tyr in the active site of CAO but found not to be on the reaction pathway to form the quinone cofactor.

The addition of *n*-butylamine hydrochloride in the biogenesis of WT- and D298A-AGAO resulted in the formation of an LTQ-like quinone but prevented the formation of TPQ. Each biogenized protein, containing the LTQ-like cofactor, showed a 40- to 1000-fold reduced activity towards substrate amine when compared to WT AGAO with TPQ cofactor. The LTQ-like quinone in those enzymes is predicted to have an increased mobility when compared to the LTQ-like cofactor in D298K-AGAO, but it was not reactive towards inhibitor. These results suggest that the putative LTQ-like cofactor formed in the reaction between WT- or D298A-AGAO and *n*-butylamine, has some mobility, and can be in the active conformation. Further, the formation of an LTQ-like cofactor in WT-AGAO occurs at a rate that is slower than the rate of LTQ cofactor formation in D298A indicating that the active site of D298A is better arranged to facilitate the amination reaction.

An attempt was made in order to generate a TPQ cofactor in LOX was made to confirm the proposal that DPQ is an intermediate in LTQ formation. In addition to the possibility of forming TPQ, it is possible that the reaction would be incomplete and DPQ would be observed directly. The mutation of Lys653 to Ala in a recombinant form of HLOXL2 resulted in the formation of a mis-folded protein that was expressed mainly as an inclusion body in *Drosophila* S2 cells as opposed to soluble secreted WT-protein. Although the conclusive identification of DPQ as an intermediate on the pathway to form LTQ was not confirmed, this result shows that Lys653 is important to the proper folding of the protein as well as the formation of LTQ.

Acknowledgements

I would like to start by acknowledging my advisor, Minae Mure, without whom this dissertation wouldn't have been possible. Thank you for introducing me to an area of research I am passionate about and look forward to continuing as a career, for giving me opportunities to hone skills in research and scholarship, and for carefully reading and re-reading my many chapter drafts. This section would be incomplete without thanking my other significant research advisor, Julian Limburg, for his guidance, intelligence and his kindness. Dr. Limburg was an integral element to my success at KU, and I am grateful. My committee, thank you for tackling an Herculean task by jump-starting this dissertation and getting it from page one to done in two intense, but well-organized months. Dr. Schowen, your help with data analysis and your kind words proved invaluable.

I extend heartfelt thanks to all my current and former lab members, especially Scott Schreiber, who helped with the stop-flow—a lot. Mary Krause, who always had a kind word, even when I sometimes didn't want to hear it, who read my orals, helped with my resume, lunched with me, and listened. Finally, thanks to Megen and Matt Culpepper, original members of the Triad, my comrades in arms, the foundation I leaned on. Thanks for the songs about Patti that got stuck in my head, Matt's inspiring new lyrics, Megen's uplifting spirit and dedication to her work, for putting up with Bella, the fierce mountain lion, and for getting it.

My parents supported my interest in the sciences with enthusiasm, financial support, home cooked meals (when Dad remembered the chicken and Mom remembered to turn on the crock pot), lawn-mowing services, retail therapy, physical therapy, psychological therapy, and a lot of laughter. My siblings for continuing to like me through this process and teasing me only a little for still being in school. My nieces, for reminding me to play, and laugh, and make something else more important for a while. My sister, Gaywyn, for sharing a home with me for the last five years, for her encouragement and advice, for being a great travel companion, for dinner, and for supporting my addictions to TV programs. Special thanks to Bella, Hector, Whitney and the Pennys, for unconditional love, tail-wags, and underappreciated face-kisses.

I must extend a special thanks to Heather Bastian, fellow Ph.D. pilgrim, model of hard work, voice of level-headed realism, best editor bar none, work-out partner, buttered watermelon teammate, dog sitter, chef, and long-suffering support system. I would also like to thank the Graduate Student Yoga Support Group without whom I would have had a headache every day, and Watkins Healthcare Staff, especially Dr. Strother and Sandy Bowman for excellent care whenever Yoga couldn't work out the kinks. Thanks for the dose of sanity.

Lastly, I would be remiss if I didn't thank KU's Department of English whose caring faculty, staff and graduate students have helped with questions about

procedures, asked about my research and actually seemed interested in my incomprehensible answers, and invited me to the best parties and conferences (Drs. Bergeron, Devitt, and Sousa).

Table of Contents

List of Figures

List of Tables

List of Schemes

List of Abbreviations

2-HP	2-Hydrazinopyridine
ABTS	2,2'-Azino-bis(3-ethylbenzthiazoline-6-sulphonic acid)
AGAO	*Arthrobacter globiformis* phenylethylamine oxidase
BSA	Bovine serum albumin
BSAO	Bovine serum amine oxidase
CAO(s)	Copper-containing amine oxidase(s)
CAPS	3-(Cyclohexylamino)-1-propanesulfonic acid
CHES	2-(Cyclohexylamino)ethanesulfonic acid
CHO	Chinese hamster ovary
CTQ	Cysteine tryptophylquinone
DDC	Sodium diethyldithiocarbamate
DPQ	Dopaquinone
ECAO	*Escherichia coli* amine oxidase
EDTA	Ethylenediaminetetraacetic acid
EMT	Epithelial-mesenchymal transitions
HEPBS	N-(2-Hydroxyethyl)piperazine-N_-(4-butanesulfonic acid)
HEPES	N-(2-Hydroxyethyl)piperazine-N_-(2-ethanesulfonic acid)
HLOXL	Human LOX-like proteins
HPAO	*Hansenula polymorpha* methylamine oxidase
HRP	Horse radish peroxidase
hVAP-1	Human vascular adhesion protein 1
ICP	Inductively coupled plasma
IPTG	Isopropyl β-D-1-thiogalactopyranoside
LB	Luria-Bertani
LOX	Lysyl oxidase
LTI	Iminoquinone tautomer of LTQ
LTQ	Lysine tyrosylquinone
MADH	Methylamine dehydrogenase
MCF7	Nonmetastatic estrogen-dependent breast cancer cells
MES	2-(N-Morpholino)ethanesulfonic acid
NBT	Nitro blue tetrazolium
PBS	Phosphate buffered saline
PBST	Phosphate buffered saline containing Tween-20
PLP	Pyridoxal phosphate
PMSF	Phenylmethanesulphonylfluoride
PQQ	Pyrroloquinoline quinone
PSB	Product-Schiff base
QHNDH	Quinohemoprotein amine dehydrogenase

SDS	Sodium dodecylsulfate
SRCR	Scavenger receptor cysteine rich
SSB	Substrate-Schiff base
TPQ	2,4,5-Trihydroxyphenylalanine quinone or topaquinone
TTQ	Tryptophan tryptophylquinone
WT	Wild-type

Chapter 1: Introduction

Post-Translationally Derived Cofactors

Several types of post-translational modifications, such as methylation, glycosylation, and cleavage of signal peptides, have been identified that regulate protein activity.[25] Cofactors, such as FAD, heme, pyridoxal phosphate (PLP), pyrroloquinoline quinone (PQQ), and NAD^+, are utilized by enzymes to assist in biochemical transformations. These transformations would otherwise be impossible due to the limited capability of amino acid side chains to perform a variety of chemical reactions. Most amino acid side chains are inert, while others, such as acidic, basic, and aromatic residues, have limited function in acid-base chemistry and electron transfer reactions. Previously, a cofactor was defined as a metal or small organic compound that is not composed of amino acids but is required for enzymatic activity. More recently, however, a new class of post-translational modifications have been identified, protein-derived cofactors, that participate in enzyme catalysis or redox chemistry.[26] Protein-derived cofactors are covalently attached to the protein and are usually derived from aromatic residue oxidation, amino acid cross-linking, or

amino acid cyclization. These cofactors are mostly located in the active site of proteins and facilitate chemistry that the unmodified amino acids could not.

Quinone Cofactors

PQQ is a cofactor that is frequently found in proteins that metabolize small molecules. It has been extracted from methanol dehydrogenase, indicating that it is not covalently bound to the proteins.[27,28] The first protein-derived cofactor to be identified was 2,4,5-trihydroxyphenylalanine quinone (TPQ) in 1990 in bovine serum amine oxidase (BSAO), which was initially believed to be a covalently attached PQQ cofactor.[26] Since then, three additional quinone cofactors have been reported, including both tyrosine- and tryptophan-derived quinone cofactors (Figure 1.1). The tyrosine-derived quinone cofactors are TPQ of copper-containing amine oxidase (CAO) and lysine tyrosylquinone (LTQ) of lysyl oxidase (LOX). Tryptophan tryptophylquinone (TTQ) of methylamine dehydrogenase (MADH) and cysteine tryptophylquinone (CTQ) of quinohemoprotein amine dehydrogenase (QHNDH) are both tryptophan-derived cofactors. The biogenesis of the tyrosine-derived cofactors occurs through an autocatalytic process requiring only Cu^{2+} and O_2,[2,29,30] while the biogenesis of TTQ requires the action of four gene products, *mauD,* mau*E, mauF* and *mauG*, in addition to the two that encode for the alpha and beta subunits, *mauA* and *mauB*, of the MADH protein.[31,32] The biogenesis of CTQ is less understood but, likely requires additional genes that have not yet been identified.[33,34] Each of these cofactors catalyzes the deamination of substrate amines to their corresponding

aldehydes with concomitant production of an ammonium ion; however, the tyrosine-derived cofactors are oxidases that transfer electrons to O_2 producing H_2O_2, while the tryptophan-derived cofactors are dehydrogenases that transfer electrons to external electron acceptors such as amicyanin, azurin, and cytochrome C_{550}.

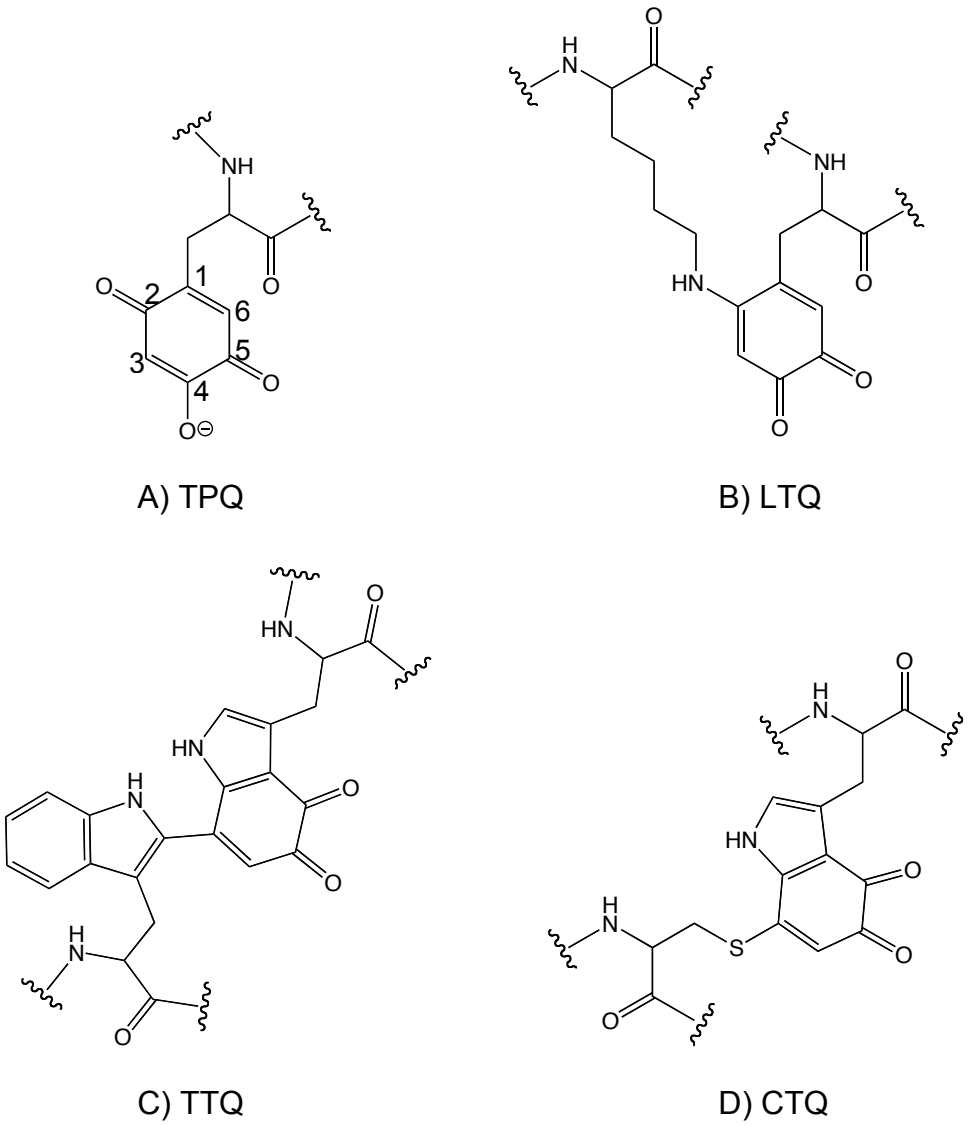

Figure 1.1 Post-translationally derived quinone cofactors. A) 2,4,5-Trihydroxyphenylalanine, B) lysyl oxidase, C) tryptophan tryptophylquinone, and D) cysteine tryptophylquinone.

CAO and the TPQ Cofactor

CAO (EC 1.4.3.6) catalyzes the oxidative deamination of various primary amines to produce their corresponding aldehydes concomitant with hydrogen peroxide and ammonia (Equation 1.1).[35]

$$RCH_2NH_3^+ + O_2 + H_2O \rightarrow RCHO + NH_4^+ + H_2O_2 \qquad (1.1)$$

CAOs are ubiquitously expressed in nature but vary with regard to their substrate specificity and their role in various organisms.[8-11] In bacteria, CAOs serve to break down amines to supply the sole source of carbon or nitrogen.[9,13] In plants, the H_2O_2 formed in CAO catalysis is proposed to play a role in cell wall formation and wound healing.[16] In higher organisms, the role of amine oxidases is more complex. Three CAOs have been identified in a variety of tissues in the human body and have potential roles in regulating the level of biogenic amines, reducing inflammation, and cell signaling.[17-21]

All of the solved crystal structures of CAO show a homodimeric protein containing one TPQ and one copper per subunit (Figure 1.2).[9,26,36-41] Each monomer contains three domains with the exception of *E. coli* amine oxidase (ECAO) that has an additional N-terminal domain (D1).[9,42] The C-terminal domain (D4) contains a β-sandwich and the protein active site. Additionally, this domain has two long β-hairpin arms that reach across from the D4 of one monomer to the D4 of the other. Although the overall structures of the CAOs are similar, the catalytic domain (D4) shares ~20%

sequence identity among all the known species of CAOs.[43] These differences likely account for the variation in substrate specificities among the CAOs from different species.[44] For example, the substrate entry channel of hVAP-1 is rich in aromatic and hydrophobic residues and appears to be gated by a Leu residue.[45] However, in AGAO, the substrate entry channel is lined with negatively charged residues that are more hydrophobic towards the active site and Tyr302 is proposed to be the gate.[9,46] TPQ, however, is derived from a conserved tyrosine residue in the consensus sequence N-Y-D/E-Y/N.[29]

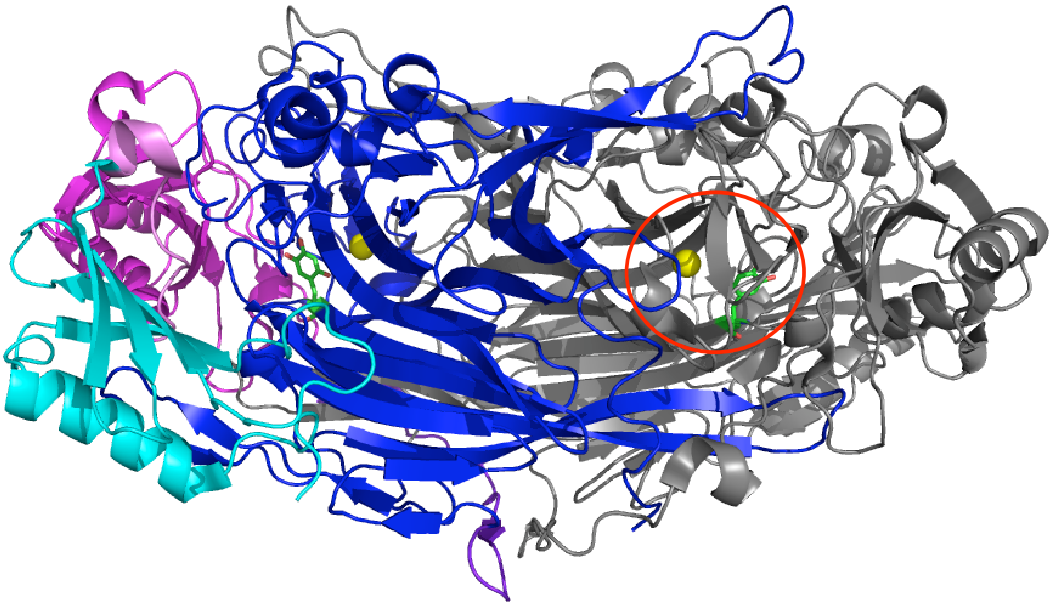

Figure 1.2 Secondary structure of the AGAO homodimer. The three domains of monomer A are shown in light blue (D2), cyan (D3), and blue (D4). Monomer B is shown in grey. Copper is shown as a yellow sphere and TPQ is shown as green sticks. The red circle indicates the location of the active site with TPQ and copper.

In the active (holo) form of AGAO, three histidines ligated to the copper along with two water molecules; one of the water molecules is on the Jahn-Teller axis (W_a) and the other is in the equatorial position (W_e) to provide a distorted square

pyramidal coordination geometry (Figure 1.3).[12] The C5 carbonyl group of TPQ_{ox} is facing the proposed substrate entry channel[9] and the conserved aspartate residue (Asp298) is proposed as an active site base.[11] Xe binding studies of AGAO indicate that the single hydrophobic O_2 binding site is on the opposite side of the active site from the substrate entry channel. O_2 bound in this site would be 7 Å from Cu^{2+} and 9 Å from TPQ.[47] Similar Xe binding studies on HPAO indicated that there are two O_2 binding sites near the active site; one is consistent with the O_2-binding site predicted for AGAO and another is in an adjacent hydrophobic pocket.[48] In HPAO, mutation of residues intended to inhibit O_2-binding in either site or mutation of residues in potential O_2-entrance channels did not alter activity, indicating that multiple channels are available to O_2 and that the importance of various O_2-binding sites vary from species to species. This study also indicated that the hydrophobic core of the β-sandwich in the D3 domain of CAOs acts as a reservoir for O_2.

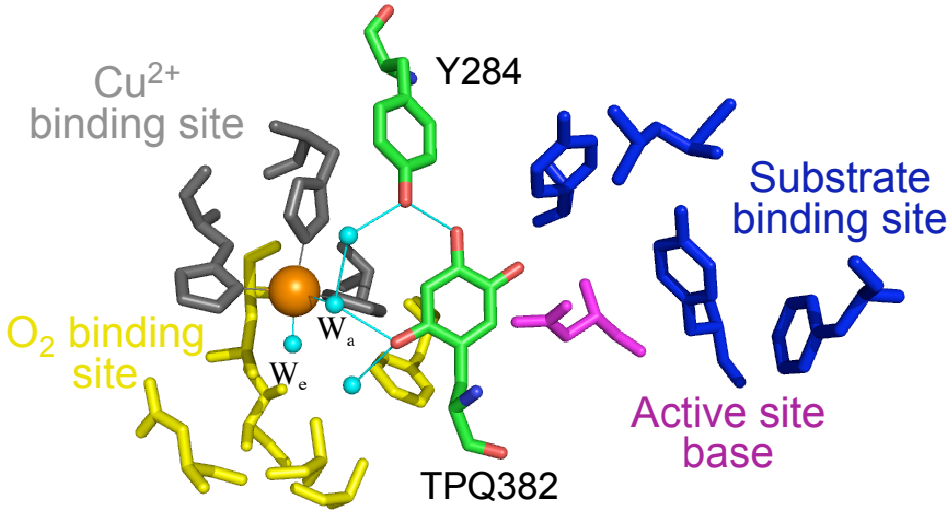

Figure 1.3 Active site of AGAO showing substrate, copper and molecular oxygen binding sites.

Xe binding studies on BSAO indicated that there is a potential O_2-binding site 8.6 Å from Cu^{2+} on the opposite side of Cu^{2+} from TPQ.[40] It is located in a hydrophobic pocket with a phenylalanine side chain between the pocket and Cu^{2+}. An additional Xe signal was observed between Cu^{2+} and TPQ and is in a position where O_2 has been predicted to bind in ECAO. Another Xe signal was observed on the opposite side of TPQ from the Cu^{2+} and is proposed to be a hydrophobic region in the wedge shaped cavity where small apolar molecules, or apolar portions of substrates, interact with the cavity.

The C2 carbonyl group of TPQ interacts with the copper through hydrogen bonding with a conserved water molecule, but neither O2 nor O5 are directly ligated to the copper. This orientation of the TPQ ring is critical for the optimal activity of CAO (Figure 1.4 a).[7] At neutral pH, TPQ exists in a resonance stabilized mono-anionic form with charge delocalization between the C2 and C4 carbonyls.[49,50] This delocalization of charge directs nucleophilic attack to the C5 carbonyl group.[50,51] In AGAO, resonance Raman studies indicate that the C5 oxygen of TPQ has more double bond character than the C2 or C4 oxygens, which explains why nucleophilic attack by substrate occurs only at this position.[52] Additionally, in HPAO, the C5 oxygen of TPQ exchanges with solvent water molecules.[52] This observation supports its proposed reactivity.

The mobility of TPQ and TPQ-derived reaction intermediates in CAOs are tightly controlled by hydrogen bonding interactions, particularly between the O4 of TPQ and the conserved Tyr (Tyr284 in AGAO) for optimal activity (Figure 1.4 a).[7]

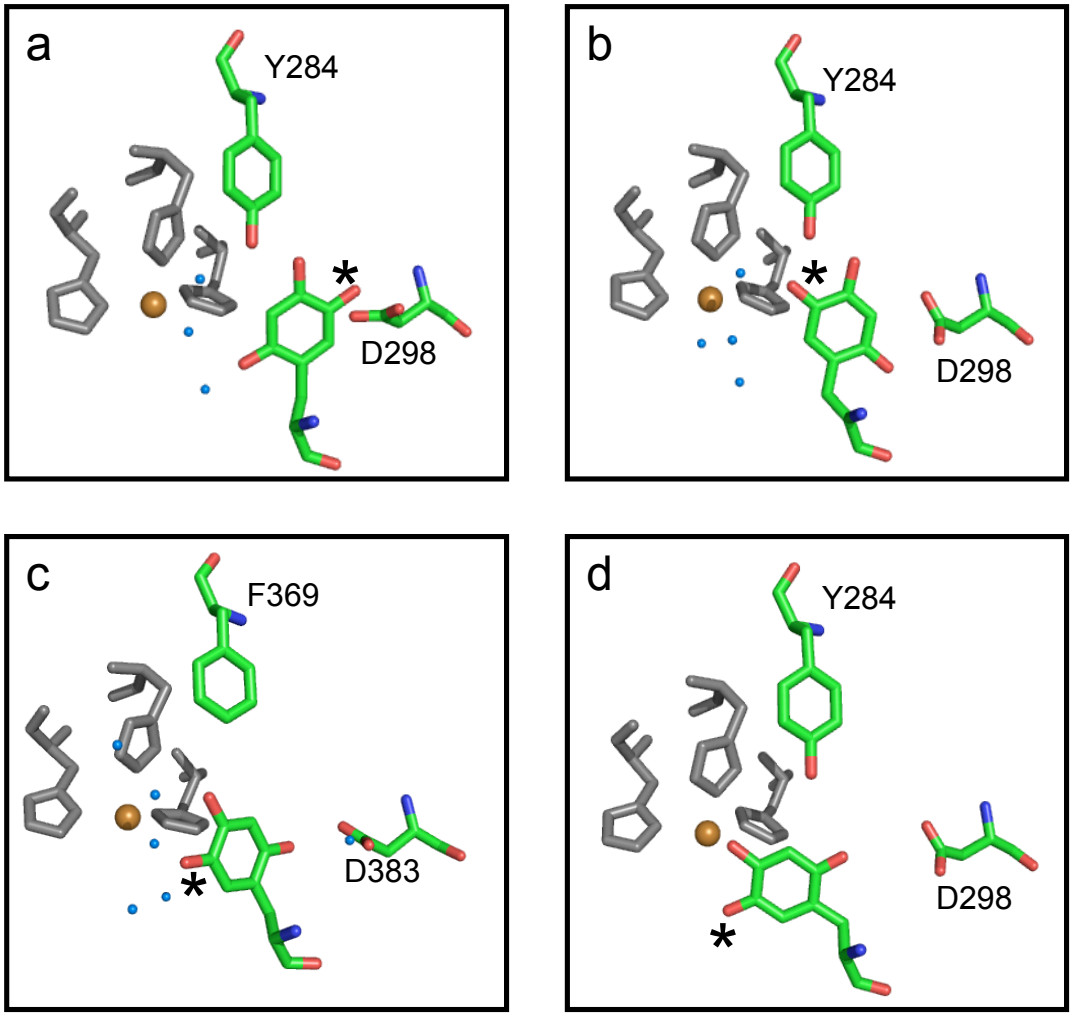

Figure 1.4 Active site structures of holo CAO.[7] a) Active conformation of AGAO (PDB code 1IU7 at 1.8 Å resolution).[12] b) Flipped conformation of AGAO (PDB code 1AV4 at 2.2 Å resolution).[9] c) Flipped and swung conformation of ECAO Y369F (PDB code 1JRQ at 2.15 Å resolution).[15] d) Cu-on conformation from AGAO (PDB code 1AVL at 2.8 Å resolution).[9] TPQ, the active site base, and the conserved Tyr (mutated to F is panel c) are green. The copper binding site is grey. Copper is shown as a golden sphere. The active site waters are blue. * indicates the C5 position of TPQ. Figures are generated by Pymol (DeLano Scientific LLC, http://www.pymol.org).

The TPQ ring is located in a wedge shaped cavity in the active site, but the mobility is limited to pivoting inside of the wedge (Figure 1.4).[7,15] When these hydrogen bonding interactions are disrupted by high salt (Figure 1.4 d), lowering pH (Figure 1.4 b), or

site-directed mutagenesis (Figure 1.4 c), the TPQ ring gains mobility and swings out from the wedge and can ultimately be trapped by ligation to the active site Cu^{2+}, all of which lead to greatly reduced catalytic activity. Disruption of the hydrogen bonding network by lowering the pH (Figure 1.4 b) shows an electron density map with density seen for the O4 atom but not for the aromatic ring, O2, or O5 indicating that the ring is free to rotate in the active site.

CAO Catalysis

The catalysis of primary amines to their corresponding aldehyde, proceeds through a ping-pong mechanism consisting of a reductive followed by an oxidative

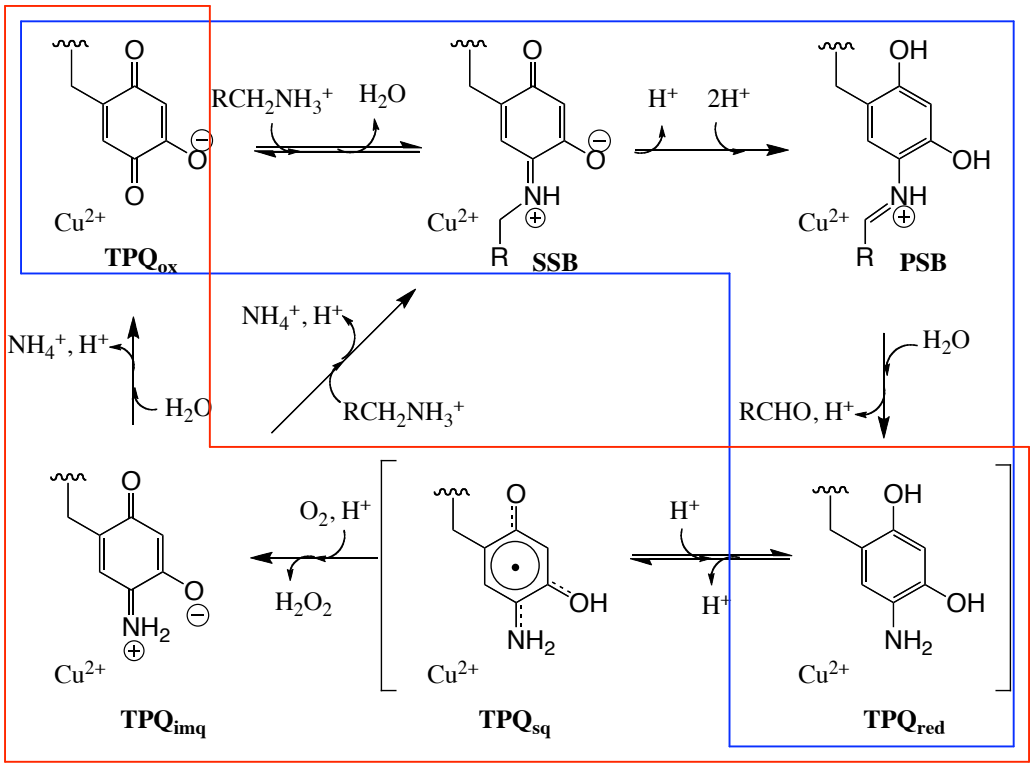

Scheme 1.1 Proposed reaction mechanism of the catalytic cycle of CAO. —The reductive half-reaction, — the oxidative half-reaction.

half-reaction (Scheme 1.1).[35] The reductive half-reaction initiates when the substrate enters the negatively charged substrate entry channel that becomes hydrophobic closer to the active site,[9] is deprotonated, potentially by the active site base (D298 in AGAO), and undergoes nucleophilic attack on the C5 carbonyl of TPQ to form the substrate-Schiff base (SSB). The SSB is converted to the product-Schiff base (PSB) by the abstraction of the substrate C1 proton by a conserved aspartate residue, and two electrons are transferred from the amine of the substrate to the oxidized TPQ. [49] The proton abstraction step in the reductive half-reaction has been shown to be stereospecific, determined by the arrangement of the active site.[53] Mutation of the active site base, D383 in ECAO or D298 in AGAO, indicates that the active site base is responsible for proton abstraction, and it is involved in positioning the substrate in the active site.[15,46,54] PSB hydrolysis releases the product aldehyde and forms an aminoresorcinol like reduced cofactor (TPQ_{red}) that exists in equilibrium with a Cu(I)-semiquinone (TPQ_{sq}). The rate limiting step in the reductive-half reaction is dependent on the source of the CAO and the mutation of active site residues. C-H bond cleavage may be more rate-limiting in some enzymes. For example, it appears to be more rate-limiting in BSAO than in HPAO.[55] While in HPAO, C-H bond cleavage is more rate-limiting with butylamine than with methylamine as a substrate. Conformational changes in the active site have been suggested to be rate-limiting in D319E of HPAO.[54]

The SSB and PSB of ECAO have been shown to have some conformational flexibility.[56] In HPAO, mutation of the tyrosine corresponding to Tyr284 in AGAO,

or of the residues flanking TPQ to alanine, led the the accumulation on a neutral form of the PSB (catalytically active PSB is the monoprotonated form) that slowly hydrolyzes; PSB was proposed to be in the flipped conformation.[30,55,57] Mutagenesis studies on ECAO showed that residues D383 and Y369, corresponding to D298 and Y284 of AGAO, are involved in limiting the mobility of the SSB and PSB.[56] When TPQ of ECAO was reacted with 2-hydrazinopyridine (2-HP), the 2-HP adduct was mainly in the hydrazone form as opposed to the azo form of the tautomer due to interactions between D383 and the pyridine ring of the TPQ adduct; the rings of TPQ and pyridine were not coplanar. When D383 was mutated to Ala or when Y369 was mutated to Phe, the equilibrium between hydrazone and azo forms of the tautomer shifted to the azo form. Additionally, by heating or increasing the pH of the enzyme solution, a new species was observed that was identified as the on-copper form of the TPQ-2HP cofactor. In the Y369F mutant, the species is formed at room temperature, indicating that the hydrogen bonding interaction between the O4 of TPQ and Y369 has a role in keeping TPQ in the active, off-copper, conformation.[56]

In the oxidative half-reaction, O_2 accepts electrons from TPQ_{red} to produce H_2O_2 and an iminoquinone (TPQ_{imq}).[58] The TPQ_{imq} can undergo hydrolysis to regenerate the resting cofactor, TPQ_{ox}, and NH_4^+ or, most likely, it undergos a transimination reaction with substrate to generate the SSB and NH_4^+.[9,35,51] An ^{18}O kinetic isotope effect study in BSAO and HPAO showed that the electron transfer from TPQ_{red} to O_2 was the rate-limiting step in the oxidative half-reaction.[58,59] Additionally, the effect of solvent viscosity on the rate of oxidation suggested that O_2

was prebound in the active site, and the binding of O_2 was not responsible for the observed kinetic isotope effect.[58] As discussed above, O_2 bound in the proposed O_2 binding site would be ~ 7 Å form the Cu^{2+} and ~ 9 Å from the TPQ.[47] Electron transfer from either Cu^{2+} or TPQ would require the O_2 molecule to move 4 – 6 Å. It is possible that O_2 reacts with either the Cu(I)-TPQ_{sq} or with Cu(II)-TPQ_{red}.[12,60] Additionally, Co^{2+} and Ni^{2+} substituted forms of the enzyme show 1000-fold decreased rate in the oxidative half-reaction.[12] Various studies on CAOs from different sources suggest that the mechanism of reoxidation of the cofactor may vary from species to species.[12,61-63]

TPQ Cofactor Biogenesis

The mechanism of TPQ biogenesis has been studied for AGAO[5,9,64-68] and HPAO.[14,55,69-74] The biogenesis of the TPQ cofactor is a self-catalyzed reaction, requiring only copper and oxygen.[29,30] The biogenesis can be initiated by addition of Cu^{2+} to the apo-protein under aerobic conditions or exposure of the Cu^{2+}-bound precursor protein prepared under anaerobic conditions to O_2.[75] The copper-free tyrosine precursor (apo) form of recombinant CAO can be prepared by removing copper from the buffers used during purification. In AGAO, the ratio of O_2 consumption to hydrogen peroxide formation is 2:1; 1 mol of H_2O_2 was produced per mole of TPQ formed (Equation 1.2), and the rate of TPQ formation is approximately that of H_2O_2 formation.[65] The rate of the reaction was zero-order in copper with

concentrations of one equivalent or more.[64] Mechanisms have been proposed that account for this stoichiometry (Scheme 1.2).

$$\text{E-Tyr} + 2O_2 + H_2O \rightarrow \text{E-TPQ} + H_2O_2 \qquad (1.2)$$

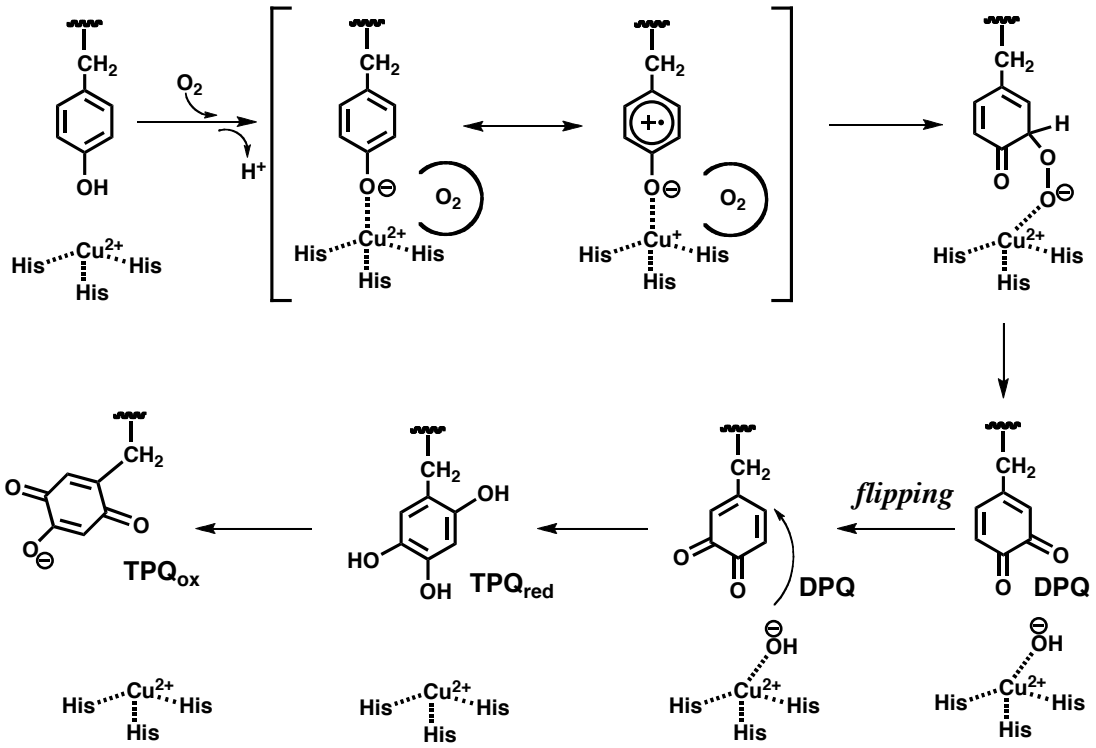

Scheme 1.2 Proposed mechanism of TPQ biogenesis[14]

In 2004, Kim et. al. performed an X-ray snapshot analysis in an attempt to freeze trap the reaction intermediates of TPQ biogenesis in AGAO (Figure 1.5).[5] The structure of the apo form of AGAO revealed that the phenolic hydroxyl group of the precursor tyrosine (Tyr382) pointed towards the vacant metal site composed of the

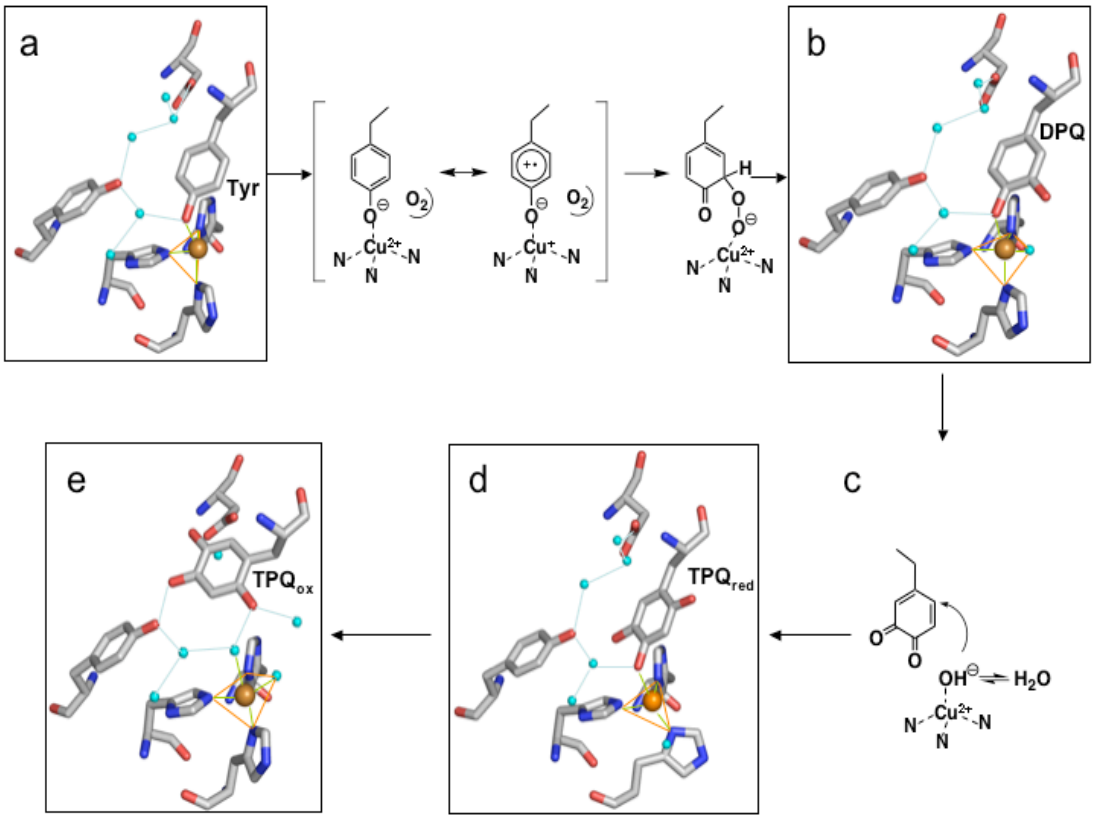

Figure 1.5. Proposed mechanism of TPQ biogenesis.[5] Panels a, b, d, e are intermediates observed in the X-ray snapshot analysis. Copper is shown as a golden sphere and water molecules are shown in light blue spheres. a) Tyr: Tyr382 precursor, b) DPQ: dopaquinone, c) proposed DPQ in a flipped form, d) TPQ_{red}: 2,4,5-trihydroxylbenzene form of the reduced TPQ, e) TPQ_{ox}: the oxidized form of TPQ. Figures are generated by Pymol (DeLano Scientific LLC, http://www.pymol.org).

three conserved histidine residues (His431, His433 and His592).[5,9] When apo protein crystals were soaked with copper anaerobically, copper was bound in a tetrahedral geometry to the three His ligands, and Tyr382 provided the fourth ligand (Figure 1.5 a). A similar observation of the precursor tyrosine ligation to the metal was seen in the crystal structure of zinc-substituted HPAO that remains unprocessed.[76] Upon exposure of the unbiogenized copper bound crystals to molecular oxygen, two

copper-bound intermediates, proposed to be dopaquinone (DPQ, Figure 1.5 b) and trihydroxybenzene (TPQ_{red}, Figure 1.5 d), respectively, were detected where the O4 hydroxyl group of the aromatic ring remained directly coordinated to Cu^{2+}. During the conversion of the putative DPQ to TPQ_{red}, the aromatic ring rotated 180° to undergo hydration by a copper-associated, solvent exchangeable water molecule (Figure 1.5 c), as shown by resonance Raman studies on AGAO.[66] In the final step of the oxidation of TPQ_{red} to TPQ_{ox}, the TPQ ring finally moved off Cu^{2+} to leave the cofactor in the active conformation (Figure 1.5 e). As a result of the conformational changes during biogenesis, the TPQ ring in the mature AGAO is in a different orientation from the precursor tyrosine (Figure 1.5 a). The C2 carbonyl of the TPQ ring is directed toward the five-coordinate distorted square-pyramidal copper where two water molecules have taken the place of the O4 atom of TPQ.

When Co^{2+} or Ni^{2+} is substituted for Cu^{2+}, the metal has a six coordinate, octahedral geometry with the addition of a second water molecule.[68] Co^{2+}, Ni^{2+}, and Zn^{2+} can all bind tightly to the metal binding site of CAO but only Co^{2+} and Ni^{2+} are capable of producing an enzyme with a fully biogenized TPQ cofactor. The rates of biogenesis of the Co^{2+} and Ni^{2+} substituted enzymes were reduced to 2.2% and 0.9%, respectively, of the rate in WT AGAO.[12] However, in AGAO and HPAO, metal substitution does not affect the rate of substrate catalysis.[12,77] Kinetic studies on the biogenesis of TPQ in Ni^{2+}-substituted HPAO indicated that the electron transfer from the metal-coordinated tyrosinate to O_2 is the rate-limiting step in the reaction.[73]

In contrast to mature TPQ, the possible mobility of the reaction intermediates in the TPQ biogenesis has not been considered. From the X-ray snapshot analysis, the precursor Tyr382 is initially bound to the Cu^{2+} residing outside the active site wedge (Figure 1.5 a).[5] Both the proposed DPQ intermediate and TPQ_{red} are both still interacting with Cu^{2+} (Figure 1.5 b, 1.5 d). Upon oxidation of TPQ_{red} to TPQ_{ox}, TPQ finally leaves the active site Cu^{2+} and swings into the wedge to be captured by Tyr284 to be in the active conformation (Figure 1.5 e). It is not known what factors cause TPQ_{ox} to leave the Cu^{2+} site.

Detailed kinetic and spectroscopic studies on the biogenesis of TPQ in HPAO revealed that the rate-determining step is the decay of a species absorbing at 350 nm that is proposed to be a Cu^{2+}-tyrosinate complex and exists in equilibrium with a Cu^{1+}-tyrosyl radical (Scheme 1.2).[72] The decay of the 350 nm species and the formation of TPQ occur concomitantly with an isobestic point indicating a precursor-product relationship.[70] The absence of a kinetic isotope effect on the rate of TPQ formation using the 3,5-ring dideuterated tyrosine precursor excluded the possibility that subsequent C-H bond cleavage step from a proposed Cu^{2+}-aryl-peroxide intermediate was rate-limiting (Scheme 1.2).[14] No spectroscopic intermediates were detected during the conversion of the 350 nm species to mature TPQ_{ox} absorbing at 472 nm. In AGAO, binding of Cu^{2+} to the precursor protein under anaerobic conditions does not appear to lead to the formation of any distinct new features in the UV/vis spectrum, in contrast to HPAO.[64] When O_2 was introduced to the system,

rapid formation of mature TPQ_{ox} (478 nm) was observed, where the reaction was complete within a couple of minutes.

The roles of various active site residues have been explored using site-directed mutagenesis. N-Y-D/E-Y (Y is the precursor of TPQ) consensus sequence residues of histamine oxidase from *A. globiformis* were mutated to N401D/Q, D403E/N and Y404F.[78] Reduced rates of biogenesis were seen in N401D/Q and D403N, but the rates of biogenesis in D403E and Y404F were comparable to wild-type protein. These results, along with those of E406Q and N404D from HPAO[57] have indicated that these residues are important in determining the rate of TPQ biogenesis. The catalytic base, D298 in AGAO, has not been proposed to be directly involved in cofactor biogenesis, but the rate of TPQ formation in the D298A mutant was ~ 40% of that seen in WT. The mutation of the strictly conserved active site Y305 from HPAO to alanine or phenylalanine slowed the rate of biogenesis by ~45-fold and 3-fold, respectively.[74] The variation in rates indicates that the bulkiness of the residue is important in restricting the movement of the precursor tyrosine or biogenesis reaction intermediates. Additionally, this mutant formed a new species ~400 nm, particularly at higher pHs, that is, most likely, a Cu-on TPQ_{ox}.[49]

LTQ Cofactor Biogenesis in LOX

Lysyl oxidase (LOX) is also a copper-containing amine oxidase but differs from CAO by being monomeric (32 kDa) and having a lysine tyrosylquinone (LTQ, see Scheme 1.3) cofactor.[3] It is known to play a role in stabilizing the extracellular

matrix by forming cross-links in collagen and elastin.[22,23] A model study suggested that 1,4-addition of the ε-amino side chain of lysine to the DPQ intermediate can form the LTQ cofactor, where the active site of LOX must be pre-organized to achieve the selectivity of the reaction (Scheme 1.3).[1] Recently, Bollinger *et al.* isolated the copper-free precursor form of recombinant LOX (apo-LOX) and showed the formation of the LTQ cofactor by extensive dialysis of the apo-LOX against copper under aerobic conditions.[2] They proposed that the biogenesis of the LTQ cofactor is a self-catalyzed process requiring only Cu^{2+} and molecular oxygen as in the case of the TPQ cofactor in CAOs. In order to identify the residues participating in the crosslink to form LTQ, a mutagenesis study was done on LOX from a rat aorta expressed in Chinese hamster ovary (CHO) cells.[3] Mutagenesis of Lys314 and Tyr349, the precursors for the LTQ cofactor, followed by activity assays, showed that both single and double mutants of these residues were inactive. However, the mutants from this study were not fully characterized. Taken together, these results support proposals that both TPQ and LTQ biogenesis proceed through a DPQ intermediate. However, to date there has been no definitive identification of DPQ in either CAO or LOX.

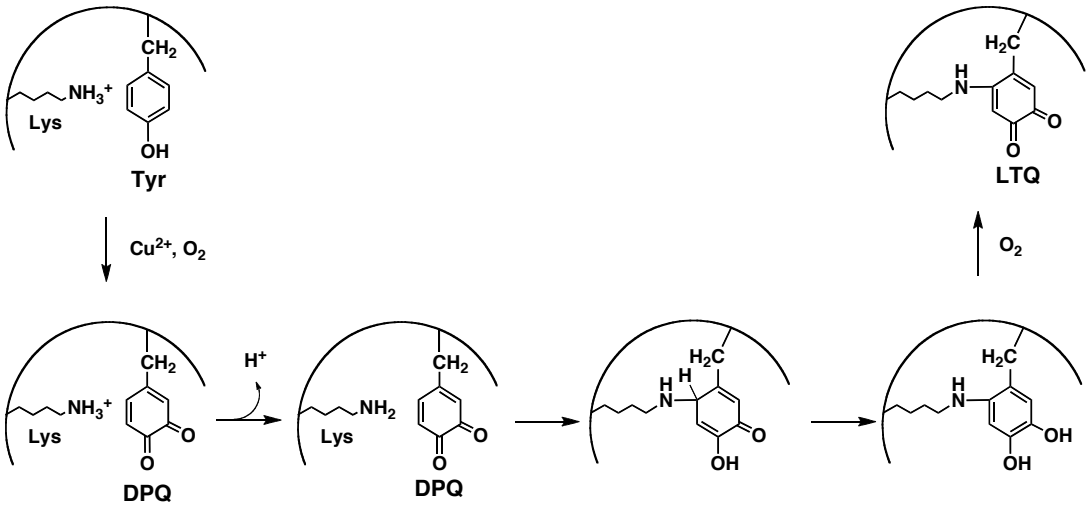

Scheme 1.3. Proposed mechanism for LTQ biogenesis.[1-3,]

Research Goals

The overall goal of this research is to determine if DPQ is a common intermediate on the pathway to form TPQ in CAO and LTQ in LOX in order to support the proposed mechanisms of TPQ and LTQ formation. In an attempt to definitively identify DPQ as the intermediate in the biogenesis of TPQ and to provide support for the intermediacy of DPQ in the biogenesis of LTQ, a lysine residue was incorporated into the active site of AGAO by site-directed mutagenesis to trap the putative DPQ intermediate. Research presented herein characterizes the cofactor formed in D298K by UV/vis and resonance Raman spectroscopy.

While determining that DPQ is an intermediate in the biogenesis of TPQ and supporting the proposed intermediacy of DPQ in the biogenesis of LTQ, the research indicated that the 1,4-addition of a lysine side chain to DPQ in the biogenesis of an LTQ-like cofactor in AGAO occurred selectively at pH 6.8 without competition from

hydration. Thus, a secondary goal of this research was proposed to determine if the hydration reaction (to form TPQ) competes with amination (to form LTQ) at lower or higher pHs. The pH-dependency on cofactor formation was studied along with the pH-dependency on the rate of biogenesis of the LTQ-like cofactor in the D298K mutant. Observations made during this study suggested a further goal of this research: to characterize the species initially forming at ~370 nm in D298K biogenesis by UV/vis spectroscopy.

Additionally, the LTQ-like cofactor generated during the initial DPQ trapping study was generated by the cross-linking of two amino acid residues causing it to be trapped in the flipped, inactive conformation. Another secondary goal of this research was to generate and characterize an LTQ-like cofactor in CAO that has increased mobility and could potentially exist in the active conformation; thus, a D298A mutant was biogenized in the presence of a free amine.

Lastly, in order to assess the intermediacy of DPQ in the biogenesis of LTQ in LOX and to determine if the active site of LOX is selectively set up to generate LTQ or capable of catalyzing the formation of TPQ (hydration reaction of DPQ), the lysine participating in the cross-link to form LTQ was removed from the active site of HLOXL2 by site-directed mutagenesis.

Chapter 2: Trapping a DPQ Intermediate in the Biogenesis of TPQ in AGAO

Introduction

Designing Active-site Mutants to Trap Dopaquinone in TPQ Biogenesis.

As discussed in chapter 1, a dopaquinone-like intermediate (DPQ) has been observed in the biogenesis of TPQ using time-resolved X-ray crystallography, but the redox state of the intermediate was not defined at 2.1 Å resolution (Figure 1.5 b). A resonance Raman spectroscopic study confirmed that the C2 oxygen of TPQ was derived from a solvent water molecule and strongly supported the proposed reaction mechanism involving 1,4-addition of water to the C2 position of a DPQ intermediate.[66] By analogy, DPQ has been suggested as an intermediate in LTQ biogenesis. In a model study, it was shown that 1,4-addition of N-methyl-*n*-butylamine to the C2 position of DPQ forms the LTQ-like quinone and the active site of LOX must be pre-organized to prevent a 1,2-addition reaction.[1] In order to gain insight into the intermediacy of DPQ both in the TPQ and LTQ cofactor biogenesis, a lysine residue was incorporated in the active site of AGAO in two positions in an attempt to trap the DPQ intermediate either before flipping (Figure 1.3 b) or after flipping (Figure 1.3 c) and to generate a LTQ-like cofactor in CAO. Based on the

model chemistry,[1] a correctly placed amine should be able to effectively trap the putative DPQ intermediate, thereby forming an LTQ-like-quinone. Based on the X-ray crystal structure of the putative DPQ intermediate,[5] a mutation of Asp298 was performed to trap the un-flipped conformation (Figure 2.1 a). To determine which residue to target for the flipped conformation, the X-ray structure of TPQ_{red} (Figure 1.3 d) was used as a model for flipped DPQ. Based on this, Met602 was found to be the closest residue to the C2 carbon (Figure 2.1 b).

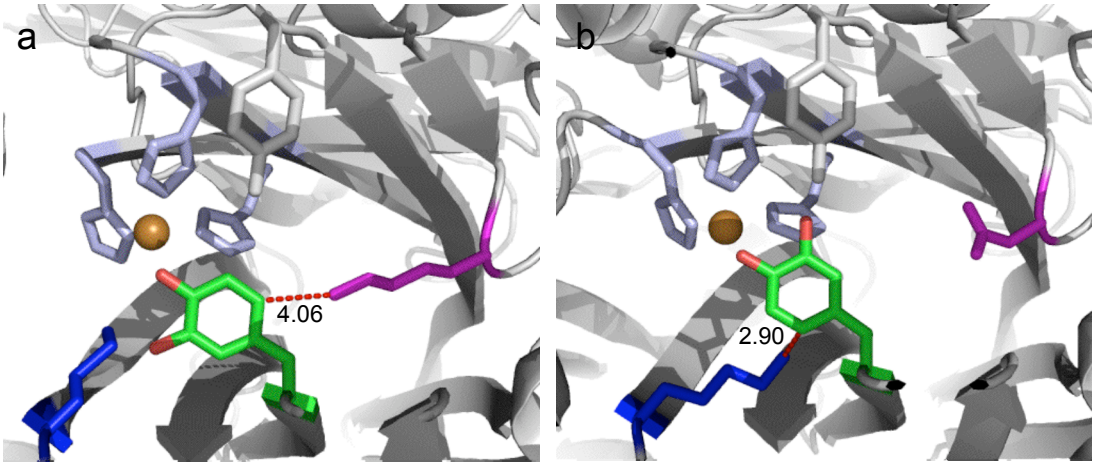

Figure 2.1 Active site structures of DPQ intermediates. Intermediates are shown in un-flipped (a) (PDB code 1IVV at 2.1 Å resolution) and flipped (b) conformations. The flipped conformation (b) of the DPQ intermediate is generated from the reduced form of TPQ (TPQ_{red}) (PDB code 1IVW at 1.8 Å resolution). The DPQ is green, D298 or D298K is magenta and M602 or M602K is blue. H431, H433, H592 (copper binding site) are light blue. Copper is shown as a golden sphere. Remaining active site residues are gray. Figures are generated by Pymol (DeLano Scientific LLC, http://www.pymol.org).

X-ray Crystal Structure of D298K.

The Tanizawa group (Osaka University) determined the crystal structure of holo-D298K at 1.7-Å resolution.[4] The cross-link between the ε-amino group of

Lys298 and the C2 atom of the side chain aromatic ring of TPQ382 was apparent even before introducing the cofactor model to the residues at the 298 and 382 positions. Then, two models including the cross-link were examined at residues 298 and 382 for a best fit compared with the electron density. One was LTQ, and the other was the iminoquinone tautomer of LTQ (LTI) (Scheme 2.1). The latter model

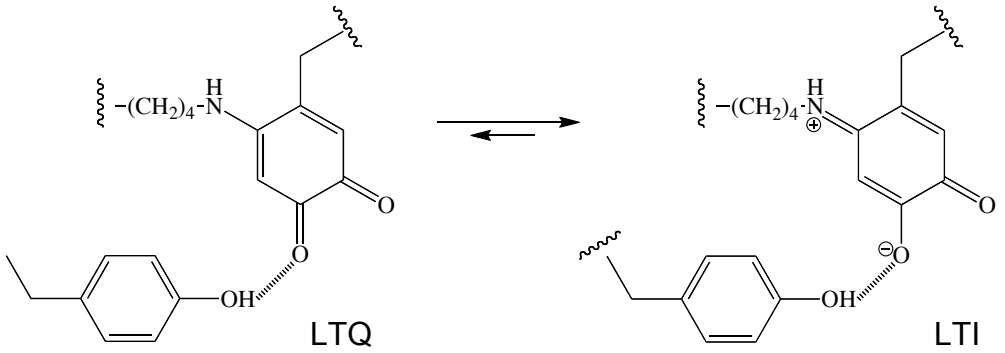

Scheme 2.1 Tautomerism of LTQ and LTI in D298K. LTQ λ_{max}= 505 nm; LTI λ_{max}= 450 nm.

indicates that an imine bond is formed between the C2 carbon of the DPQ and the side chain ε-amino group of Lys298. The dictionaries for these two models were created by linking the C2 atom of the DPQ and the ε-amino group of Lys298 through distinct types (single or double) of a covalent bond whose lengths are indistinguishable crystallographically at the present resolution. The extra electron density at the O5 position was very clear, suggesting a carbonyl group. The two models fitted equally well to the electron density in the $F_o - F_c$ simulated annealing (sa) omit map viewed perpendicularly to the dopaquinone ring (Figure 2.2 a, c). However, close inspection of the lysyl side chain portion of the models revealed that the LTI model fit better to the omit map than the LTQ model. Particularly in a view

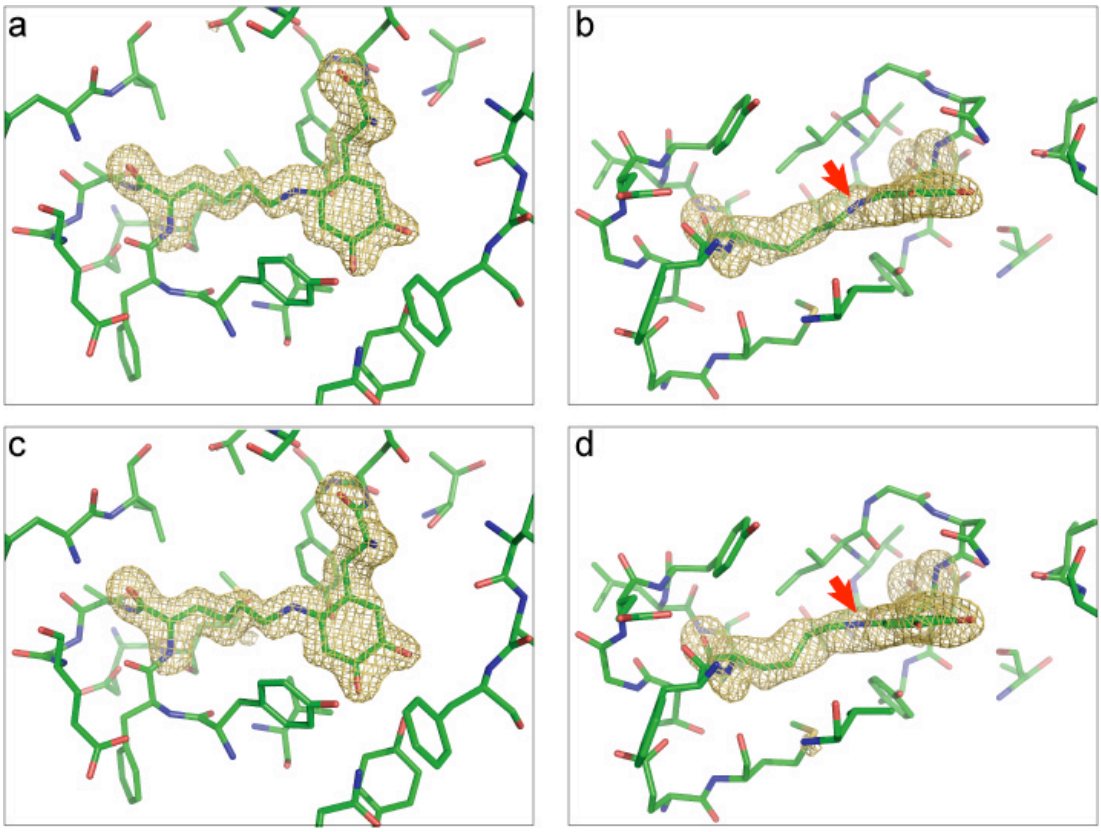

Figure 2.2 Electron density map of the active site of D298K at 1.7 Å resolution. Simulated annealing (sa) omit maps (contoured at 4.5 σ) are shown with the structure models of LTQ (a, b) and LTI (c, d). a, c) Views perpendicularly to the dopaquinone ring. b, d) Views parallel to the dopaquinone ring. Red arrows show N^{ε} atoms of Lys298.[4]

parallel to the dopaquinone ring, both of the N^{ε} and CE atoms of Lys298 are positioned nearly in the middle of the electron density in the LTI model (Figure 2.2 d), whereas those in the LTQ model are located in the periphery of the electron density (Figure 2.2 b). The plane of the quinone ring is also better accommodated inside the electron density in the LTI model than in the LTQ model. The planarity is extended to the CE atom of Lys298 (Figure 2.2 d) and is permitted only for the sp^2 N^{ε} atom of LTI. These data suggested that the cross-link formed between dopaquinone

and Lys298 has an imine double bond character and that the quinone is stabilized as LTI rather than LTQ. The O4 of TPQ is in hydrogen bonding contact with the conserved Tyr284 in WT. A similar hydrogen bonding interaction appears to be present in D298K, which may help to stabilize LTI over LTQ (Figure 2.3). The orientation of LTI in D298K is in a flipped, inactive conformation where the active carbonyl group at C5 is facing away from the proposed substrate entry channel.[9]

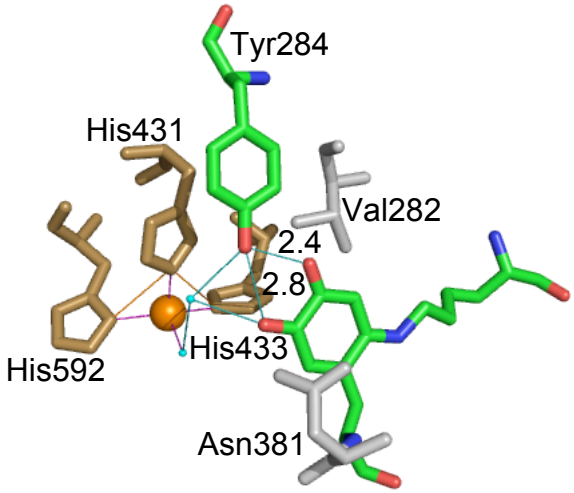

Figure 2.3 Active site structure of D298K and the putative dopaquinone intermediate seen in TPQ biogenesis in WT. a) D298K (PDB code 2YX9 at 2.7 Å resolution). Copper is shown as a golden sphere and water molecules are shown in light blue spheres. Val282 and Asn381 forming a wedge-shape pocket are shown in gray. Figures are generated by Pymol (DeLano Scientific LLC, http://www.pymol.org).

Along with 1,4-additions to DPQ, 1,6-additions could also potentially occur. In nature, *o*-quinones react with amino acid side chains, such as lysine, cysteine, and histidine, in 1,2-, 1,4-, and 1,6-additions. The addition reactions initiate polymerization, and are a source of pigmentation in a variety of plant and animal species.[79,80] Studies of the reaction between *o*-quinone and cysteine occurring in

insects have shown that 1,6-additions to *o*-quinones are preferred to 1,4-additions.[81] Additionally, a model study of the reaction between *o*-dopaquinone and *N*-acetylcysteine in the presence of oxygen resulted in the formation of the 1,6-addition product, but the 1,4-addition product was not observed.[82] In the biosynthesis pathway of pheomelanin, a type of melanin with a red hue, cysteine is added to dopaquinone through a 1,6-addition forming the catechol, cysteinyldopa (Figure 2.4).[83,84] Cysteinyldopa has been detected in the plasma and urine of individuals with melanoma.[85] Cysteinyldopa levels are monitored in patients who have had melanoma due to its usefulness as a specific and sensitive marker in the prediction of metastases. In order to determine if DPQ in CAO could be trapped by a 1,6-addition, a cysteine residue was incorporated into the active site in the D298 position.

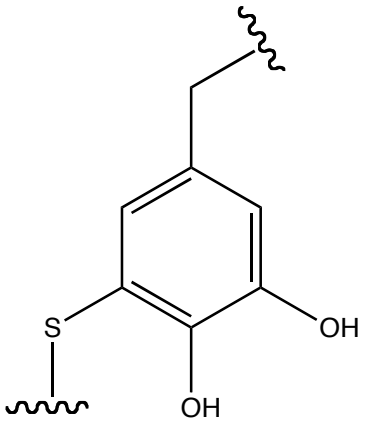

Figure 2.4 Structure of cysteinyldopa, the 1,6-addition product of cysteine and dopaquinone.

Materials and Methods

Materials

HEPES, MES, CHES, ammonium sulfate, sodium hydroxide, potassium hydroxide, hydrochloric acid, potassium phosphate, Tris, ethylenediaminetetraacetic acid (EDTA), urea, potassium chloride, sodium borate, PVDF membrane, sodium diethyldithiocarbamate (DDC), phenylmethanesulphonylfluoride (PMSF), Pepstatin A, Leupeptin, Luria-Bertani (LB) (Miller) broth/agar, ampicillin HCl, sodium dodecylsulfate (SDS), glycine, TEMED, acetic acid, methanol, brilliant blue R-250, and a Sonic Dismembrator 500 were purchased from Fisher Scientific. 2-phenylhydrazine, antipain, lysozyme, DNase, RNase, potassium acetate, horse radish peroxidase (HRP), 2,2'-azino-bis(3-ethylbenzthiazoline-6-sulphonic acid) (ABTS), 30% hydrogen peroxide, 2-phenylethylamine, 2-hydrazinopyridine hydrochloride, 4-nitrophenylhydrazine, copper sulfate ($CuSO_4$) and ethylenediamine were purchased from Sigma Aldrich. CAPS, 85% glycerol, potassium pyrophosphate, and isopropyl β-D-1-thiogalactopyranoside (IPTG) were purchased from Acros. The BCA assay kit, Slide-A-Lyzer cassette, and SnakeSkin dialysis tubing were purchased from Thermo Scientific Pierce Protein Research Products. TOYO PEARL HW55-F size exclusion resin, TOYO PEARL DEAE 650-M anion exchange resin, and TOYO PEARL Butyl 650-M hydrophobicity resin were purchased from Tosoh Bioscience. Ammonium persulfate, 30% acrylamide/bis solution, and chelex were purchased from Bio-Rad Laboratories. Open column chromatography was done with an Econo pump EP-1, an Econo UV monitor EM-1, and a BioLogic BioFrac Fraction collector (Bio-

Rad). FPLC chromatography was done with an AKTA FPLC, a HiPrep 16/10 Butyl FF column, and HiLoad 16/60 Superdex 200 sizing column purchased from GE Healthcare (Amersham Biosciences). The FPLC DEAE column was manually packed into a XK 16/40 jacketed column (GE Healthcare). Ethanol was purchased from Decon. The Amicon Ultra 30K MW cutoff concentrators were purchased from Millipore. Nitro blue tetrazolium (NBT) used for quinone staining was purchased from CalBiochem. Synthetic oligonucleotides were purchased from Operon Biotechnologies, Inc. PCR was performed on a DNA Engine PTC-200 Peltier Thermal Cycler (Biorad). Plasmids were prepared using a QIAprep Spin Miniprep kit (Qiagen). DNA sequencing was performed at the UC Berkeley DNA sequencing facility.

Site-directed Mutagenesis.

The expression plasmids for D298K-, M602K-, Y384K-, D298C-, and Y284A-AGAO were generated by site-directed mutagenesis using a Quikchange mutagenesis kit from Stratagene on pPEAO-02[29] as a parent vector. The DNA primers used for D298K were 5′-CCTGGCAGAACTACTTCAAGACGGGGGAGTACCTGGTG-3′ (forward) and 5′-CACCAGGTACTCCCCCGTCTTGAAGTAGTTCTGCCAGG-3′ (reverse) (underlined nucleotides correspond to the sites of mutation). The DNA primers used for M602K were 5′-GGACTGGCCCATCAAACCGGTGGACACCGTC-3′ (forward) and 5′-GACGGTGTCCACCGGTTTGATGGGCCAGTCC-3′ (reverse). The DNA primers

for Y384K were 5′-CCACTATCGGCAACTACGACAAAGGCTTCTACTGGTACCTCTAC-3′ (forward) and 5′-GTAGAGGTACCAGTAGAAGCCTTTGTCGTAGTTGCCGATAGTGG-3′ (reverse). The DNA primers for D298C were 5′-CTGGCAGAACTACTTCTGCACGGGGGAGTACCTG-3′ (forward) and 5′-CAGGTACTCCCCCGTGCAGAAGTAGTTCTGCCAG-3′ (reverse). The DNA primers for Y284A were 5′-GATGGTGGTGCCGGCGGGCGATCCGTCCC-3′ (forward) and 5′-GGGACGGATCGCCCGCCGGCACCACCATC-3′ (reverse). The DNA primers for D298A were 5′-AGAACTACTTCGCTACGGGGGAGTACCTG-3′ (forward) and 5′-CAGGTACTCCCCCGTAGCGAAGTAGTTCT-3′ (reverse). An expression plasmid for the double mutant, Y284F/D298K was generated from the D298K-AGAO expression vector using the DNA primers, 5′-GATGGTGGTGCCGTTCGGCGATCCGTCC-3′ (forward) and 5′-GGACGGATCGCCGAACGGCACCACCATC-3′ (reverse). The double mutants of Y284F/M602K and Y284F/Y384K were also prepared from the M602K- and Y384K-AGAO expression vectors using the Y284F primers seen above. All plasmids were fully sequenced and the point mutations were confirmed. Plasmids were grown in *E. coli* DH5α cells and purified using high-speed plasmid mini- and midi-prep kits from Qiagen.

Enzyme Expression and Purification.

Wild-type (WT) and mutant AGAO expression plasmids were transformed into *E. coli* BL21(DE3) or CD03, a mutant strain of *E. coli* BL21(DE3) where two out of three catalase genes were disrupted.[12] The mature forms the of WT, D298K, M602K, Y384K, Y284F/D298K, and Y284F/M602K enzymes were produced by growing the transformants in LB-ampicillin media at 37°C and induced with 0.1 mM IPTG and 50 μM Cu^{2+} at an OD_{600} between 0.6 and 0.8. The precursor form of D298C was produced by growing the transformants in LB-ampicillin media at 37°C and induced with 0.1 mM IPTG at an OD_{600} between 0.6 and 0.8. Expression was allowed to continue overnight at 26°C. The cells were harvested by centrifugation at 3,000 x g, 4°C, for 15 min and stored at -80°C until use. The enzymes were purified to homogeneity following the published procedure.[86] All steps of this procedure were completed at 4°C unless otherwise noted. Cells were thawed in 30 mM KPi with 10 μM $CuSO_4$ at a final volume of 500 mL. 500 μL 1000x protease inhibitors: PMSF, antipain, pepstatin A, and leupeptin were added along with 500 μL 1000x DNase and RNase. Small amounts of lysozyme were also added. Disruption of the cells was achieved by sonication at an amplitude of 60%. Cycles of one sec on/one sec off for one min were repeated every five min for a total of five cycles. The cells were centrifuged at 57,000 x g for 1 hr. The supernatant was mixed with 1 M acetate buffer pH 5.0 (10% v/v). This mixture was stirred 20 min and centrifuged 20 min at 12,000 x g. The pH of the supernatant was adjusted to 6.5 with KOH. $(NH_4)_2SO_4$ (45% saturated) was added and allowed to stir for 20 min followed by centrifugation

at 12,000 x g for 20 min. The pellet was collected and dissolved in a minimal amount of 20 mM KPi pH 6.5 with 10 μM $CuSO_4$. The sample was dialyzed against 1 L of this same buffer with 50 mM KCl three times (1 hr, 1 hr, overnight).

The sample was removed from dialysis and centrifuged at 57,000 x g for 20 min before being loaded onto a pre-equilibrated 100 mL DEAE column connected to a peristaltic pump and UV detector at 4 mL/min. The column was washed with 225 mL of the pre-equilibration buffer (20 mM KPi pH 6.5 with 10 μM $CuSO_4$ and 50 mM KCl). The protein was then eluted with a four column volume gradient containing 50 to 200 mM KCl in buffer. Fractions were collected every 1.0 min. The column was washed with three column volumes 200 mM KCl in buffer and re-equilibrated in three column volumes 50 mM KCl in buffer. SDS-PAGE gels were run on every fourth fraction, along with activity assays for CAO and catalase. Fractions containing active CAO protein were pooled. $(NH_4)_2SO_4$ (70% saturated) was added and the mixture was stirred for 20 min. After 20 min of centrifugation at 12,000 x g, the pellet was dissolved in a minimal amount of 20 mM KPi pH 6.5 with 10 μM $CuSO_4$ and 50 mM KCl and dialyzed against 1 L of the same buffer three times (1 hr, 1 hr, overnight).

The dialysis product was loaded onto the DEAE column, and the column was washed with 100 mL of 20 mM KPi pH 6.5 with 10 μM $CuSO_4$ and 50 mM KCl. The column was further washed with 250 mL of 20 mM KPi pH 6.5 with 10 μM $CuSO_4$ and 90 mM KCl and the protein was eluted with a four column volume gradient of 90 to 200 mM KCl in buffer. SDS-PAGE gels were run on every fourth

fraction along with activity assays for CAO and catalase. Fractions containing active CAO protein were pooled and $(NH_4)_2SO_4$ was slowly added, with stirring, to a final concentration of 20%.

Pooled protein was loaded onto a pre-equilibrated 50 mL Butyl column. The column was washed with 250 mL of equilibration buffer (50 mM KPi pH 6.5 with 10 μM $CuSO_4$ and 20% sat. $(NH_4)_2SO_4$). The protein was eluted with an eight column volume gradient from 20 to 0% $(NH_4)_2SO_4$ in buffer. SDS-PAGE gels were run on every third fraction along with activity assays for CAO and catalase. Fractions containing active CAO protein and lacking catalase activity were pooled and concentrated in a spin column, or by adding $(NH_4)_2SO_4$ to a concentration of 70%, and dialyzing the sample into 20 mM KPi pH 6.5. Protein concentrations were determined by BCA assay. Protein was stored at -80°C in 50 μL aliquots at 20 mg/mL containing 25% glycerol as a cryoprotectant. The Y284F/D298K mutant was not very stable and the purification was performed in the minimal time (2 ~ 3 days).

The precursor forms of WT, D298K, and Y284F/D298K were optimally expressed using the following procedure: After transformation, the cells were plated on LB-ampicillin agar plates and allowed to incubate at 37°C overnight. A colony was picked the following morning and added to a 125 mL of LB-ampicillin media (starter culture) and grown at 37°C, 225 rpm to an OD_{600} of ~1.4 (~8 hrs). Fifteen mL of starter culture was used to induce 1.5 L of LB-ampicillin media, which was grown at 37°C to an OD_{600} of 0.6-0.8 (~3.5 hrs). The culture was placed on ice for 15 min and then induced with 0.1 mM IPTG. The culture was returned to the shaker and

grown overnight at 26°C, 225 rpm. The cells were harvested by centrifugation at 3,000 x g, 4°C, for 15 min and stored at -80°C until use.

The purification procedure was modified from a procedure described previously.[29,12] All steps of this procedure were completed at 4°C unless otherwise noted. All buffers were chelexed. The cells were thawed at room temperature in 10 mM HEPES pH 6.8 with 1 mM EDTA and 1 mM DDC to a final volume of 300 mL. 300 μL of 1000x protease inhibitors: PMSF, antipain, pepstatin A, and leupeptin were added along with 300 μL of 1000x DNase and RNase. Small amounts of lysozyme were also added. Disruption of the cells was achieved by sonication at an amplitude of 70%. Cycles of one sec on/one sec off for one min were repeated every five min for a total of five cycles. The cells were centrifuged at 57,000 x g for 1 hr. The supernatant was mixed with 1 M acetate buffer pH 5.0 (10% v/v). This mixture was stirred 20 min and centrifuged 20 min at 57,000 x g. The pH of the supernatant was adjusted to 6.8 with KOH. $(NH_4)_2SO_4$ was added to 45% saturated and allowed to stir for 20 min followed by centrifugation at 57,000 or 12,000 x g for 20 min. The pellet was collected and dissolved in a minimal amount of 10 mM HEPES pH 6.8 with 1 mM EDTA and 1 mM DDC. The sample was dialyzed against 1 L of the same buffer three times (1 hr, 1 hr, overnight).

The sample was removed from dialysis and centrifuged at 57,000 x g for 20 min before being loaded, at 4 mL/min, onto a pre-equilibrated 250 mL DEAE column connected to a peristaltic pump and UV detector. The column was washed with two column volumes of the pre-equilibration buffer (10 mM HEPES pH 6.8 with 1 mM

EDTA and 1 mM DDC). The protein was then eluted with a four column volume gradient containing 100-300 mM KCl in pre-equilibration buffer. Fractions were collected every 1.5 min. SDS-PAGE was run on every third fraction and fractions containing CAO were pooled. $(NH_4)_2SO_4$ was added to 70% saturated and the mixture was stirred 20 min. After 20 min of centrifugation at 57,000 or 12,000 x g the pellet was dissolved in a minimal amount of 10 mM HEPES pH 6.8 with 1 mM EDTA and 1 mM DDC and dialyzed against 1 L of the same buffer three times (1 hr, 1 hr, overnight).

The sample was removed from dialysis and centrifuged at 57,000 x g for 20 min before being loaded onto a pre-equilibrated 80 mL DEAE FPLC column. (Buffer A: 10 mM HEPES pH 6.8 with 1 mM EDTA and 1 mM DDC). The column was washed with two column volumes of the buffer with 5 % buffer B (Buffer A + 1 M KCl). The protein was eluted with an eight column volume gradient from 5-30% buffer B. The column was washed with one column volume of 40% buffer B followed by two column volumes of 50% buffer B and two column volumes of H_2O. The column was re-equilibrated in 10 mM MES pH 5.8 with 1 mM EDTA and 1 mM DDC. An SDS-PAGE gel was run on every third fraction and fractions containing CAO were pooled. Pooled fractions were precipitated by adding $(NH_4)_2SO_4$ to 70% saturated and stirring 20 min. After 20 min of centrifugation at 57,000 or 12,000 x g the pellet was dissolved in a minimal amount of 10 mM HEPES pH 6.8 with 1 mM EDTA and 1 mM DDC and dialyzed against 1 L of the same buffer three times (1 hr, 1 hr, overnight).

The sample was removed from dialysis and $(NH_4)_2SO_4$ was added to 25% saturated. The sample was stirred 20 min and centrifuged 20 min at 57,000 x g. Half of the sample was loaded onto a pre-equilibrated 20 mL Butyl FPLC column (Buffer B: 10 mM HEPES pH 6.8 with 1 mM EDTA, 1 mM DDC and 25% saturated $(NH_4)_2SO_4$). The column was washed with two column volumes of 75% buffer B and the protein was eluted with a seven column gradient from 75-20% buffer B. The column was washed with two column volumes of buffer A (buffer B without $(NH_4)_2SO_4$), re-equilibrated, and the same method was run on the other half of the sample. An SDS-PAGE gel was run on every third fraction, and fractions containing CAO were pooled. Pooled fractions were precipitated by adding $(NH_4)_2SO_4$ to 70% saturated and stirring 20 min. After 20 min of centrifugation at 57,000 or 12,000 x g, the pellet was dissolved in a minimal amount of 10 mM MES pH 5.8 with 1 mM EDTA and 1 mM DDC and dialyzed against 1 L of the same buffer three times (1 hr, 1 hr, overnight).

The sample was removed from dialysis and centrifuged at 57,000 x g for 20 min before being loaded onto a pre-equilibrated 80 mL DEAE FPLC column. (Buffer A: 10 mM MES pH 5.8 with 1 mM EDTA and 1 mM DDC). The column was washed with two column volumes of the buffer with 10% buffer B (Buffer A + 1 M KCl). The protein was eluted with a seven column volume gradient from 10-35% buffer B. An SDS-PAGE gel was run on every third fraction, and fractions containing CAO were pooled. Pooled fractions were concentrated in a spin column to about two mL. An additional FPLC sizing column was run on D298A samples being purified

for crystallography using 10 mM HEPES pH 6.8 with 1 mM EDTA and 1 mM DDC. All protein samples were dialyzed in a spin column into 10 mM HEPES pH 6.8 (5 x 15 mL). Protein concentrations were determined spectrophotometrically by using extinction coefficients at 280 nm of 12.3 and 13.2 for 1% (w/v) solutions of the apo and holo forms of AGAO, respectively.[29] Protein not being used immediately was stored at -80°C in 40 mg/mL aliquots containing 25% glycerol as a cryoprotectant.

Activity Assay

The holo enzyme activity was assayed by one of two methods. The first method measures the production of hydrogen peroxide using horseradish peroxidase (HRP)–2,2'-azino-bis(3-ethyl)-benzthiazoline-6-sulfonic acid (ABTS) coupled assay, according to published procedure.[29,44,87] In this assay, CAO produces H_2O_2, which acts as a substrate for HRP to give an activated form. The activated HRP oxidizes ABTS to give a λ_{max} of 414 nm. UV/vis spectroscopy was performed on a Shimadzu UV-2501 PC dual beam UV/vis spectrophotometer equipped with a temperature-controlled cell holder at 30 ± 0.2 °C (path length of 1 cm). A 5 mL stock solution of 50 mM KPi pH 7.2, 2.5 μL of 10 mg/mL HRP, and 250 μL of 20 mM ABTS was made. 100 μL of the stock solution was placed in a 100 μL cuvette followed by 1 μL of 10 mM 2-phenylethylamine and a variable amount of enzyme of known concentration. The absorbance at 414 nm was observed with a cycling time of 0.2 sec for a total of 240 sec. The activity was calculated from the change in absorbance between 30-120 sec.

The second method was to measure the amount of O_2 consumed using a Clark type polarographic electrode (Hansatech Instruments) using 2-phenylethylamine as a substrate with variations from the published procedure.[12,29] The temperature of the reaction was maintained at 30°C with the use of a circulating water bath. The chamber of an O_2 electrode was filled with 500 μL of 50 mM KPi pH 6.5 and 50 μL of 5 mM 2-phenylethylamine. The reaction was started with the addition of a variable amount of enzyme of known concentration.

The redox activity of holo D298C was determined by adding two equivalents of $NaIO_4$ (1 μL) to the 70 μL of 0.128 mM sample after biogenesis. Spectra were taken every 30 sec for 10 min. The reaction was incubated at room temperature overnight and an additional spectrum was taken. An equal volume of 12 M urea was added and the sample was heated at 30°C 1.5 hrs followed by heating at 50°C 1 hr. The reaction was monitored by UV/vis.

Catalase activity was measured by an ABTS coupled assay with hydrogen peroxide as the substrate. UV/vis spectroscopy was performed on a Shimadzu UV-2501 PC dual beam UV/vis spectrophotometer equipped with a temperature-controlled cell holder at 30 ± 0.2 °C (path length of 1 cm). A 10 mL stock solution of 0.1 M KPi pH 6.5 with 10 μL of 1 M H_2O_2 and 500 μL of 20 mM ABTS was prepared. A stock solution of 100 μL was placed in a 100 μL cuvette followed by 5 μL of enzyme of unknown concentration. The absorbance at 414 nm was observed with a cycling time of 0.2 sec for a total of 240 sec. The activity was calculated from the change in absorbance between 30-120 sec.

Phenylhydrazine Titration

A phenylhydrazine titration was preformed after protein purification in order to determine the amount of active TPQ in the sample. The experiment was conducted on a monochromator type UV-vis equipped with a thermostatted cell chamber set to 30°C. A known concentration (5 μM subunit for WT) of enzyme in 20 mM KPi pH 6.5 was added to a 500 μL cuvette. Phenylhydrazine was added in 2.5 μL aliquots containing 0.025 to 0.1 equivalents. Spectra were taken until no further change in absorbance at 438 nm was observed. Aliquots of phenylhydrazine were added in this manner until addition of phenylhydrazine no longer produced a change in absorbance at 438 nm.

Quinone Staining

The presence of a quinone in WT and mutants of CAO was determined by the standard quinone-staining method.[88] An SDS-PAGE gel was run on the samples, which were transferred to a PVDF membrane. The membrane was rinsed three times with water before covering the membrane in 2 M potassium glycinate pH 10.0 with a few milligrams of NBT. The membrane was allowed to shake in the solution, in the dark, for 45 min. The membrane was then rinsed with 0.1 M sodium borate ($Na_2B_4O_7$) pH 10.0. The membrane was dried between paper towels in the dark.

ICP Analysis

Inductively coupled plasma (ICP) analysis was done by StatAnalysis Corp. on holo samples of WT (7.14 mg/mL), D298K (7.14 mg/mL), Y284F/D298K (11.16 and 11.7 mg/mL), and M602K (8.33 mg/mL) in order to quantify the amount of Cu^{2+} in each of the samples. Samples were dialyzed into 20 mM KPi buffer at pH 6.5 with 1 mM EDTA to remove excess Cu^{2+} followed by dialysis into the same buffer without EDTA.

Reaction with 2-Hydrazinopyridine, 4-Nitrophenylhydrazine and Ethylenediamine.

In order to determine the reactivity of the enzyme samples with inhibitors, enzyme solutions of 10 μL of 20 mg/mL WT, D298K, or M602K samples were added to 90 μL of 20 mM KPi pH 6.5 with 10 μM $CuSO_4$ and 5 μM KCl or 20 mM Tris pH 7.8, followed by 2 μL of 7 mM (five molar equivalents) of the hydrazine or ethylenediamine. The mixture was incubated at 30 °C and the absorption spectra was taken on a Shimadzu UV-2501 PC dual beam UV/vis spectrophotometer equipped with a temperature-controlled cell holder at 30 ± 0.2°C. In some cases, the temperature of the reaction was increased to 60°C and the sample was incubated 30 min and 3 hrs before spectra were taken.

Reaction with Urea

Enzyme solutions of holo WT and D298K CAO were dialyzed in a slide-a-lyzer into 20 mM Tris pH 7.8 with 1 mM EDTA or 0.1 M KPi pH 6.8 with 1 mM EDTA, then was dialyzed again without EDTA. The enzyme solution was then

dialyzed in an Amicon concentrator into buffer with 2, 6, 8 or 9 M urea in order to disrupt the hydrogen bonding interactions within the active site of CAO. Alternatively, an equal volume (35 μL) of enzyme solution and 12 M urea were combined for a final concentration of 20 mg/mL enzyme in 6 M urea. UV/vis spectroscopy was performed on a Shimadzu UV-2501 PC dual beam UV/vis spectrophotometer equipped with a temperature-controlled cell holder at 30 ± 0.2 °C (path length of 1 cm). Following the reaction with 12 M urea, samples were further reacted with five molar equivalents 2-hydrazinopyridine or 4-nitrophenylhydrazine (1.4 μL 70 mM stock solution). The reactions were monitored by UV/vis for one hour.

pH Jump

In order to determine if the LTI cofactor is sensitive to alkaline hydrolysis, holo D298K CAO samples were dialyzed into 0.1 M KPi pH 6.5 to remove excess Cu^{2+}. The pH of the samples was adjusted either by overnight dialysis into 20 mM K_2CO_3 pH 10, dialysis in a spin column into 110 mM pyrophosphate (PPi) buffer pH 9.5, or by the addition of 90 μL of 1 or 2 M KOH to 10 μL of 20 mg/mL enzyme sample. WT and M602K samples at pH 6.5 and 9.5 were reacted with one equivalent 2-hydrazinopyridine and spectra were taken at 10 and 20 min after incubation of the sample at room temperature. Holo WT and M602K samples were reacted with phenylhydrazine followed by the addition of KOH or HCl. A sample of 100 μL of 2 mg/mL WT or M602K was reacted with 2 μL of 7 mM phenylhydrazine (5 molar

equivalents), and the reaction was monitored by UV/vis for one hour. The excess phenylhydrazine was removed by dialysis against 1 L of 20 mM KPi pH 6.5 for 1 hr and again overnight. To half the sample was added 4 M KOH or 2 M HCl and the product was observed by UV/vis. UV/vis spectroscopy was performed on a Shimadzu UV-2501 PC dual beam UV/vis spectrophotometer equipped with a temperature-controlled cell holder at 30 ± 0.2 °C (path length of 1 cm).

UV/vis Biogenesis Study

The biogenesis study of WT and D298K was performed as previously described for WT.[29,68] The biogenesis of WT and D298K was monitored by UV/vis spectroscopy on an Agilent HP 8453 photo diode array UV/vis spectrophotometer equipped with a temperature-controlled cell holder at 30 ± 0.2 °C (path length of 1 cm). The spike in the spectra at 483 nm is an artifact of the instrument. Protein samples (25-50 μL) were dialyzed in an Amicon concentrator five times against 500 μL of 100 mM HEPES pH 6.8. D298K biogenesis reactions were carried out in the presence of water saturated O_2 or air. For samples run in concentrated O_2 conditions, a 50 μL sample of 0.2 mM protein was added to a cuvette, which was fitted with a T-shaped connector. A balloon was attached to the connector at a right angle to the cuvette, and a septum was used to seal the connector from the top (in line with the cuvette). The cuvette was purged with O_2 bubbled through water for 15 min. Care was taken to ensure that the sample was not bubbled. The balloon was allowed to fill, followed by the addition of 50 μL O_2 purged 1 mM $CuSO_4$ directly into the sample

through the septa in line with the cuvette. The instrument was blanked with water. The sample was mixed quickly and placed into the instrument. Spectra were taken every 10 sec for 10 min, followed by spectra taken every 2 min for 50 min and every 10 min for 1 hr for the D298K samples. The spectra for the WT samples were taken every 10 sec for 10 min and every 1 min for 20 min in air. The reaction was run in air without the balloon fitting or water saturation. D298K samples were run in air with 1 mM $CuSO_4$. The rates of formation of the 500-nm and 454-nm chromophores were determined spectrophotometrically in a reaction mixture containing 0.1 mM apo-D298K and 0.5 mM $CuSO_4$ in 50 mM buffer at pH 6.8. The final concentrations of enzyme were determined spectrophotometrically by using extinction coefficients at 280 nm of 13.2 for 1% (w/v) solutions of the holo form of AGAO.[29]

The biogenesis of apo D298C was done by adding 37.5 μL of 1 mM $CuSO_4$ to 37.5 μL of 0.063 mM D298C in 10 mM HEPES pH 6.8. The sample was incubated at room temperature two days before taking a spectrum. Alternatively, 37.5 μL of 1 mM $CuSO_4$ was added to 37.5 μL of 0.255 mM D298C in 10 mM HEPES pH 6.8. The sample was mixed rapidly and placed in a cuvette. UV/vis spectra were taken every 30 sec for 10 min, every 5 min for 50 min, and every 1 hr overnight.

Results

Expression and Purification of Wild-type and Mutant AGAOs

Each method of protein expression yielded approximately 105-110 g of wet *E. coli* cells. However, the amount of protein recovered varied based on mutant, growth conditions, and purification method. Although yields varied, mutants behaved the same as WT during expression and purification. Table 2.1 shows a summary of the yields. The purity of the samples was ~99% as estimated from SDS-PAGE gels.

Table 2.1 Protein yields for holo protein growth and purification conditions and for optimized apo protein growth and purification conditions. * not optimized

Protein yields (mg/L)	Holo protein	Apo protein
WT	5.03	32.8
D298K	6.95	23.5
M602K	12.1	
D298C		7.64*

UV/vis Spectroscopic Properties of Holo-D298K and Holo-M602K.

Figure 2.5 shows the UV/vis absorption spectra of D298K, M602K and WT. The purified holo-D298K and holo-M602K were yellowish brown, which contrasts with the characteristic pink color of WT-AGAO. WT shows a typical broad absorbance with a λ_{max} at 476 nm.[12] At physiological pH, the TPQ cofactor exists as a resonance stabilized mono-anion where the 4-hydroxyl group is deprotonated.[7] The λ_{max} of the WT-AGAO reflects the extent of resonance delocalization of the O4 oxo-

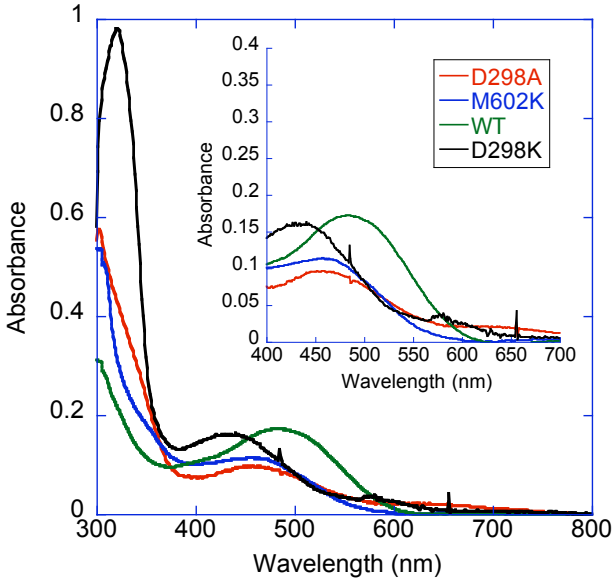

Figure 2.5 UV/vis absorption spectra of D298K, M602K, D298A, and WT-AGAO. Spectra are normalized to ~0.1 mM and were run in 50 mM HEPES buffer at pH 6.8. — D298K, — M602K, —D298A, — WT.

anion of the TPQ cofactor. The O4 of TPQ is in hydrogen bonding contact with the conserved Tyr284, and O2 of TPQ is in hydrogen bonding contact with two water molecules. D298K and M602K have a λ_{max} at ~450 nm that is ~30 nm blue-shifted from that of WT-AGAO. A similar 30 nm blue-shift in λ_{max} has been seen for the TPQ cofactor in D298A-AGAO[46] and also in D383A-ECAO[15] where, in these mutants, it is likely a result of the partial localization of electrons at O4 of TPQ. In the D298A-AGAO crystal structure,[46] the distance between O4 and the hydroxyl group of Tyr284 is a little shorter (2.3 Å) than that seen in the WT structure (2.5 Å), consistent with a localization of the charge at O4.[12] In addition to the absorbance at 450 nm, D298K also contains a prominent strong absorbance at 320 nm that is absent in WT, D298A and M602K. Such a band has been seen for LOX isolated from bovine aorta[89] as well as a recombinant form of LOX-like protein from *Drosophila*

melanogaster.[2] These observations suggested that the blue-shift in the visible spectrum of D298K might not simply be due to a change in charge distribution in the TPQ cofactor.

Reactivity of D298K and M602K towards Amine Substrate and Hydrazine Inhibitors.

The UV/vis spectra of D298K and M602K indicated the presence of a quinone that is different from TPQ in WT. The presence of a quinone in these mutants was determined by the standard quinone-staining method (Figure 2.6).[88] Both D298K and M602K were positive for quinone staining although staining was significantly weaker than WT.

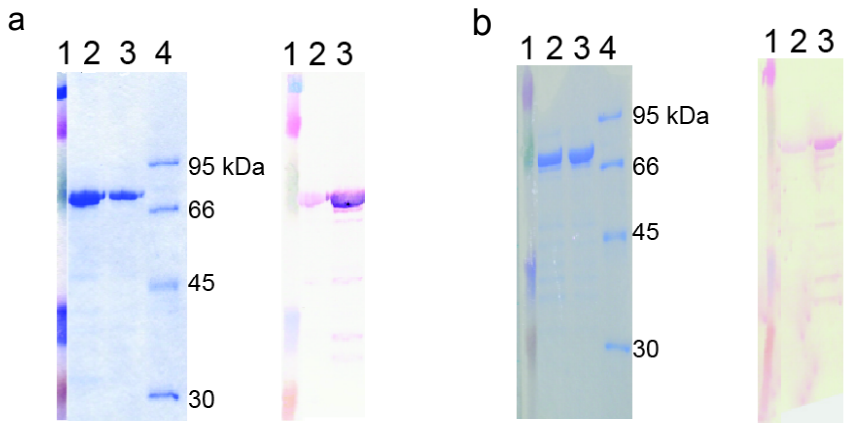

Figure 2.6 SDS-PAGE gels and PVDF-membranes stained for quinone detection. a) Lane 1: Kaleidoscope molecular marker, lane 2: WT-AGAO, lane 3: D298K-AGAO, lane 4: molecular marker, b) lane 1: Kaleidoscope molecular marker, lane 2: M602K, lane 3: WT, lane 4: molecular marker

The TPQ cofactor in CAO forms an intense chromophore with hydrazines and the chromophore formation has been used to titrate the amount of TPQ in CAOs.[90] In WT-AGAO, TPQ can be converted to hydrazone-azo derivatives with

phenylhydrazine,[12] 2-hydrazinopyridine[56] or 4-nitrophenylhydrazine.[29] M602K reacted with phenylhydrazine, and the titration indicated that the protein sample contained 40% active quinone (a typical result for WT is 65% titratable) (Figure 2.7). Consistent with the presence of a reactive quinone, M602K showed 0.45% activity towards 2-phenylethylamine in comparison to WT using a Clark O_2 electrode to assay O_2 consumption. The resonance Raman spectrum of the phenylhydrazine-derivatized M602K was very similar to that of the TPQ-phenylhydrazone adduct (Figure 2.8). This clearly indicated that the quinone in M602K is TPQ and that no cross-link had occurred between the ε-amino side chain of Lys602 and dopaquinone. For this reason, we did not pursue further characterization of M602K.

In contrast to M602K and WT, the quinone in D298K did not react with any of the hydrazines; no spectral change was observed even after prolonged

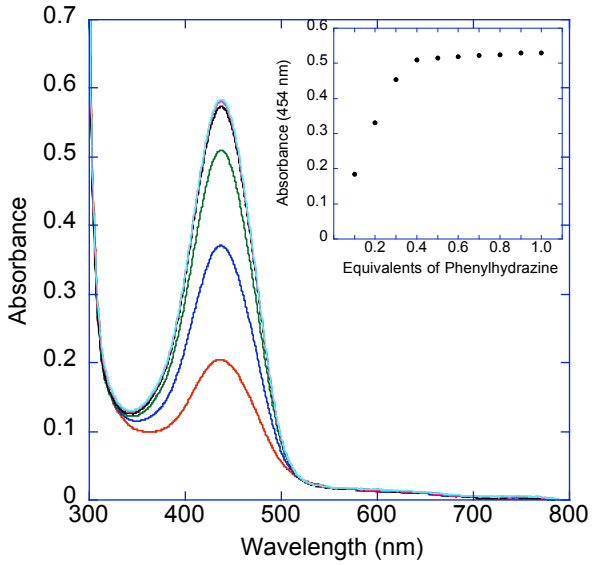

Figure 2.7 Phenylhydrazine titration of M602K. Phenylhydrazine was added in 0.1 equivalents. Final spectra were taken after 15 min for each equivalent. Insert shows the change in absorbance at 454 nm 15 min after the addition of each 0.1 equivalent.

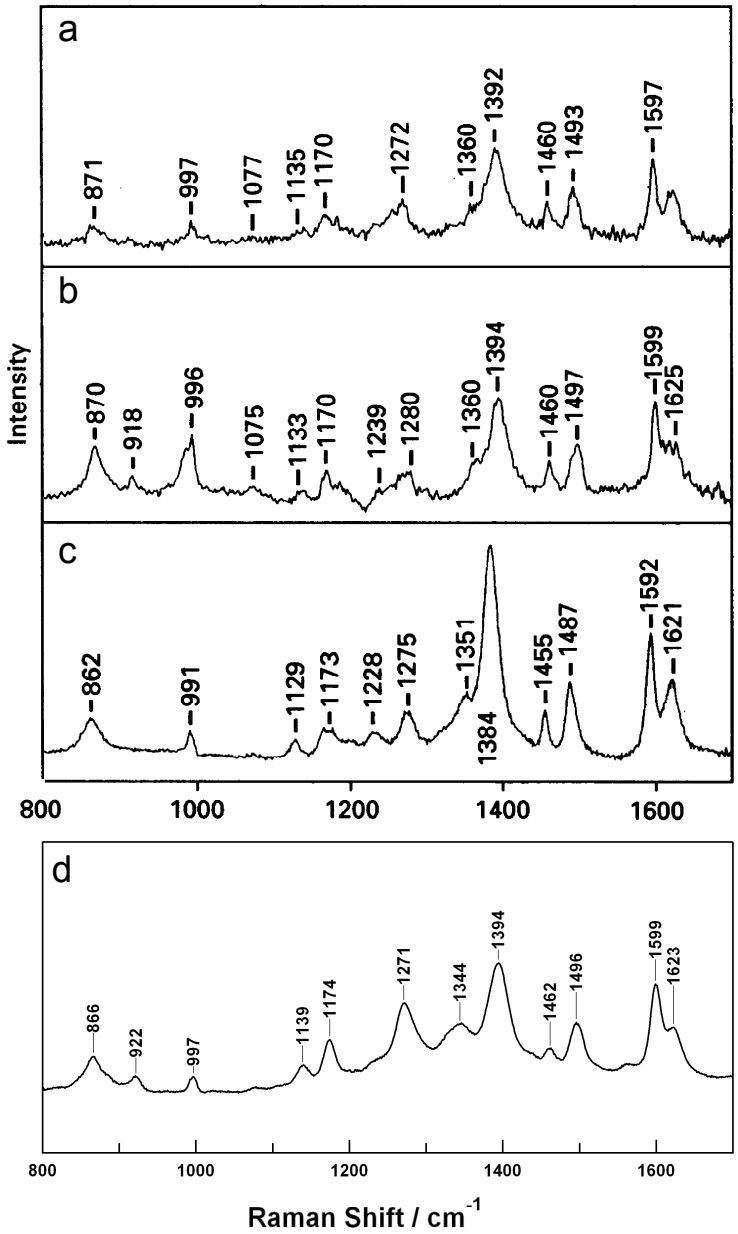

Figure 2.8 Resonance Raman spectrum of phenylhydrazine adducts. a) Arthrobacter P1 amine oxidase (AGAO), b) E. coli K-12 amine oxidase (ECAO), c) 3,4,6-trihydroxyphenylalanine quinone (TOPA),[6] and d) M602K AGAO. Panals a-c were reproduced with permission from Cooper, R. A.; Knowles, P. F.; Brown, D. E.; McGuirl, M. A.; Dooley, D. M., **1992**, *Biochemical Journal 288*, 337-340. Copyright the Biochemical Society. http://www.biochemj.org

incubation. D298K also showed no activity towards oxidative deamination of 2-phenylethylamine. This showed that the quinone formed in D298K was trapped in a

conformation that could not react with amines. The crystal structure of D298K shows LTI in the flipped conformation, with the C5 carbonyl group facing away from the proposed substrate entry channel. In agreement with these data, D298K is not active towards oxidative deamination of substrate amine and does not react with inhibitors such as 4-nitrophenylhydrazine and 2-hydrazinopyridine. The combination of UV/vis and resonance Raman spectroscopies (shown below) and the structural data suggested that D298K contains a quinone other than TPQ. ICP analysis of the Cu^{2+} content in D298K indicated that the species contained ~75% Cu^{2+} while WT contained ~72%.

Comparison of UV/vis Spectra of D298K with LTQ and LTI Model Compounds

Figure 2.9 shows the UV/vis spectra of an LTQ model compound, 5-*tert*-butyl-4-*N*-*n*-butylamino-1,2-benzoquinone at pH 7 and pH 11 (see Scheme 2.2). At physiological pH, the model compound is stabilized as an *ortho*-quinone with λ_{max} at 504 nm as seen in LTQ in LOX.[91] The pK_a of the amino group of the *n*-butylamino side chain of the related model compound, 5-ethyl-4-*N*-*n*-butylamino-1,2-benzoquinone, has been determined to be 10.3 by UV/vis spectroscopic pH titration.[1] 5-*tert*-Butyl-4-*N*-*n*-butylamino-1,2-benzoquinone[92] was used in this study as the 5-ethyl-quinone was not stable in alkaline conditions. Upon deprotonation, a 50-nm blue-shift in λ_{max} was observed due to the formation of the monoanionic form of LTI (Scheme 2.2). The monoanionic form of LTI resembles the chromophore in D298K (Figure 2.5) although it lacks the large absorption around 320 nm. Nonetheless, the visible spectrum of D298K is similar to that of the monoanionic LTI, supporting the

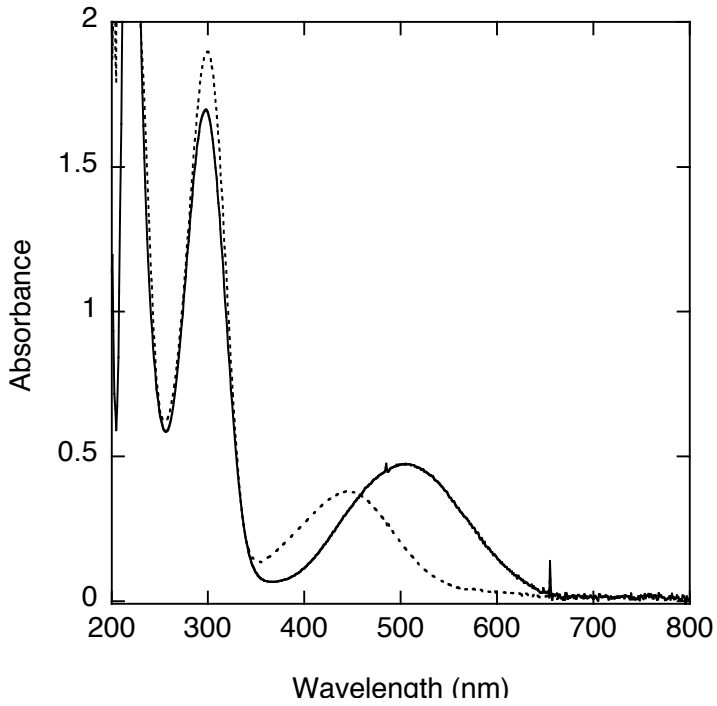

Figure 2.9 UV-vis spectra of LTQ and LTI (mono-anionic form) model compounds. [LTQ] = 1.7 mM in 50 mM HEPES buffer, pH 6.8; [LTI] = 1.7 mM in 0.1 M NaOH.— LTQ, ---LTI.

tentative assignment of the quinone in D298K as the iminoquinone tautomer of LTQ. The differences in the UV spectrum between D298K and the model compound may arise from the difference in protonation states, where the quinone in D298K would be expected to be neutral as opposed to monoanionic.

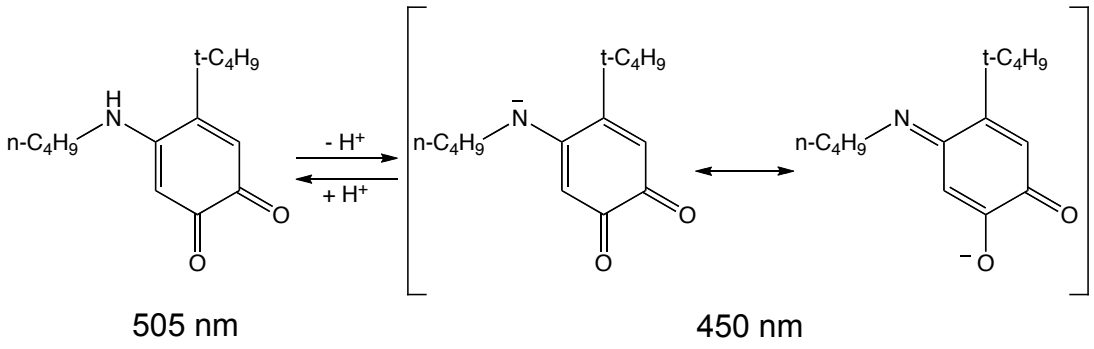

Scheme 2.2 Acid dissociation of LTQ to form the monoanionic form of LTI in the model system

Effect of pH on the UV/vis Spectrum of D298K.

It has been shown in model studies that the C5 carbonyl group of TPQ undergoes nucleophilic addition of substrates and inhibitors, whereas the C2 carbonyl group is unreactive.[51] The C2 carbonyl group is less electrophilic than that at C5 due to the resonance delocalization of the O4 oxoanion at physiological pH. This selective reactivity of nucleophiles at C5 of the TPQ cofactor over C2 has also been confirmed in CAO.[35] In addition to the resonance effect, the C5 carbonyl group is located near the proposed substrate entry channel[9] and the active site base, Asp298, for optimal activity. For this reason, it is less likely that the C2 carbonyl group of the TPQ cofactor reacts with the ε-amino side chain of Lys298 to form LTI in D298K. Alternatively, it could be possible that TPQ is formed initially in D298K, but the C5 carbonyl group of TPQ reacted with ε-amino side chain of Lys298 to form an iminoquinone similar to the substrate Schiff base intermediate in the catalytic cycle.[35,51] If so, the C5 imino group should be sensitive towards alkaline hydrolysis. To test for this possibility, D298K was incubated in pH 10 buffer. Under these conditions, we did not see any red-shift of λ_{max} to 480 nm, suggesting that the hydrolysis to TPQ did not occur. This is consistent with the cross-link between the ε-amino side chain of Lys298 and the quinone being at the C2 position, as revealed by the X-ray crystal structure. However, when D298K was reacted with 1 M KOH for 1 min a red shift of ~30 nm was observed. Additionally, peaks around 340 and 370 nm were observed (Figure 2.10). The peak at 510 nm is like that seen in the model

compound of LTQ as well as LOX isolated from bovine aorta[89] and a recombinant form of LOX-like protein from *Drosophila melanogaster*.[2]

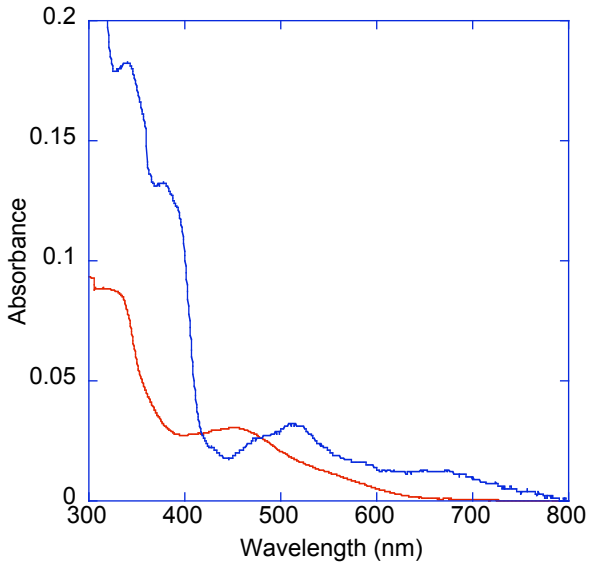

Figure 2.10 UV/vis spectra of D298K at increased pH. —D298K was slowly dialyzed into 20 mM K_2CO_3 pH 10. The sample was warmed to 30°C and the spectrum was taken after 1 hr. The final concentration of enzyme was normalized to ~0.056 mM. —D298K was reacted with 1 M KOH. The spectrum was taken after 1 min. The final concentration of enzyme was normalized to ~0.056 mM.

Effect of Disrupting the Hydrogen Bonding Interaction between O4 and Tyr284 on the UV/vis Spectrum of D298K.

The X-ray crystal structure of D298K (Figure 2.11) suggested a strong hydrogen bonding interaction (2.4 Å) between O4 of the quinone and the conserved Tyr284 (Scheme 2.1). In order to assess whether this hydrogen bonding interaction contributes to stabilizing the LTI tautomer in D298K, we disrupted the interaction by denaturation with 8 M urea at pH 7. The denaturation yielded a drastic spectral change to form a large absorbance around 350 nm but almost no absorbance above

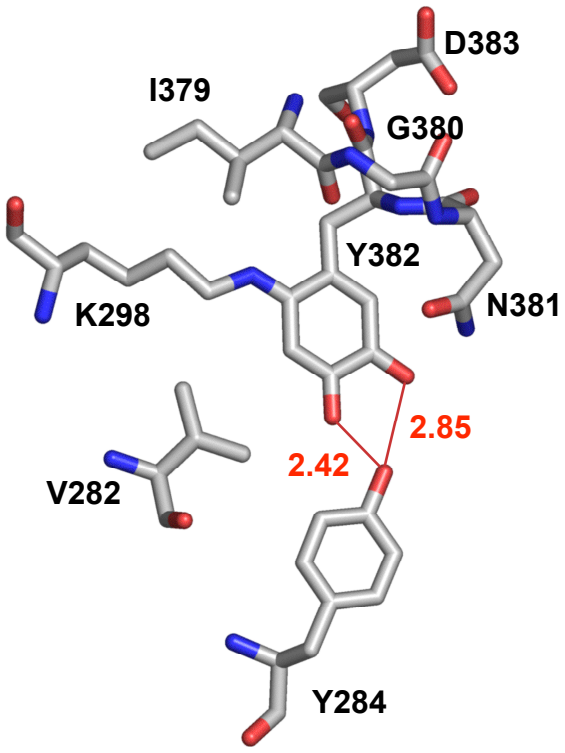

Figure 2.11 Hydrogen bonding interaction stabilizing the LTQ-like quinone as the tautomer, LTI (PDB code 2YX9 at 2.7 Å resolution).

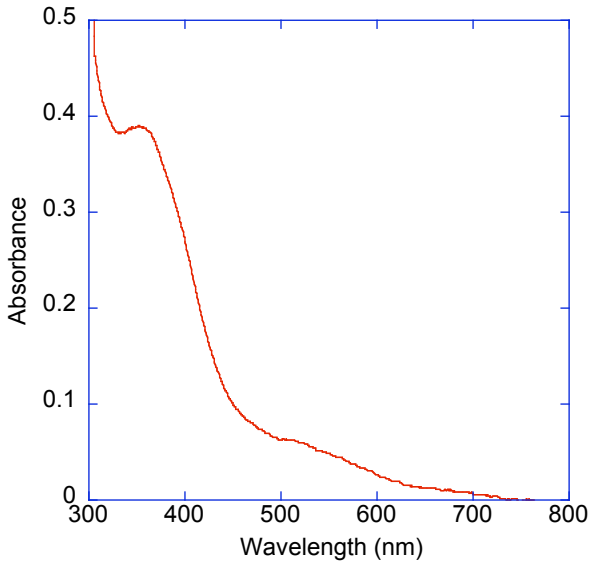

Figure 2.12 UV/vis spectrum of D298K in urea. 0.28 mM D298K in 0.1 M KPi pH 6.8 and 8 M urea. Incubation for 2 hr at 50°C.

450 nm (Figure 2.12). Interestingly, a very similar spectral change was observed upon copper removal from LOX isolated from bovine aorta in 6M urea where the 350 nm species was proposed to be derived from a covalent modification of the LTQ with an amino acid side chain.[89] It could be possible that the similar modification took place on the LTQ-like quinone in denatured D298K.

In order to define the role of the hydrogen bond between Tyr284 and the O4 of the quinone in D298K in stabilizing LTI over LTQ, we prepared a double mutant Y284F/D298K. The yields for the double mutants are shown in Table 2.2. The Y284F/D298K double mutant was positive for quinone-staining (Figure 2.13) but did

Table 2.2 Protein yields for double mutant holo protein growth and purification conditions.

Y284F/D298K	0.667
Y284F/M602K	1.764

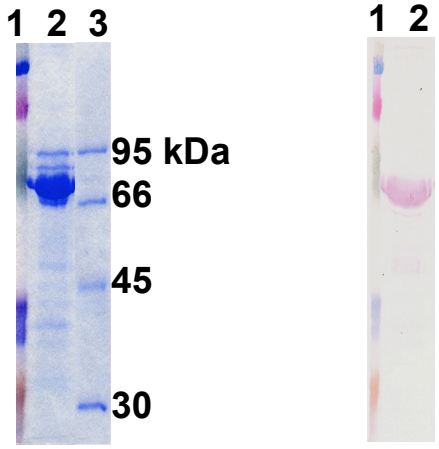

Figure 2.13 SDS-PAGE gel and PVDF-membranes of Y284F/D298K a) 10 % SDS-PAGE gel and b) PVDF-membrane stained for quinone detection. Lane 1: Kaleidoscope molecular marker, lane 2: Y284F/D298K-AGAO, lane 3: molecular marker.

not react with phenylethylamine and hydrazines as in the case of D298K. This was predicted as the quinone had been fixed in the inactive orientation due to the cross-link; therefore, the active carbonyl group at C5 is not accessible by nucleophiles. The UV/vis spectrum of Y284F/D298K has a broad absorbance at 504 nm very similar to the LTQ cofactor (Figure 2.14).[1] This red-shift compared to the quinone in D298K would be expected if the LTQ tautomer dominated the equilibrium. Further characterization of this mutant was not possible due to the instability of the quinone, which readily formed a 350 nm species similar to that seen in urea denaturation of D298K discussed above. We were only able to prepare the holo form of the double mutant by growing host cells (*E. coli*) in the presence of Cu^{2+}; any attempts to isolate and reconstitute apo-Y284F/D298K were unsuccessful. The UV/vis spectrum of the holo-Y284F/D298K was taken immediately after purification. These results suggest that the quinone in D298K is stabilized as LTI through a hydrogen bonding

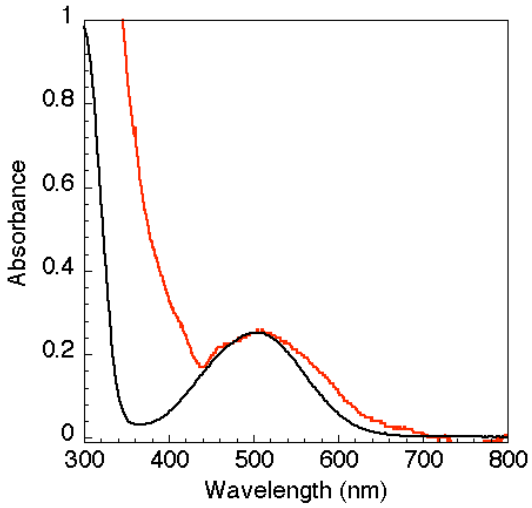

Figure 2.14 UV/vis spectra of an LTQ model compound and Y284F/D298K. [LTQ] = 1.7 mM, [Y284FD298K] = 0.1 mM in 50 mM HEPES buffer, pH 6.8. —LTQ model — Y284F/D298K.

interaction with Tyr284 and such an interaction must be absent for the LTQ cofactor in LOX.

Biogenesis and UV/vis Spectroscopic Properties of D298C

In order to determine if a Cys side chain at D298 position could trap the DPQ intermediate, the D298C mutant was prepared. The reaction of apo D298C with $CuSO_4$ did not appear to produce a quinone from the UV/vis spectrum (Figure 2.15 a). A cysteinyldopa quinone would be expected to show a broad quinone peak around

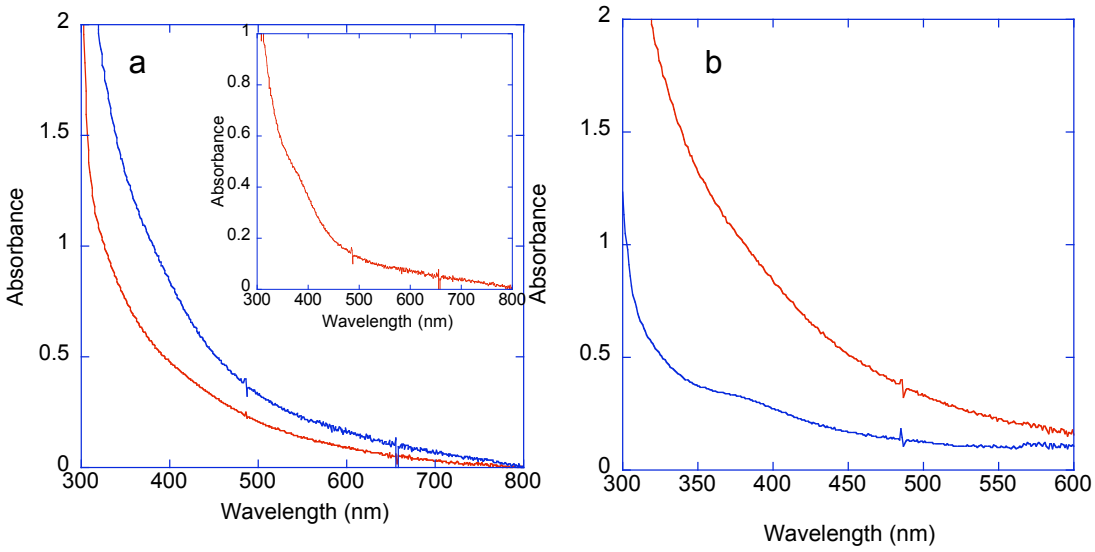

Figure 2.15 UV/vis spectra of D298C a) —apo D298C and —holo D298C. Final concentrations were 0.1 mM D298C, 50 mM HEPES pH 6.8 and 0.5 mM $CuSO_4$ (holo only). The insert shows the difference spectra of holo-apo D298C. b) Holo D298C with (—) and without (—) reaction with 2 eq. $NaIO_4$ in 6 M urea.

450 to 500 nm as amino- and indolquinones.[1,93,94] This is not unexpected as the formation of a 1,6-crosslink to DPQ most likely results in a reduced catechol species as observed in the mechanism of melanin formation.[84] In order to determine whether a catechol species was formed, the reaction product was tested for redox activity by

reacting it with 2 eq. $NaIO_4$ in the presence of 6 M urea (Figure 2.15 b). Again, the spectral features of a quinone were not observed, indicating that a catechol was also not formed from the reaction. The increase in absorbance of the holo species in comparison to the apo species is likely the result of baseline drift due to protein precipitation. It is likely that the DPQ is not accessible by the SH of the cysteine or that DPQ was not formed at all. If DPQ was not formed and the Tyr precursor remained, there may be some conformational change in the protein by the incorporation of the cysteine residue. The initial steps of the biogenesis reaction occur at the copper binding site. The cysteine residue is away from the copper binding site and should not directly inhibit the initial steps of biogenesis; thus, DPQ should be formed unless some change in the conformation of the copper binding site occurred. Further investigation of this mutant was not done.

Biogenesis of LTI in D298K.

In WT-AGAO, the formation of TPQ occurs directly from the Cu^{2+}-bound tyrosine precursor where no spectroscopic intermediates have been observed. The formation of TPQ is rapid and complete within a couple of minutes under saturating concentrations of O_2 at pH 6.8. The time course of LTI formation in D298K at pH 6.8 was similarly followed by UV/vis spectroscopy (Figure 2.16). The apo-D298K was prepared by the standard procedure used to prepare apo-WT.[12,29] The apo-D298K was mixed with a Cu^{2+} solution at saturating concentrations of O_2 (1.1 mM at 30 °C). The initial reaction did not produce LTI, but instead produced a pink species with a

broad visible absorbance centered at ~500 nm. The ~500 nm pink species formed followed by its absorption slowly decreasing (~4 hours to completion) concomitant with the increase in absorbances at 454 nm and 320 nm to give a final spectrum that

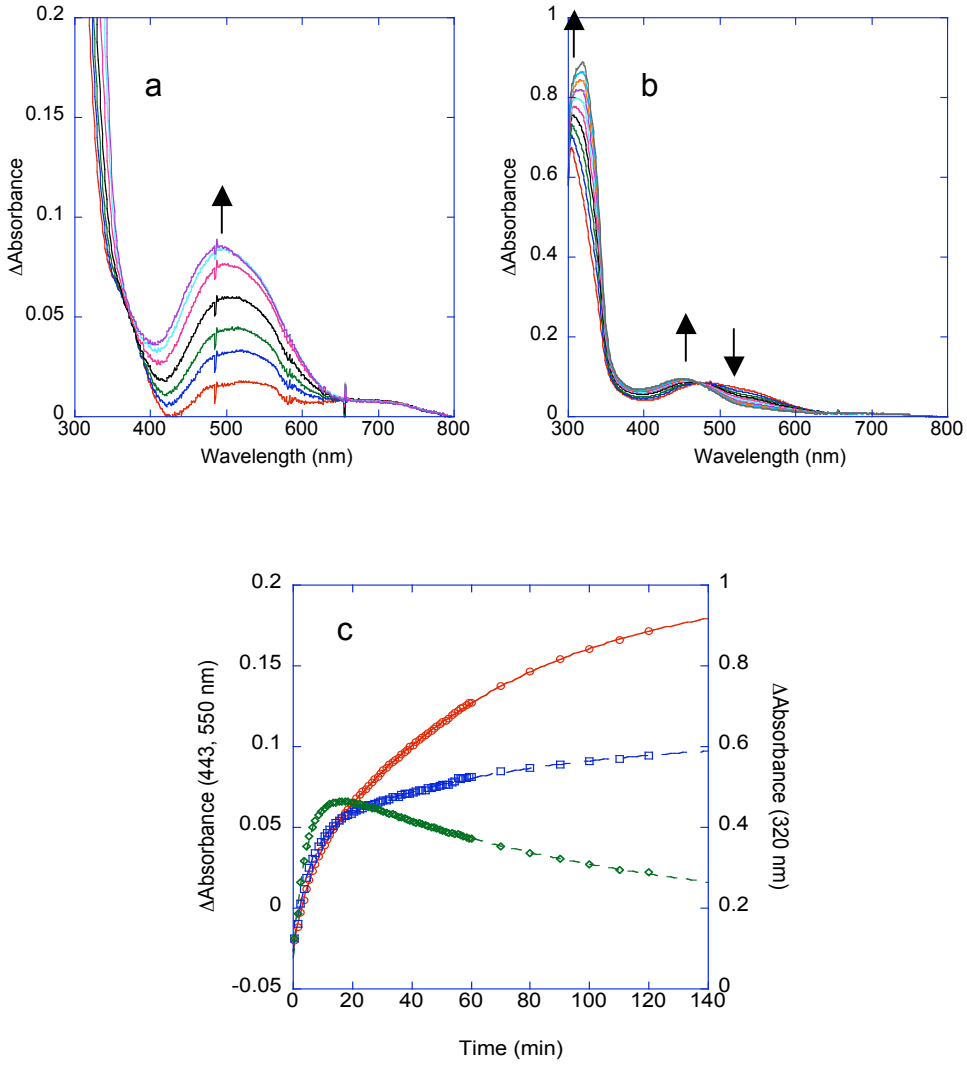

Figure 2.16 UV/vis spectral changes after addition of Cu^{2+} to apo-D298K under O_2-saturating conditions ([O_2] = 1.1 mM) at 30 °C. a) First phase: absorption spectra were recorded at 2.5, 3.5, 4.5, 6.5, 10.5, 15.5, and 20.5 min. b) Second phase: absorption spectra were recorded at 30.5, 40.5, 50.5, 60, 70, 80, 90, 100, 110, and 120 min. Arrows indicate the direction of the spectral changes. c) Absorbance changes at 320 (○), 454 (□), 550 nm (◇) were plotted against time and fitted to sum of two exponentials by the non-linear least-squares method (see Table 2.2).

was identical to that of LTI in holo-D298K described above. An isosbestic point at 473 nm was observed for the conversion of the ~500 nm species to the 454 nm species. The rate constant of formation of the 500-nm species is 0.22 min^{-1} at pH 6.8 in concentrated O_2, and this rate is about 1/6 of that of TPQ biogenesis in WT (1.50 min^{-1}).[68] The 500-nm intermediate could be either TPQ, which reacts with the lysine side-chain to form the cross-link, or it could be an LTQ-like quinone that slowly converts to the LTI tautomer (Scheme 2.3). In both of these cases, there is an O_2-

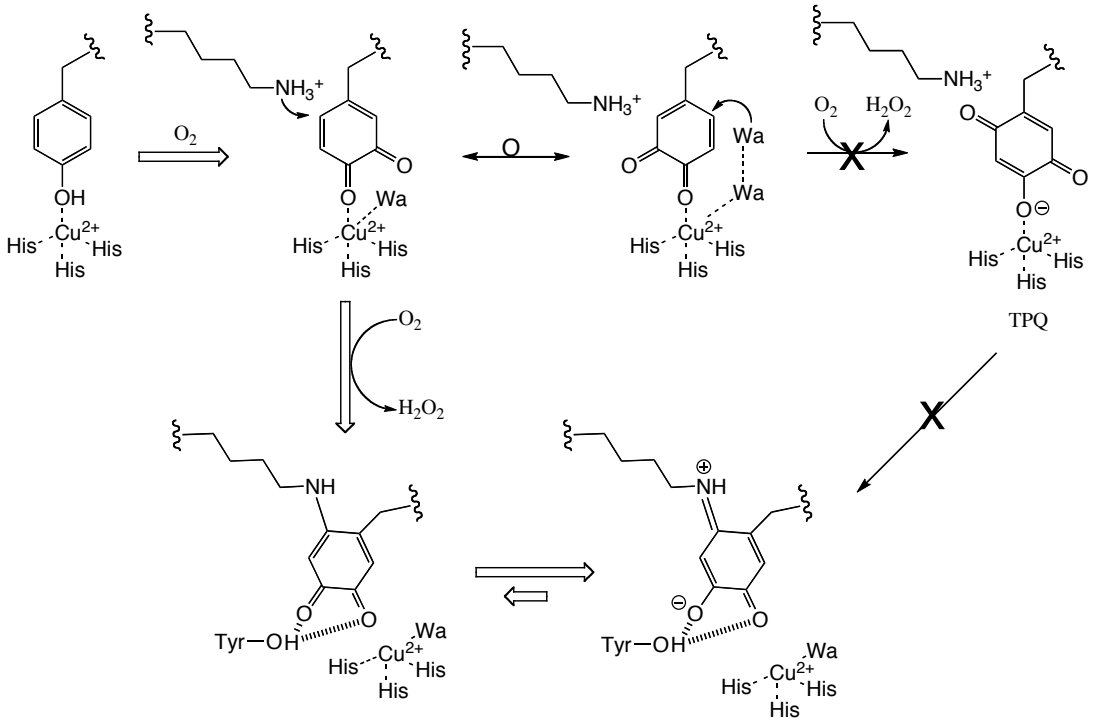

Scheme 2.3 Possible mechanisms for LTI formation in D298K.

dependent step (formation of the 500-nm species) and O_2-independent step (formation of LTI from the 500-nm species). When the biogenesis reaction was performed at atmospheric O_2 concentrations (225 μM at 30 °C), the rate of formation of the 500-nm species decreased to 0.05 min^{-1}, but the rate of the formation of LTI was

unchanged versus saturated O_2 (Table 2.3). This is consistent with both of the possible mechanisms for the formation of LTI from the 500-nm species. If the 500 nm species was an LTQ-like quinine, these results would suggest that the rate-limiting step in the biogenesis of the 500-nm species in D298K versus TPQ in WT is the same. This is consistent with TPQ biogenesis in D298A where the removal of the carboxyl side chain of Asp298 has only a minimal effect on the rate of biogenesis of TPQ (40% reduction).[46]

Table 2.3 Rates of Biogenesis of D298K

$[O_2]$	first phase (min^{-1})	second phase (min^{-1})
1.1 mM	0.2212 ± 0.0028	0.0093 ± 0.0005
225 μM	0.050 ± 0.006	0.0111 ± 0.004

The 500-nm intermediate is not reactive towards hydrazines, suggesting that it is not TPQ. This result rules out the mechanism where the ε-amino side chain reacts with C2 carbonyl of TPQ to form the iminoquinone. This was expected as the C2 carbonyl of TPQ is intrinsically unreactive.[35,51] The cross-link has most likely already formed in the 500-nm species from the reaction of the amine with dopaquinone. Based on our observation that the LTI tautomer is stabilized by a hydrogen bonding interaction with Tyr284, we propose that the slow conversion of the 500-nm species to LTI is controlled by a subtle conformational change in the active site where LTI is the thermodynamic product in D298K.

In order to gain further insight into the identity of the 500-nm species observed at the early stage of the biogenesis, the time course of the biogenesis of the

quinone in D298K was followed by resonance Raman spectroscopy ([O_2] = 225 μM) (Figure 2.17). Under the reaction conditions used for resonance Raman spectroscopy, the rate of the biogenesis was significantly slower (most likely due to high concentration of enzyme (1 mM) used where O_2 becomes a limiting reagent), but the overall trends of the spectral change were similar to what was observed in the UV/vis spectroscopy experiment. During the initial phase of the biogenesis, peaks at 1186, 1364, 1393, 1554, 1688 cm^{-1} appeared where these species were associated with the 500-nm species (Figure 2.17). As the absorbance at ~500 nm decays, the peaks at 1186, 1554, and 1688 cm^{-1} then disappeared; and therefore, they are likely derived solely from the 500-nm intermediate. The peaks observed during the biogenesis at 1364 and 1393 cm^{-1} are very close in energy to those associated with holo-D298K (at 1361 and 1391 cm^{-1}, Figure 2.17) but the observed ratio of the two peaks is different: holo, 1361<1391; intermediate, 1364>1393. One interpretation of the resonance Raman spectrum at 6 hr (holo-D298K) is that at 514.5 nm we are selectively probing the 500-nm species over LTI and are therefore observing a small amount of the 500-nm species that remains in equilibrium with LTI. This would explain the decrease in intensity of the features over time course of the reaction.

a

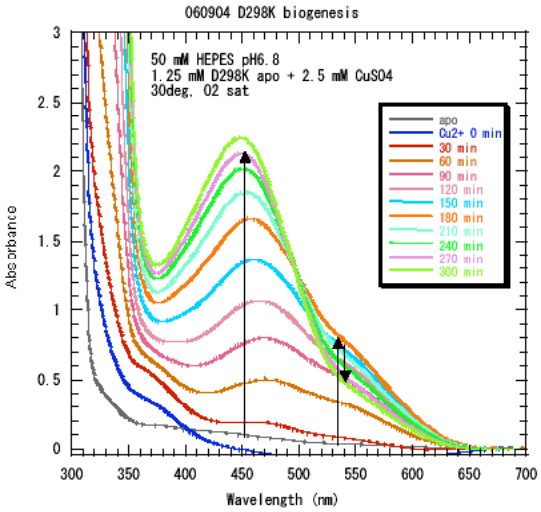

b

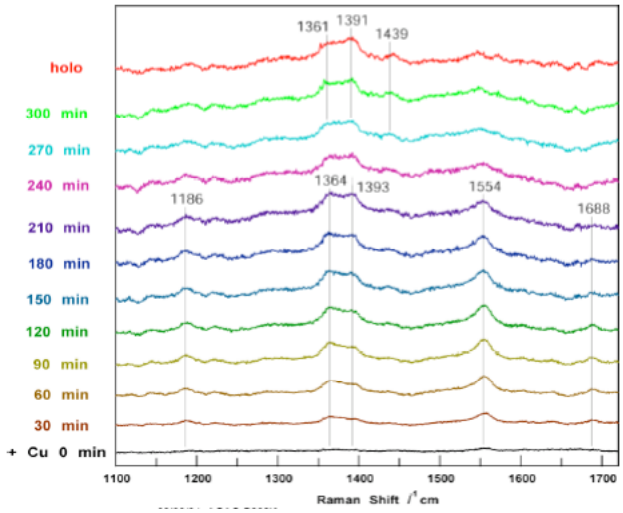

Figure 2.17 UV/vis and resonance Raman spectra of the time course of D298K biogenesis. a) UV-vis spectral change following incubation of apo-D298K (1.25 mM) and Cu^{2+} (2.5 mM) in 50 mM HEPES buffer at pH 6.8 at 30°C. b) Resonance Raman spectral change. Accumulation time = 1 sec x 100 scans x 1 set at room temperature, references are toluene and acetone.

Figure 2.18 shows the comparison of D298K-500-nm species (c), holo-D298K (b) and WT-AGAO (TPQ) (a) in comparison to model compounds of LTQ (d) and monoanionic LTI (e). The D298K-500-nm species is clearly neither TPQ nor LTI, thereby making a biogenesis mechanism where TPQ is an intermediate less

likely. The 500-nm species is very similar to the LTQ model compound, but does have some differences. Most likely the protein environment is modulating the electronic structure of the quinone in D298K-500-nm species, thereby making it difficult to compare directly to LTQ in solution.

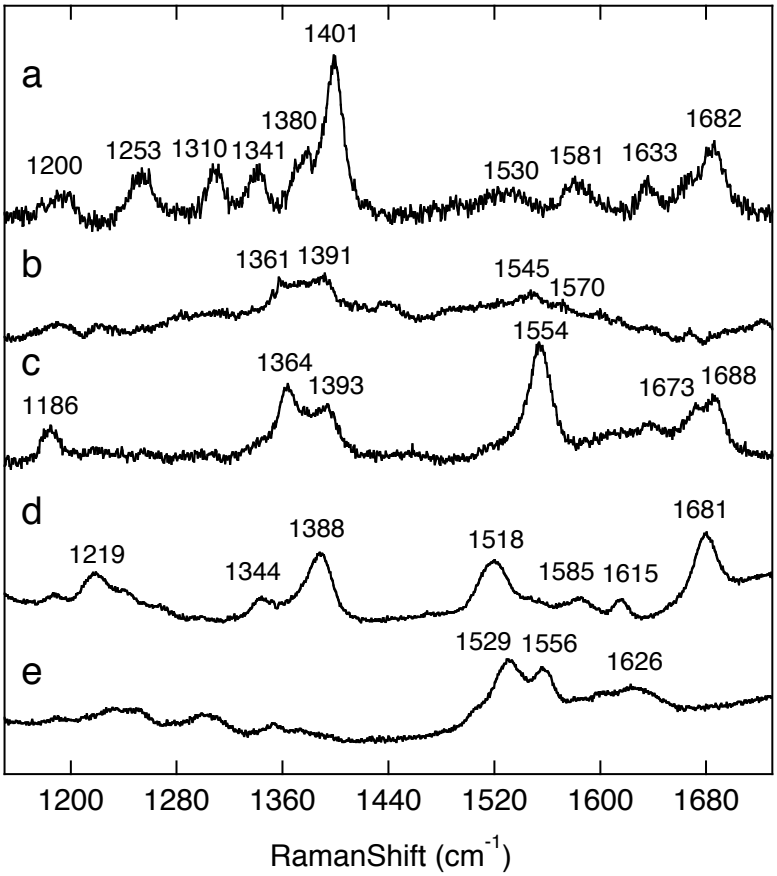

Figure 2.18 Resonance Raman spectra of holo-D298K, the 500-nm intermediate seen in the biogenesis of D298K, TPQ in WT, LTQ model compound in 50 mM HEPES, pH 6.8, and mono-anionic form of LTI model compound in 0.1 M KOH. a) WT (TPQ), b) holo-D298K, c) the 500-nm intermediate, d) LTQ model compound, e) mono-anionic form of LTI model compound. Excitation wavelength = 514.5 nm

Conclusion

In the present study we were able to effectively trap the DPQ intermediate by incorporating Lys at the D298 position (D298K). This strongly supports the intermediacy of DPQ in the biogenesis of TPQ and suggests that DPQ is, likely, also on the pathway of LTQ formation. The formation of an LTQ-like quinone in D298K showed that the proposed dopaquinone intermediate (Figure 1.2 b) has mobility and can leave the Cu^{2+} site and swing into the active site wedge to react with Lys298. The quinone in D298K is in the flipped orientation, making it inactive. An attempt was made to trap the dopaquinone with a lysine residue incorporated at position 602 in AGAO (M602K). Met602 is on the opposite side of the active site compared to Asp298 and, should a cross-linked quinone be formed, it would be expected to be in an active conformation. However, the holo-M602K contained TPQ where no such cross-link formed. The most likely explanation for this is that the lysine (Lys602) is not accessible to the C2 position of the flipped dopaquinone, and thereby cannot compete effectively with hydration. An attempt was also made to trap the dopaquinone with a cysteine residue in the D298 position. Cysteine has been known to add to dopaquinones in a 1,6-addition as opposed to the 1,4-addition in D298K. In that study, it appeared that the protein precipitated during biogenesis and a cross-link was not formed. It is likely that either DPQ was not formed or that the DPQ is not accessible by the SH group on cysteine.

An important observation from this study is the absence of any detectable amount of TPQ in D298K. The active site of AGAO is arranged to optimize the 1,4-

addition of copper associated water to dopaquinone intermediate to form TPQ. A recent model study suggested that an appropriately placed Cu^{2+} ion can catalyze the 1,4-addition of water to dopaquinone.[95] The mutation site to incorporate the lysine residue in D298K is away from the copper site and it is less likely that the environment around copper is significantly altered when compared to WT. The rate of formation of the 500-nm species is close to that of WT and D298K suggesting that initial steps of biogenesis, activation of Tyr382 and subsequent oxidation to dopaquinone, are not perturbed in D298K. However, in D298K the dopaquinone intermediate is selectively trapped by the amino group of Lys298 to form LTI. This suggests that 1,4-addition of the ε-nitrogen of Lys298 to the dopaquinone intermediate in CAO is much more efficient than the addition of copper associated water, even though the latter is the natural reaction. A similar phenomenon was observed in the model study of the LTQ biogenesis, where dopaquinone can be trapped efficiently by secondary alkyl amines to form LTQ, but not by solvent water to form TPQ.[1] In this model study, primary amines reacted rapidly with the carbonyl groups of dopaquinone in preference to 1,4-addition. That such chemistry did not occur in D298K and is also not seen in LOX strongly suggests that the positioning of the reactive amine in the active site is key in controlling the chemistry (1,4- vs. 1,2-addition and hydration vs. amination).

The X-ray crystal structure of D298K (Figure 2.10) suggested a strong hydrogen bonding interaction (2.4 Å) between O4 of the quinone and the conserved Tyr284. This hydrogen bond has been shown to stabilize the quinone as the tautomer,

lysyl tyrosyl iminoquinone (LTI). Such an interaction is likely absent in LOX. Tautomers are proposed as opposed to resonance forms based on the UV/vis data in which the absorbance spectra of LTQ is red-shifted by ~50 nm from that of LTI. The double mutant Y284F/D298K was prepared to eliminate the hydrogen bond between the quinone and Tyr284. The UV/vis spectrum of Y284F/D298K has a broad absorbance at 504 nm very similar to the LTQ cofactor (Figure 2.13).[1] These results suggest that the quinone in D298K is stabilized as LTI through a hydrogen bonding interaction with Tyr284 and such an interaction must be absent for the LTQ cofactor in LOX.

Chapter 3: pH Dependency of UV/vis Spectra and Rate of Biogenesis of an LTQ-like Cofactor in D298K

Introduction

As discussed in chapter 2, the biogenesis of an LTQ-like cofactor occurred selectively in D298K by the DPQ intermediate reaction with a 1,4-addition of a lysine side chain, as opposed to the copper bound water molecule as occurs in the natural reaction. This finding is consistent with results shown for the model study in which the 1,4-addition of *N*-methyl-*n*-butylamine to an *in situ* generated DPQ at pH 7.2 forms an LTQ-like cofactor exclusively.[1] In order to determine if hydration can compete with amination at lower or higher pHs and to determine how the active site environments of CAO and LOX contribute to the formation of their corresponding cofactors, the pH dependency of the rate of biogenesis in D298K was examined.

In HPAO, a study on the pH-dependency of cofactor formation provided information about the protonation states of the residues in the active site that participate in the biogenesis reaction. The pH-dependency of the rate of biogenesis in HPAO showed a sigmoidal curve with a single pK_a of 8.45 (Figure 3.1).[69] The pK_a was assigned to the precursor tyrosine of TPQ even though the typical pK_a for the hydroxyl group of tyrosine residue in solution is ~10. Similarly reduced pK_as for tyrosine residues have been observed in other proteins including glutathione S-transferase (8.3-8.5), human aldose reductase (8.25), and Fe-containing superoxide dismutase (8.5).[96-98]

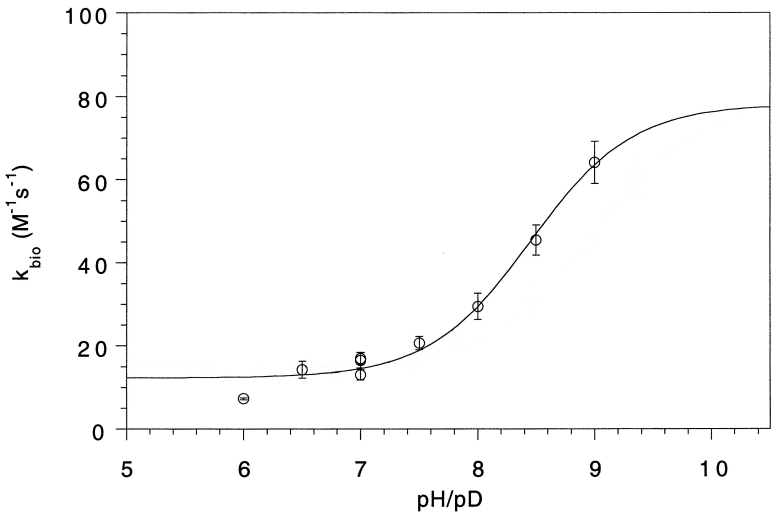

Figure 3.1 Effect of pH on the rate of TPQ biogenesis in WT HPAO. k_{bio} was determined in buffers varying in pH (○). The data were fit to a function with differing rates at low and high pH. The value is equal to 12 M^{-1} s^{-1} at low pH and 78 M^{-1} s^{-1} at high pH, with a pK_a of 8.45. Adapted with permission from Schwartz, B.; Dove, J. E.; Klinman, J. P. *Biochemistry* **2000**, *39*, 3699-3707. Copyright 2000 American Chemical Society.

In HPAO two UV-vis spectroscopically distinguishable species have been observed at ~380 nm and ~350 and were proposed to be tyrosine-copper charge transfer complexes.[69,70] The species at ~380 nm in HPAO, grew in over ~3 min and decayed at about the same rate as the formation of TPQ.[70] The ~ 380 nm species formed and decayed at the same rates when Cu^{2+} was added to apo enzyme anaerobically, indicating that its formation was not O_2-dependent. Additionally, mutagenesis of the active site residues immediately flanking the precursor tyrosine residue, N404D and E406Q respectively, slowed the rate of TPQ formation, but the rate of formation and decay of the ~380 nm species remained the same, suggesting that the two are not kinetically coupled. Zn^{2+} is known to bind tightly to the active site of apo protein and inhibit the formation of TPQ. The ~380 nm species was observed when Zn^{2+} was pre-bound in the active site of the protein and Cu^{2+} was subsequently

added, as well as when excess Cu^{2+} was added to holo-protein. Taken together, these results suggest that the formation of the ~380 nm species is not the Cu^{2+} - precursor Tyr (Tyr405) charge-transfer complex and that it is likely resulting from a site away from the active site.

Anaerobic formation and decay of the ~380 nm species in HPAO followed by aeration of the sample lead to the formation of a new species absorbing at ~350 nm.[70] The decay of the ~350 nm species occurs concomitantly with the formation of TPQ. This species was assigned to a Cu(II) – precursor Tyr (Tyr405) charge-transfer complex leading to the formation of TPQ. The ~350 nm species grew in to a greater extent at pH 8.6 than at pH 7.0.[69] The increased absorbance could be due to either a higher extinction coefficient for the deprotonated versus protonated tyrosine or due to a more favorable pre-equilibrium between the ligated and unligated precursor tyrosine.

Neither the ~ 380 nm nor the ~ 350 nm species have been observed in the biogenesis of TPQ in the wild-type AGAO.[64] The rate of TPQ biogenesis in AGAO (1.5 ± 0.2 min^{-1})[65] is ~19-times faster than that in HPAO (0.08 ± 0.03 min^{-1}).[69] In order to characterize the proposed charge-transfer species in AGAO, the UV-vis spectroscopic studies of the cofactor biogenesis in D298K were conducted, where the rate of the formation of the LTQ-like quinone (0.05 ± 0.006 min^{-1}) is 30-fold slower than that of TPQ formation in the wild-type at pH 6.8 (Chapter 2).

Materials and Methods

Materials

See the Materials section in Chapter 2 for a more comprehensive list of materials. HEPBS buffer was purchased from Sigma-Aldrich. Pyrogallol and $ZnSO_4$ were purchased from Acros. The biogenesis of WT and D298K was monitored by UV/vis spectroscopy on an Agilent HP 8453 photo diode array UV/vis spectrophotometer equipped with a temperature-controlled cell holder at 30 ± 0.2 °C (path length of 1 cm). The spike in the spectra at 483 nm is an artifact of the instrument. The biogenesis was also monitored by stopped-flow UV/vis spectroscopy using a stopped-flow spectophotometer (SX.18MV-R) equipped with a diode array accessory from Applied Photophysics.

UV/vis spectroscopy

The biogenesis study of WT and D298K was performed as previously described in chapter 2. Protein samples (25-50 μL) were dialyzed in an Amicon concentrator five times against 500 μL of the appropriate buffer. Buffers of 100 mM were used for dialysis. From pH 6.0 to 6.5, MES buffer was used. HEPES buffer was used for pH values from 6.8 to 7.8. HEPBS buffer was used for pHs 8.0 to 9.0 and CHES buffer was used for pHs 9.2 to 9.5. CHES buffer was made fresh before each use. WT and D298K biogenesis reactions were carried out in air. The spectra for the WT samples were taken every 10 sec for 10 min and thereafter, every 1 min for 20 min in air. D298K samples were aerobically incubated with 1 mM $CuSO_4$ and

with 400 mM $CuSO_4$ for comparison with stopped-flow results. The rates of formation of the 500-nm and 454-nm chromophores were determined spectrophotometrically in a reaction mixture containing 0.05 mM apo-D298K and 0.25 mM $CuSO_4$ in 50 mM buffer at the appropriate pH. The spectra for the D298K samples were taken every 10 sec for 10 min, every 2 min for 50 min, and every 10 min to 1 hr. The final concentrations of enzyme were determined spectrophotometrically by using extinction coefficients at 280 nm of 13.2 for 1% (w/v) solutions of the holo form of AGAO.[3]

Stopped-flow UV/vis Spectroscopy

WT and D298K samples (150-250 μL) were dialyzed in an Amicon concentrator five times against 500 μL of the appropriate buffer. Buffer (100 mM) was used for dialysis. From pH 6.1 to 6.5, MES buffer was used. HEPES buffer was used for pH values from 6.8 to 7.8. HEPBS buffer was used for pH values from 8.0 to 9.0 and CHES buffer was used for pH values from 9.2 to 9.5. CHES buffer was made fresh before each use. The enzyme was diluted to approximately 0.2 mM and initial concentrations of enzyme were determined spectrophotometrically by using extinction coefficients at 280 nm of 12.3 for 1% (w/v) solutions of the apo form of AGAO.[3] The instrument was blanked with H_2O and rinsed with the appropriate buffer (injection port A) or 400 mM $CuSO_4$ (injection port B). Sample was loaded following the buffer into injection port A. Sample and CuSO4 were injected

simultaneously in equal volumes to a final volume of ~100 μL. Up to 1600 spectra were taken from 200 to 712 nm over ~20 min.

UV/vis Absorption Spectrum of the Biogenesis Reaction at t = 0

UV/vis spectra were taken of enzyme samples diluted to 0.1 mM (apo sample) at each pH. Samples were degassed with argon using a set-up similar to the one used for oxygenating samples in chapter 2. Argon was passed through an alkaline pyrogallol solution prior to purging the cuvette and enzyme solution for 15 min. A balloon was filled and degassed; 1 mM $CuSO_4$ or $ZnSO_4$ was added to the cuvette by a gas tight syringe. UV/vis spectra were taken immediately, 5 min and 10 min after mixing. The cuvette was then opened to air to expose the contents to O_2 and allow biogenesis to take place. After at least 30 min, the concentration of the sample was determined spectrophotometrically by using the extinction coefficient at 280 nm of 13.2 for 1% (w/v) solutions of the holo form of AGAO.[3]

UV/vis Spectral Change Following the Addition of Metal to Holo-AGAO

Holo-WT and holo-D298K were prepared by incubation with an excess (four molar equivalents) of Cu^{2+} and the corresponding apo-proteins at pH 6.8 in 100 mM HEPES or pH 8.5 in 100 mM HEPBS. The holo samples were dialyzed in the same buffer in an Amicon concentrator to remove excess Cu^{2+}. The protein concentration was adjusted to ~ 0.2 mM and UV/vis spectra were recorded. An equal volume of 1 mM $CuSO_4$ was then added to each sample and UV/vis spectra were taken immediately, 5 min and 10 min after mixing. The concentrations of the samples were

determined spectrophotometrically by using extinction coefficients at 280 nm of 13.2 for 1% (w/v) solutions of the holo form of AGAO.[3] Zn^{2+}-containing WT and D298K samples at pH 6.8 and 8.5 were dialyzed to remove excess Zn^{2+}. The protein concentration was adjusted to ~ 0.2 mM. A spectrum was taken and an equal volume of 1mM $CuSO_4$ was added to the sample. Spectra were taken immediately, 5 min and 10 min after mixing. The concentrations of the samples were determined spectrophotometrically by using extinction coefficients at 280 nm of 13.2 for 1% (w/v) solutions of the holo form of AGAO.[3] Apo-WT and apo-D298K samples were incubated aerobically with 1 mM $ZnSO_4$ pH 6.8 and 8.5 for 1 hour. The sample was dialyzed to remove excess Zn^{2+} and a spectrum was taken. Samples were further dialyzed in the presence of 10 mM EDTA and the appropriate buffer. Dialysis to remove excess EDTA was done prior to taking a spectrum of each sample. The concentration of the sample was adjusted to 0.1 mM and an equal volume of 1 mM $CuSO_4$ was added to each sample. Spectra were taken immediately, 5 min and 10 min after mixing. The concentration of the samples were determined spectrophotometrically by using extinction coefficients at 280 nm of 12.3 for 1% (w/v) solutions of the apo form of AGAO.[3]

Data Analysis

The UV/vis spectra were baseline corrected at 800 nm and normalized to a concentration of 0.1 mM enzyme. The observed rate constants (k_{obs}) for formation and decay of 500 nm chromophore and formation of the 454 nm chromophore were

determined by fitting absorbance changes at 320 nm, 454 nm and 550 nm plotted versus time by least square fitting to the sum of two single exponentials (Equation 3.1) using Kaleidagraph (Synergy software). The plot of rate versus pH for the first phase was fit to equation 3.2 and the plot for the second phase was fit to equations 3.2 (sigmoidal curve) and 3.3 using (bell shaped curve) Kaleidagraph (Synergy software). Average values of at least two independent measurements are taken.

$$\text{rate} = \text{Abs}_1 * 10^{(-k_1 * t)} + \text{Abs}_2 * 10^{(-k_2 * t)} + \text{Abs}_3 \quad (3.1)$$

$$\text{rate} = k_{\max} / (1 + 10^{(\text{p}K_\text{a} - \text{pH})}) \quad (3.2)$$

$$\text{rate} = k_{\max} / (1 + 10^{(\text{p}K_{\text{a1}} - \text{pH})} + 10^{(\text{pH} - \text{p}K_{\text{a2}})}) \quad (3.3)$$

Results

pH-Dependence of the UV-vis Spectra of the LTQ-like Quinone and LTI Biogenesis in D298K

In order to determine the effect of pH on the biogenesis of the LTQ-like cofactor in D298K, the time-course of biogenesis was followed by UV/vis spectroscopy at various pHs from 6.8 to 9.5 under aerobic conditions. Buffer outside this pH range could not be used due to protein precipitation/denaturation. Over the pH range studied, similar spectroscopic changes were observed as those of the biogenesis at pH 6.8, described in chapter 2, in which the peak at ~500 nm, proposed to be an LTQ-like quinone, forms quickly followed by its slow decay and an increase of absorbencies at ~450 nm and ~320 nm from LTI. Although the overall spectral

changes are consistent, there is a shift in the λ_{max} of the ~500 nm species across the pH range. At pH 6.8, the λ_{max} is ~496 nm (Figure 2.16 a), which shifts to ~502 nm from pH 7.5 to 8.7 (Figure 3.2 a) but shifts to ~518 nm at pH 9.5 (Figure 3.3 a). This shift in λ_{max}, most likely, corresponds to the amount of LTI present at the end of the

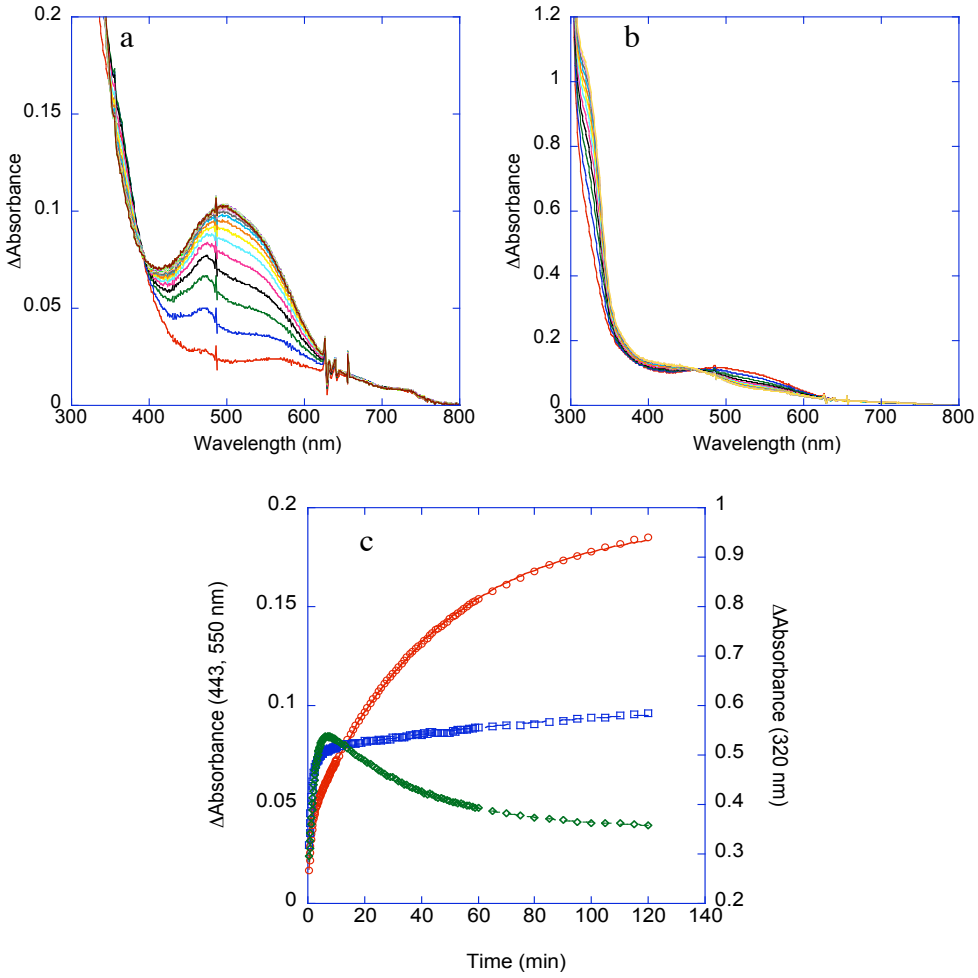

Figure 3.2 D298K biogenesis at pH 8.4. UV/vis spectral changes after the addition of Cu^{2+} to apo-D298K in air at pH 8.4 (final concentrations: 50 mM HEPBS, 50 μM D298K, 250 μM $CuSO_4$). Data were normalized to 0.1 mM D298K and the spectra of apo D298K at the corresponding pH was subtracted a) First phase: absorption spectra were recorded at 0.5, 1, 1.5, 2, …10 min. b) Second phase: absorption spectra were recorded at 10, 20, 30,…120 min. c) Absorbance changes at 320 (○), 454 (□), 550 nm (◇) were plotted against time and fitted to sum of two exponentials by the non-linear least-squares method.

first phase. The neutral form of the LTQ model compound in solution that is fully solvated, shows a λ_{max} of 504 nm and when the butylamino side chain is deprotonated, the λ_{max} shifts to 450 nm where the pK_a was determined to be 10.33 ± 0.07.[1] The methylation of the nitrogen of the butylamino side chain resulted in 20 nm red-shift in

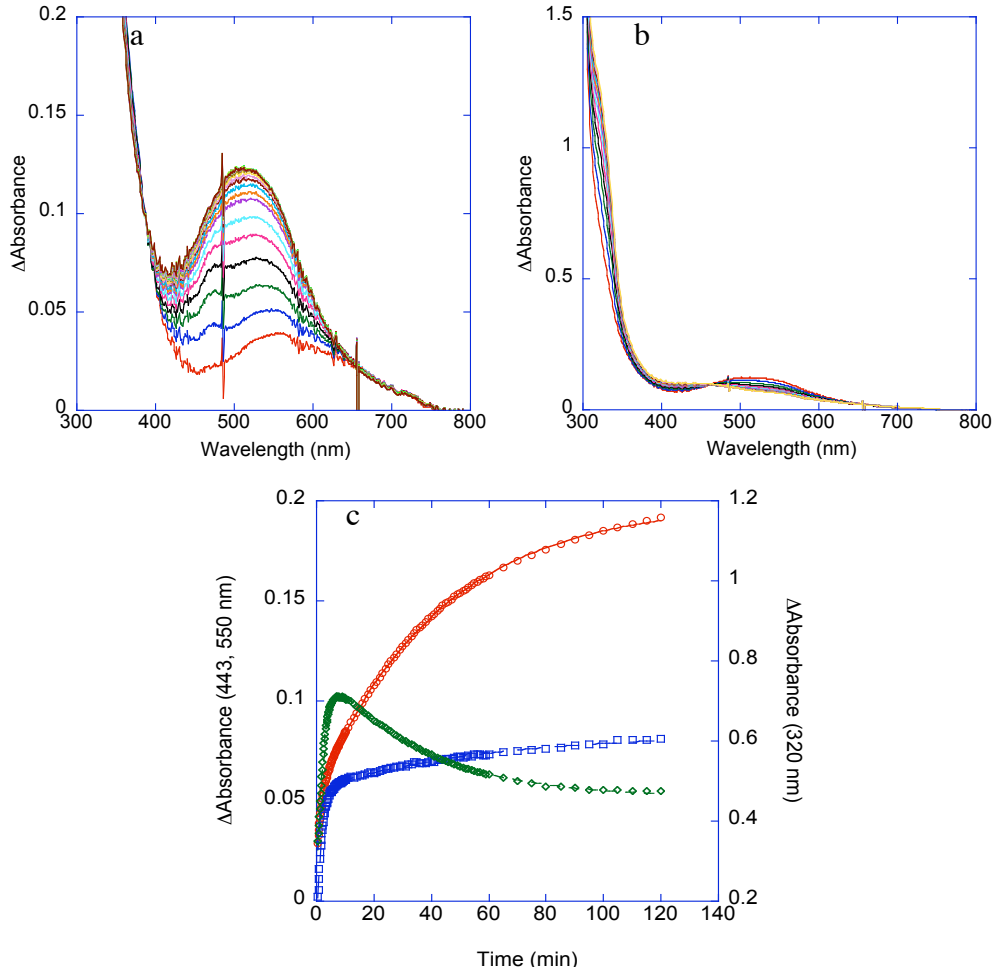

Figure 3.3 D298K biogenesis at pH 9.5. UV/vis spectral changes after the addition of Cu^{2+} to apo-D298K in air at pH 9.5 (final concentrations: 50 mM CHES, 50 μM D298K, 250 μM $CuSO_4$). Data were normalized to 0.1 mM D298K and the spectra of apo D298K at the corresponding pH was subtracted a) First phase: absorption spectra were recorded at 0.5, 1, 1.5, 2,…10 min. b) Second phase: absorption spectra were recorded at 10, 20, 30,…120 min. c) Absorbance changes at 320 (○), 454 (□), 550 nm (◇) were plotted against time and fitted to sum of two exponentials by the non-linear least-squares method.

λ_{max}.[1] The origin of the 20 nm red-shift observed for the LTQ-like quinone in D298K at pH 9.5 is not clear. At all pHs the conversion of the ~500 nm species to the ~450 nm species occurs with an isosbestic point at ~465 nm, and the peak ~450 nm does not appear to be shifted at any pH under the reaction conditions (Figures 3.2 and 3.3 panel b). It should be noted that, within the pH range studied, the formation of TPQ was not observed as in the case of the model study.[1] This result suggests that, in general, the amination of the DPQ intermediate is more efficient than hydration.

pH-Dependence on Rate for the Biogenesis of an LTQ-like Cofactor in D298K

The pH-rate profile for the biogenesis of the LTQ-like species should provide information about the protonation states of titratable active site residues that are involved in the cofactor biogenesis. The effect of pH on the rate of biogenesis of the first phase yielded a bell shaped curve with optimal pH of ~8.8 with the maximum

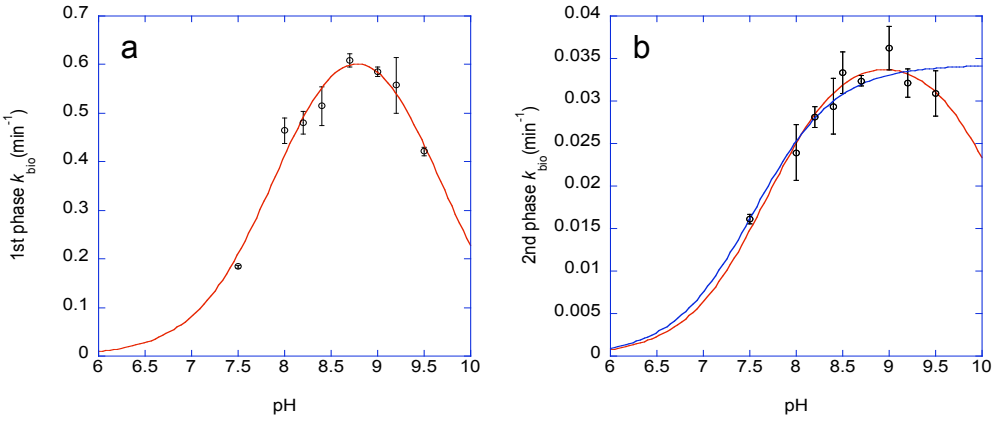

Figure 3.4 Effect of pH on the rate of biogenesis of the 505 nm (a) and 450 nm (b) species in D298K were determined in buffers of varying pH. Rates were determined from plots of Δabsorbance at 550 nm or 443 nm, respectively, vs. time, like those seen in Figures 3.3 and 3.4 panels c. The data were fit to least-square curves using equations —3.2 and —3.3.

rate of 0.77 ± 0.063 min^{-1} under aerobic conditions (Figure 3.4 a). pK_a^1 of 7.93 ± 0.10 and pK_a^2 of 9.62 ± 0.13 were determined by the least-square fit analysis of data using equation 3.2. Similarly, the pH-profile of the second phase of biogenesis was also fit to equation 3.2, resulting in a bell shaped curve that was slightly broader than that of the first phase (Figure 3.4 b). The optimal pH for the second phase is ~8.9 with a maximum rate of 0.037 ± 0.002 min^{-1}, pK_as of 7.68 ± 0.086 and 10.23 ± 0.22, and an R^2 value of 0.945 were determined by the least-square curve fit analysis using equation 3.2. Alternatively, the pH-profile of the second phase was fit to equation 3.3 resulting in a sigmoidal curve (Figure 3.4 b). The optimal pH for the second phase with this fitting is above ~9.5 with a maximum rate of 0.034 ± 0.001 min^{-1}, a pK_a of 7.55 ± 0.093, and an R^2 value of 0.897. Although the curve fitting of equation 3.2 fits better to the data for the second phase, it is possible that the rate of the second phase plateaus and the slight decrease in observed rate is due to partial denaturation of the protein. Therefore, it is not possible to determine the accuracy of the pK_a of 10.23 due to the denaturation of the protein above pH 9.5.

The pK_a of 7.93, observed in the first phase of D298K biogenesis, is 0.5 pH unit-lower than the value reported for the wild-type of HPAO; it is most likely that the pK_a corresponds to the precursor tyrosine as well. The later pK_a of 9.62 has not been seen previously in CAOs. The active site of D298K lacks Lys or Arg residues, with pK_as of ~11-13, other than K298. However, the active site does contain several Tyr residues. Deprotonation of the residue responsible for the pK_a of 9.62 results in a slower rate of biogenesis of the LTQ-like cofactor in D298K. If the amino group of

K298 were being titrated and the rate of the reaction between deprotonated K298, and DPQ became rate limiting, a spectral feature for DPQ (λ_{max} ~ 380 nm)[99,100] should be apparent in the UV/vis spectra. Additionally, slowing the reaction between DPQ and K298 could allow for a competition between hydration and amination. However, at higher pHs, spectral features were not observed for the DPQ intermediate or TPQ; therefore, it is unlikely that K298 was being titrated. It is more likely that the pK_a was the result of an active site Tyr residue.

Examination of the active site of the D298K crystal structure shows four Tyr residues near the LTQ-like cofactor (Figure 3.5 a). However, upon closer inspection, it is apparent that the OH groups of two of the residues, Tyr296 and Tyr302, are pointing away from the cofactor and, most likely, are not involved in the biogenesis reaction (Figure 3.5 b).

Tyr296 and Tyr302 are both outside the wedge-shaped cavity in the active site of CAO.[7] The wedge-shaped cavity is formed by Val282 and Asn381 positioned on either side of TPQ. Additionally, Tyr284 appears to serve a role as a gate keeper, holding TPQ in the wedge so that it does not move out of the wedge and get trapped by Cu^{2+}. Mutation of the residue corresponding to Tyr284 in ECAO resulted in the TPQ being flipped and swung out of the wedge, decreasing the rate of catalysis ~ 50 fold.[101] D298 is positioned on the opposite side of TPQ from Tyr284. Mutation of this residue to Ala in ECAO resulted in the increased mobility of TPQ, thus decreasing the rate of catalysis.[15] Mutation to Glu in ECAO led to a decrease in the mobility of

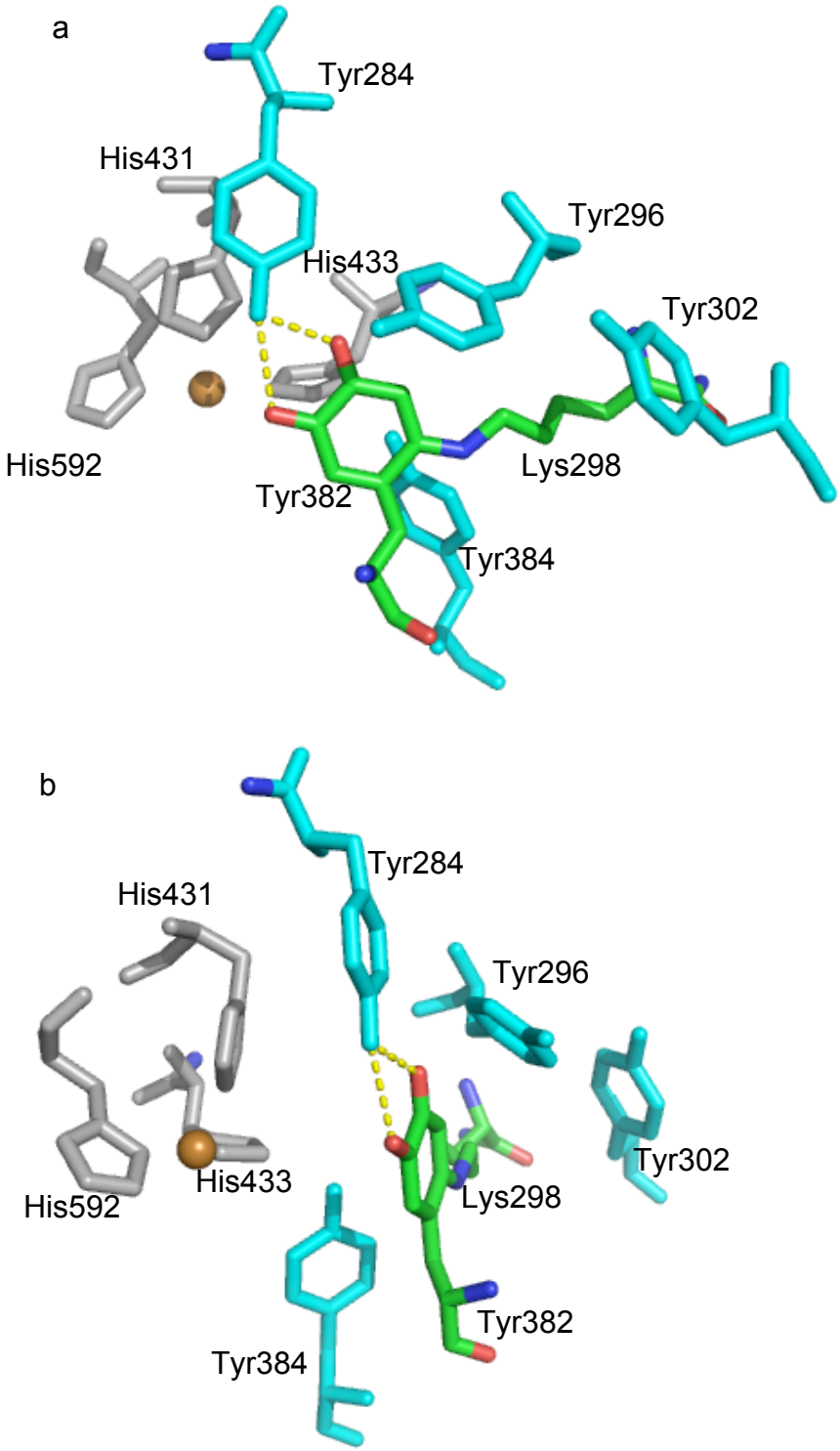

Figure 3.5 Active site structure of D298K a) in the perpendicular view of the LTI cofactor and b) in the nearly parallel view of the LTI cofactor. Residues potentially responsible for the pK_a seen at 9.62 and 10.23 are shown in blue.

TPQ[15] while in HPAO the corresponding mutation led to an increase in mobility.[54] However, both mutations lead to a decrease in the rate of catalysis suggesting that TPQ requires some mobility but that movements of TPQ are tightly controlled for optimal activity. Tyr296 is located at the base of the proposed substrate entry channel but is not part of the active site cavity. [7]Similarly, Tyr302 is near the bottom of the proposed substrate entry channel and may have a role in hydrogen bonding or π-stacking but is not part of the active site cavity.[44,102]

Tyr384 is also near the wedge-shaped cavity; it is ~3.7 Å from the ε-amino group of Lys298. Mutation of the corresponding residue, Tyr404, to Phe in histamine oxidase from *A. globiformis* had no effect on cofactor biogenesis.[78] It did, however, decrease the rate of catalysis and altered the substrate specificity indicating that this residue plays a role in substrate binding. Deprotonation of this residue in D298K may lead to a salt bridge with the protonated ε-amino group of the lysine residue prior to cross-linking. This may hold Lys298 in a position where it is unable to react with DPQ. If this were the case, a spectral feature for DPQ should be observed ~ 380 nm, as discussed previously,[99,100] but this is not observed experimentally. Therefore, it is unlikely that this residue is being titrated in the pH-profile.

It is possible, during the first phase of biogenesis of the LTQ-like cofactor, that a hydrogen bonding interaction exists between Tyr284 and the C4 carbonyl group of DPQ to position the quinone and allow the 1,4-addition to occur. As discussed in chapter 2, DPQ can be trapped by Lys298 so it must have mobility in the active site that is similar to the mobility of TPQ and it must be able to come off Cu^{2+}. If Y284 is

hydrogen bonding with DPQ, Tyr284 could be responsible for the pK_a of 9.62 seen in the first phase of biogenesis. Deprotonation of Y284 would inhibit hydrogen bonding and could result in DPQ swinging out of the wedge and onto Cu^{2+}.

In the second phase of D298K biogenesis, LTQ is thought to be converting to the more thermodynamically favored LTI. Tyr284, most likely, facilitates the conversion. As discussed in chapter 2, the mutation of Tyr284 to a Phe, in D298K, results in an unstable species with λ_{max} ~505 nm, and conversion to the ~450 nm species does not occur. If the pK_a were from the amino group of LTQ, it would be lower in the enzyme (~ 7.55 - 7.68) than in the model system (10.33) and LTQ would be deprotonated at pH 8.8. The LTQ/LTI monoanion would have an absorbance of ~450 nm as seen in chapter 2 for the model compounds. However, the rate of conversion of the ~505 nm species to the ~450 nm species, although slightly faster, remains very slow, where at pH 8.8 the 450 nm species should form very fast, making this possibility very unlikely. Therefore, it is likely that the pK_a of 7.55 - 7.68 results from a tyrosine residue, most likely Tyr284.

In the resting state, TPQ exists as a resonance stabilized mono-anion where resonance occurs between the C2 and C4 carbonyls and deuterium exchange of the C3 proton has been observed.[26,49,50,66,103] However, LTQ exists as a neutral ortho-quinone where deuterium exchange at C3 was not observed.[1,91] If Tyr284 is being titrated in the pH profile of the second phase, deprotonation of Tyr284 would be catalyzing the rate of thermodynamic equilibrium between LTQ and LTI (Scheme 3.1). When Tyr284 is deprotonated, LTI can still hydrogen bond with Y284,

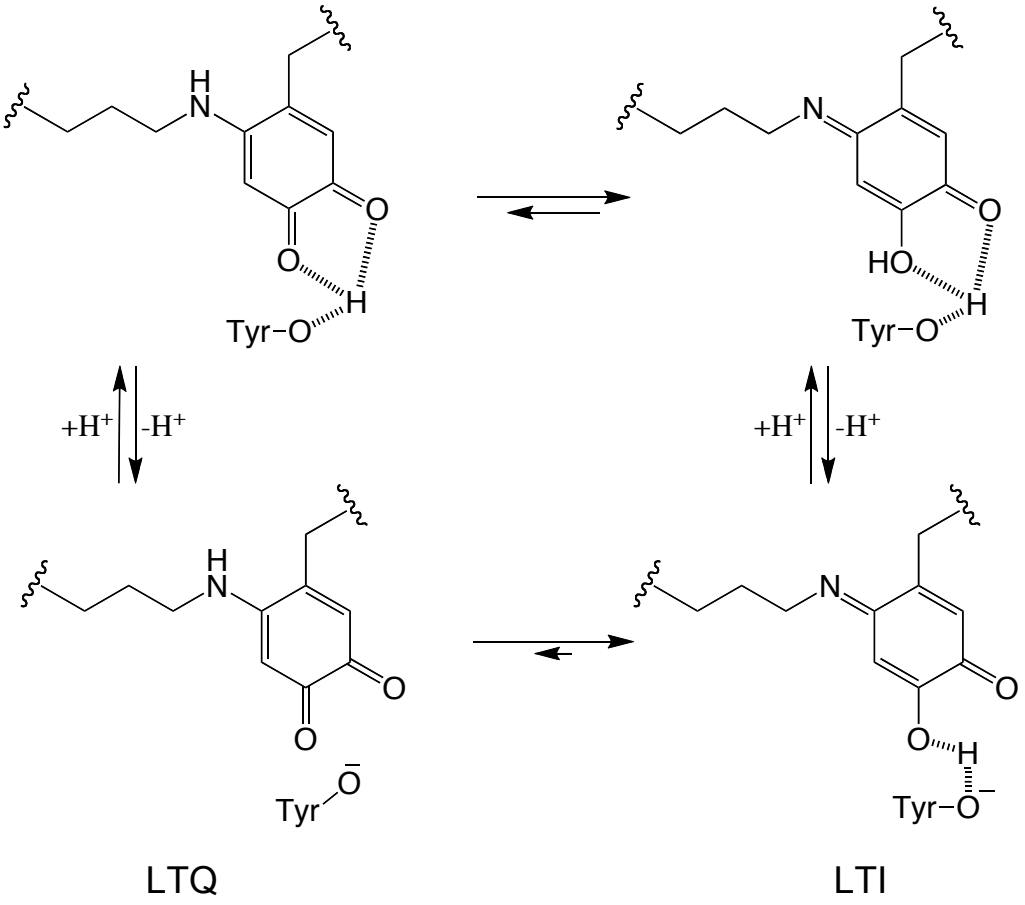

Scheme 3.1 Possible mechanism for LTI stabilization by protonated versus deprotonated Tyr284

stabilizing it over LTQ. The extent of hydrogen bonding between residues is known to directly effect the pK_a of the residues. Therefore, it is possible for Tyr284 to have a pK_a of 9.65 in the first phase and ~7.5 in the second phase. In CAOs, the active site base, a conserved aspartate residue with a typical pK_a of ~ 4, has a pK_a of 7.5 in AGAO that shifts to 6.5 in the enzyme substrate complex,[46] 8.1 in HPAO,[55] 8.0 in BSAO that shifts to 5.6,[40,104] and 6.2 in ECAO.[15] The increased pK_as of the active site bases in CAOs have been attributed to a charge repulsion between the C4 oxoanion of

TPQ and the active site base[35,55] as well as the hydrophobic environment of the active site.[55] The pK_a of a phenol in water is ~10[105] but it is ~18 in DMSO.[106] The OH group is more ionizable when it is able to participate in hydrogen bonding interactions. It is likely that the hydrogen bonding interaction between Tyr284 and DPQ in the first phase is weaker than the hydrogen bond between Tyr284 and LTQ/LTI in the second phase.

pH-Dependence of the UV/vis Absorbance Spectra of the Charge Transfer Complex Formed During the Biogenesis of an LTQ-like Cofactor in D298K

During the initial seconds of cofactor biogenesis in D298K, a peak at ~370 nm was observed which had not been observed in WT biogenesis in AGAO.[64] The species can, however, be seen during the biogenesis of the TPQ cofactor in WT AGAO when monitored by stopped-flow spectroscopy (Figure 3.6) but the species is no longer visible after ~ 3 sec. In WT HPAO, however, two similar species have been observed at ~380 nm and ~350 nm both of which are proposed to be tyrosine-copper charge transfer species.[69,70] The species resulting in the absorbance ~380 nm was determined to be independent of O_2 while the species with an absorbance of ~350 nm was O_2-dependent. In order to determine if the ~370 nm species observed in D298K was O_2-dependent, the time course of the reaction was monitored by UV/vis spectroscopy under anaerobic conditions.

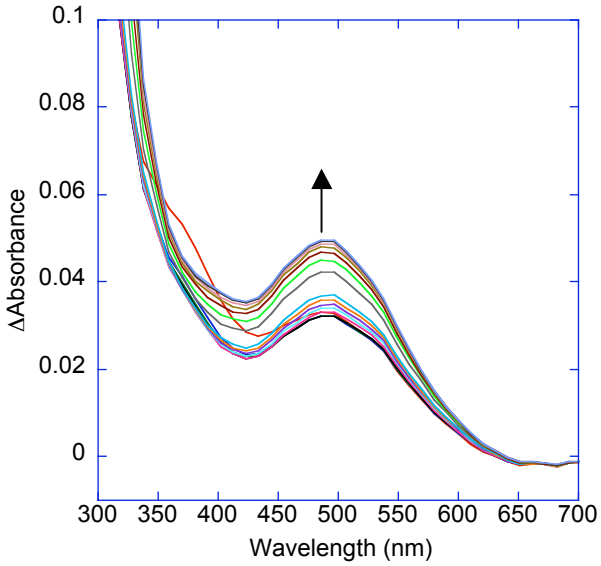

Figure 3.6 Biogenesis of 0.1 mM WT with 0.5 mM $CuSO_4$ in HEPES at pH 7.2 monitored by stopped-flow UV/vis spectroscopy. —0.1638 sec, —3.441 sec, —6.717 sec, —9.994 sec, —23.1 sec, —32.93 sec, —42.76 sec, —52.59 sec, —62.42 sec, —121.4 sec, —180.4 sec, —242.4 sec, —301.6 sec, —360.6 sec, —422.9 sec, and —481.9 sec

The ~ 370 nm species appeared to be fully formed in the mixing time of the reaction (30 sec) and the species decayed over the next several minutes (Figure 3.7), indicating that the formation of the species is not O_2-dependent. However, the rate of decay of the species appears to be faster under aerobic conditions (less that one minute) than under anaerobic conditions (5 – 10 minutes). Moreover, the rates of cofactor biogenesis do not seem to coincide with the rate of ~370 nm species decay, and an isosbestic point was not observed, indicating that the species does not convert directly to the fully formed cofactor. In HPAO, the species leading to the formation of TPQ was proposed to be an O_2 dependent Cu^{1+} - tyrosyl radical (Scheme 3.2 species C); however, this species has not been observed by EPR.[69] If the same mechanism is occurring in WT- and D298K-AGAO, it is possible that the ~ 370 nm species is

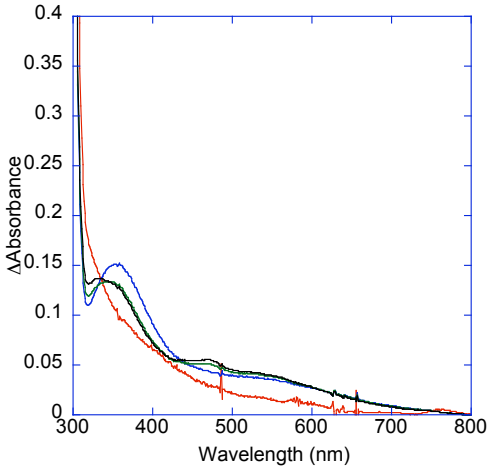

Figure 3.7 UV/vis spectra of the 370 nm species seen in the reaction of apo D298K with Cu^{2+} under anaerobic conditions at pH 8.5 —apo, —30 sec, —5 min, —10 min. Samples were blanked with buffer (apo) or a mixture of buffer and copper.

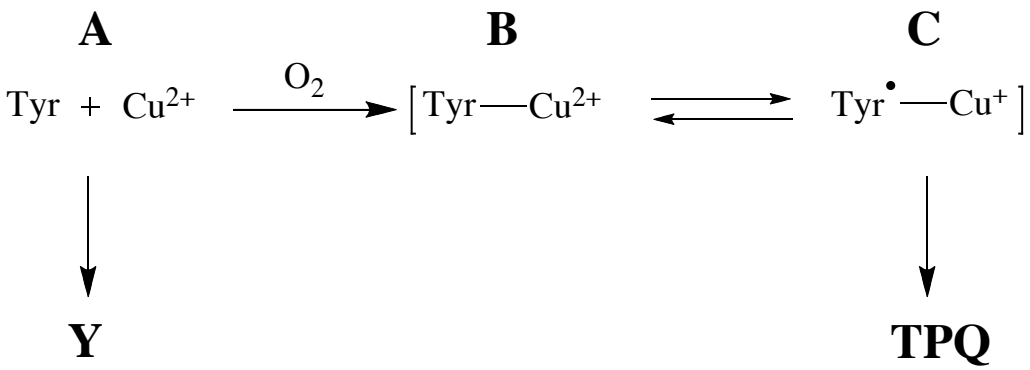

Scheme 3.2 Proposed mechanism of charge-transfer complex formation in HPAO.

forming off pathway and prior to the reaction with O_2 as shown in Scheme 3.2 A to Y.

It is possible that in AGAO, species C could form anaerobically, leading to the absorbance of ~ 370 nm (Scheme 3.3). The species would exist in equilibrium with Tyr + Cu^{2+} (A) and the Cu^{2+} - tyrosinate complex (B) and, under anaerobic conditions, the decay of the peak ~ 370 nm could be attributed to the equilibrium

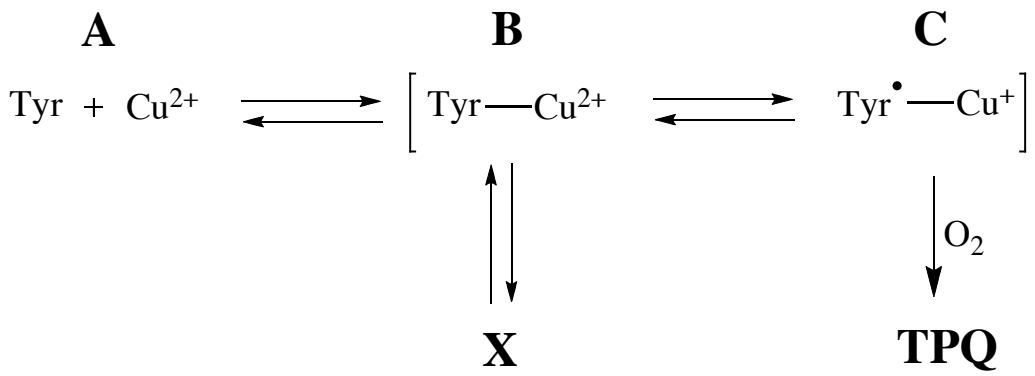

Scheme 3.3 Possible mechanism of ~ 370 nm species formation.

shifting to the thermodynamically favored species. If this were the case, under aerobic conditions the conversion of species C to TPQ should occur concomitantly and an isosbestic point would be observed. Neither were observed, indicating that species C is not the ~ 370 nm species.

The 370 nm species could be forming off pathway where the ~370 nm species (Scheme 3.3 species X) is in equilibrium with A or B, or it could be forming in a site other that the active site. In order to determine if this charge transfer complex is forming between the precursor tyrosine and Cu^{2+} (i.e. in the active site), the apo WT and D298K proteins were reacted with Zn^{2+}, which binds tightly in the active site of the protein but inhibits the formation of the cofactor. Upon the addition of Cu^{2+} to the Zn^{2+} substituted protein (dialyzed in EDTA to remove excess Zn^{2+}), the peak ~370 nm was not observed, indicating that the ~370 nm species is resulting from a charge transfer complex forming between the precursor tyrosine in the active site and Cu^{2+}, as opposed to forming outside of the active site like the ~ 380 nm species observed

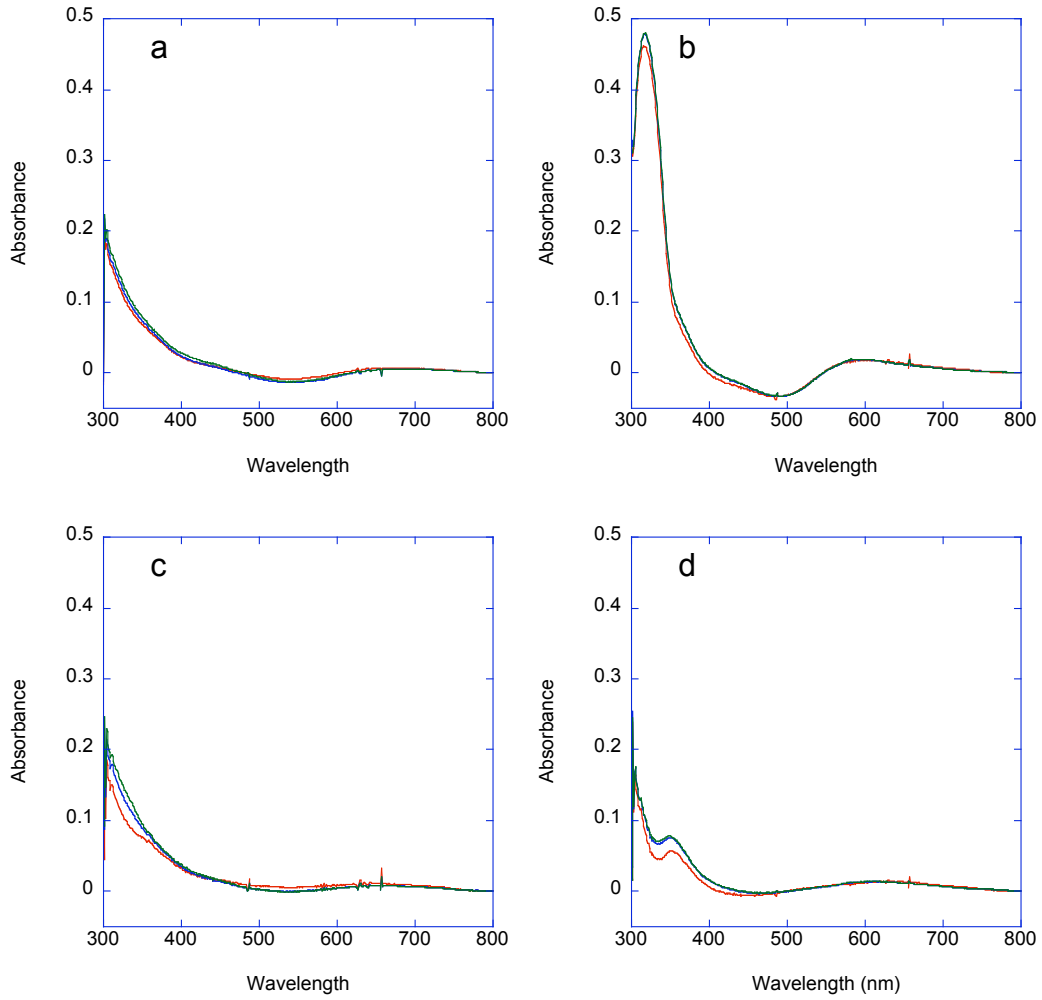

Figure 3.8 UV/vis difference spectra of holo WT (panels a and b) or D298K (panels c and d) upon the addition of copper at —30 sec, —5 min and —10 min minus holo WT or D298K without excess copper at pH 6.8 (panels a and c) and 8.5 (panels b and d)

for HPAO. The addition of excess Cu^{2+} to holo-proteins resulted in a peak at ~ 320 nm in WT and ~350 nm in D298K at pH 8.5 that was not observed at pH 6.8 (Figure 3.8). The peaks are not fully formed at 30 sec and do not decay in the time course of the experiment. Additionally, the ~ 320 nm species in WT accumulates to a much greater extent than ~ 350 nm species in D298K or in either apo protein. It is likely

that these new absorbencies are not resulting from the same potential charge transfer species seen at ~370 nm but a species that is forming outside of the active site. The 370 nm species, however, is likely a charge transfer species formed in the active site of WT- and D298K-AGAO but not on the pathway to form the cofactor.

A pH-dependency of the UV-vis spectrum of the species was also observed under anaerobic conditions, in which the UV/vis spectra taken 30 sec after the addition of Cu^{2+} to D298K produced a more defined peak at pHs from 7.8 to 9.0 where the rate of cofactor formation was the fastest (Figure 3.9). However, pH did not appear to consistently effect the extent of accumulation of the ~370 nm peak as was seen in HPAO.[69] The anaerobic spectra of WT protein taken at pH 6.8 and 8.5 also resulted in the rapid formation of the ~370 nm species, but the peaks were not well defined at either pH.

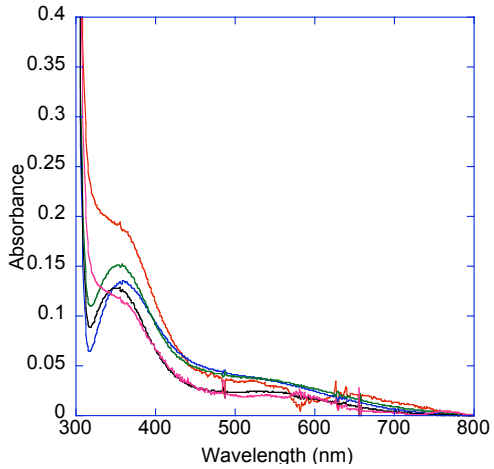

Figure 3.9 UV/vis spectra of the 370 nm species seen in the reaction of apo D298K with Cu^{2+} under anaerobic conditions at 30 sec and pHs of —6.8, —7.8, —8.5, —9.0, and —9.2. Samples were blanked with buffer (apo) or a mixture of buffer and copper.

Conclusion

The time course of the UV-vis spectral change observed during the biogenesis reaction in D298K varied based on the pH at which the reaction took place. At pH 6.8 the absorbance of the initially formed species was ~496 nm. A shift to 505 nm occurred with a change in pH from 7.5 to 8.7. At a pH of ~9.5, the species shifted to ~518 nm. This shift in λ_{max}, likely corresponds to the amount of LTI present at the end of the first phase. The conversion of this species to the 450 nm species occurred with an isosbestic point at ~465 nm and produced a peak at ~ 450 nm at each pH. The formation of TPQ was not observed at any pH indicating that amination out competes hydration at the pH range studied.

The pH-profile of D298K biogenesis, followed by UV/vis spectoscopy, indicated that the rate of biogenesis of the 505 and 450 nm species are both pH-dependent. The pH-dependency on the rate of formation of the LTQ-like species in the first phase produces a bell-shaped curve with pK_as of ~7.93 and 9.62. The rate for the formation of this species was the fastest at a pH of ~ 8.8 with a rate of 0.77 min^{-1}. Deprotonation of the residue in the active site with a pK_a of ~ 7.9, increases the rate of the reaction and the residue is proposed to be the precursor tyrosine, as was seen previously in HPAO with a pK_a of ~8.45.[69]

Protonation of the residue with a pK_a of 9.62 in the first phase, increases the rate of the reaction; this pK_a has not been observed previously in CAOs. This pK_a was proposed to be Tyr284, where it most likely is involved in a hydrogen bonding

interaction with DPQ, holding DPQ in the wedge shaped cavity to react with Lys298 and keeping it from being trapped by Cu^{2+}.

In the second phase of biogenesis, Tyr284 is known to hydrogen bond to LTQ/LTI to stabilize the LTI tautomer over LTQ. When Tyr284 was mutated to Phe in D298K, the ~ 505 nm peak for LTQ was observed but did not convert to the ~ 450 nm LTI peak (as seen in chapter 2). In the second phase, the deprotonated form of Tyr284 was proposed to increase the rate of LTQ to LTI conversion although the conversion is thought to be thermodynamically dependent. Deprotonation of Tyr284 may be influencing the thermodynamic equilibrium.

The differences in the pK_as of Try284 in the first and second phase is most likely due to the different environments of Tyr284 in the two phases. In the first phase, Tyr284 is probably only weakly hydrogen bonded to DPQ. In chapter 2, DPQ was shown to have mobility in the active site. It would have to move out of the active site wedge and interact with Cu^{2+} to undergo a hydration reaction to form TPQ in WT. Therefore, the hydrogen bond between Tyr284 and DPQ should be fairly weak. However, the hydrogen bonding interaction formed between LTQ/LTI and Tyr284 is likely stronger, as indicated by the lower pK_a.

In the initial minute of cofactor biogenesis in WT- and D298K-AGAO, an absorbance at ~370 nm, proposed to be a charge-transfer species, was observed. The formation of the species was not O_2-dependent as it forms under both aerobic and anaerobic conditions. The putative charge transfer species may be formed off pathway, as suggested by the different rates of cofactor formation and ~ 370 nm

species decay and by the lack of an isosbestic point between the 370 nm and 505 nm species. However, it is probably formed in the active site of the protein because it was not observed when Zn^{2+} was prebound in the active site or when Cu^{2+} was added to holo protein. A different putative charge transfer species was observed when Cu^{2+} was added to holo protein, which likely originates from outside of the active site.

Chapter 4: LTQ Biogenesis in WT- and D298A-AGAO in the Presence of n-Butylamine

Introduction

Copper amine oxidase, containing TPQ, catalyzes the oxidative deamination of amine substrates to their corresponding aldehydes. As discussed in chapter 1, the reaction is divided into reductive- and oxidative-half reactions. In the reductive half reaction, the C5 carbonyl group of TPQ reacts with substrate to form a substrate Schiff base. A conserved aspartic acid residue (Asp298 in AGAO) then acts as a general base to abstract the α proton of the substrate, leading to the product Schiff base.[35] Mutation of Asp298 to Ala reduced the catalytic efficiency about 10^6 fold compared to that of WT.[46] Similarly, when D298A was reacted with phenylhydrazine, the rate of the reaction was slowed ~170 fold.[46] In the biogenesis reaction of TPQ in D298A-AGAO, the rate of the reaction was 40% slower than that of WT.[46] However, the TPQ content was approximately that of WT, indicating that Asp298 is not directly involved in the biogenesis of TPQ.

In chapter 2, Asp298 was mutated to a Lys residue and was shown to form an LTQ-like cofactor during biogenesis, which was stabilized in the form of the LTI tautomer. The cofactor was formed through the cross-linking of two amino acid residues, making it immobile and unable to rotate freely like the TPQ cofactor. In the flipped orientation, the C5 active carbonyl is away from the substrate entry channel and Asp298, making it inactive. In an attempt to trap the DPQ cofactor with a free amine and to generate an LTQ-like cofactor in AGAO (Scheme 4.1) with an

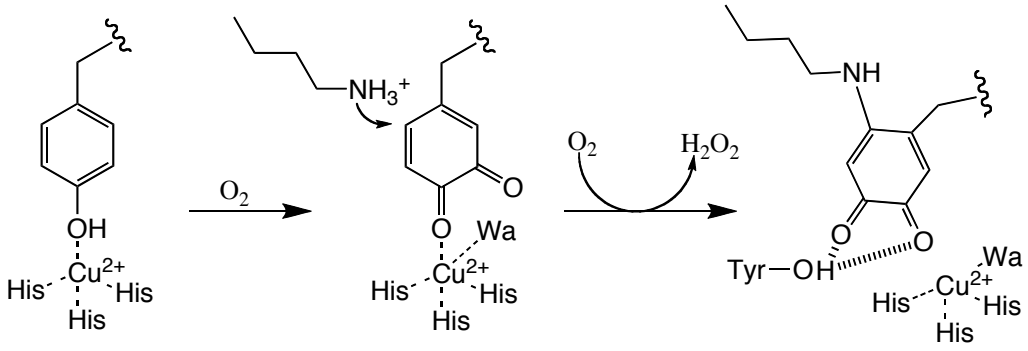

Scheme 4.1 Possible mechanism for LTQ formation in WT and D298A in the presence of *n*-butylamine

increased mobility, WT- and D298A-AGAO were biogenized in the presence of *n*-butylamine. In chapter 2, the proper placement of the Lys residue in the active site was required for the formation of LTQ. In that study, the Asp298 residue was mutated to a Lys to form LTQ. Therefore, the mutation of Asp298 to Ala should create room in the active site to accommodate the *n*-butylamine at a position to allow a cross-link to form.

Materials and Methods

Materials

See the Materials section in Chapters 2 and 3 for a more comprehensive list of materials. Potassium sodium tartrate, magnesium acetate, methylamine hydrochloride, and sodium periodate were purchased from Sigma Aldrich. Dioxane, CAPS, butylamine, and potassium carbonate were purchased from Acros. Sodium cacodylate and PEG 8000 were purchased from Fluka. The 50 μL microdialysis buttons and microdialysis membrane disks of 12,000-14,000 MW cut off were purchased from Hampton Research.

Site-directed Mutagenesis.

The expression plasmid for D298A-AGAO was generated by site-directed mutagenesis using a QuikChange mutagenesis kit from Stratagene using pPEAO-02[35] as the parent vector. The DNA primers for D298A were 5′-AGAACTACTTCGCTACGGGGGAGTACCTG-3′ (forward) and 5′-CAGGTACTCCCCCGTAGCGAAGTAGTTCT-3′ (reverse). The plasmid was fully sequenced and the point mutation was confirmed. The plasmid was propagated in *E. coli* DH5α cells and purified using high-speed plasmid mini- and midi-prep kits from Qiagen.

Enzyme Expression and Purification.

The precursor forms of WT and D298A were optimally expressed using the procedure described in chapter 2 for the precursor form of WT and D298K proteins. Protein concentrations were determined spectrophotometrically by using extinction coefficients at 280 nm of 12.3 for 1% (w/v) solutions of the apo form of AGAO.[29] Protein not being used immediately was stored at -80°C in 40 mg/mL aliquots with the addition of 25% glycerol as a cryoprotectant.

Biogenesis Study

To determine if an LTQ-like quinone could be made by cross-linking of DPQ to a free amine, the biogenesis of apo WT and D298A was done in the presence and absence of *n*-butylamine hydrochloride at 30°C. A 50 μL solution of 0.2 mM enzyme

in 100 mM HEPES pH 6.8, 100 mM CAPS pH 10, 100 mM CHES pH 9, or 100 mM HEPBS pH 8.5 was mixed with 50 μL 1 mM $CuSO_4$. Methylamine hydrochloride or *n*-butylamine hydrochloride (25 μL of 4 mM or 400 mM in 500 mM buffer) was added to 25 μL of 0.4 mM enzyme. The solution was incubated at room temperature a few minutes before adding 50 μL of 1 mM $CuSO_4$. The progress of the reaction was monitored by UV/vis spectroscopy. Spectra were taken every 10 sec for 10 min and every 2 min for 50 min. UV/vis spectroscopy was performed on an Agilent HP 8453 photo diode array UV/vis spectrophotometer equipped with a temperature-controlled cell holder at 30 ± 0.2 °C (path length of 1 cm).

WT and D298A samples were biogenized in the presence of amine hydrochloride salts, as described above, for 30 min at pH 8.5, 9, and 10. Spectra were taken before spin dialysis 5x into 100 mM HEPES pH 6.8. The samples were diluted to 0.1 mM and spectra were taken again. The final concentrations of enzyme were determined by using extinction coefficients at 280 nm of 13.2 for 1% (w/v) solutions of the holo form of WT-AGAO.[29]

Reaction with 2-Hydrazinopyridine or Methylhydrazine

Enzyme solutions of 100 μL of 28.2 mg/mL D298A with *n*-butylamine hydrochloride were prepared in 200 mM KPi pH 7.2. Five molar equivalents of 2-phenylhydrazine were added (25 μL of 0.1 mM) and the solution was incubated at room temperature overnight. Spectra were taken before and after dialysis to remove excess hydrazine.

Crystallization

The purified D298A apo-protein (0.4 mM) was incubated at room temperature for 5 min with 377 mM *n*-butylamine hydrochloride in 471 mM CAPS pH 10. An equal volume of 0.5 mM Cu^{2+} was added, and the reaction was incubated at 30°C for one hour to complete the cofactor biogenesis. The product was dialyzed against 1 L 50 mM HEPES pH 6.8 twice (1 hour and overnight). Samples were diluted to 5, 10, and 15 mg/mL, and crystal trays were set up using both the hanging drop vapor diffusion and button dialysis methods. The hanging drop method used 1-2 μL enzyme and an equal volume of crystallization buffer. The well contained 750 μL crystallization buffer. The button method was carried out in 50 μL buttons; ~27 μL enzyme and crystallization buffer were added to the button. The well contained 1.5 mL crystallization buffer. All crystal trays were incubated at 20°C. Four crystallization buffers were used based on previous CAO crystallization experiments: 1) 200 mM magnesium acetate, 20% (m/v) PEG 8000, 100 mM sodium cacodylate pH 6.5[107] 2) 1.6 M ammonium sulfate, 10% (v/v) dioxane, 100 mM MES pH 6.5[107] 3) 1.6 M ammonium sulfate, 12% (v/v) dioxane, 100 mM MES pH 6.5[107] 4) 1.05 M potassium sodium tartrate, 25 mM HEPES pH 6.8.[12]

Results

Expression and Purification of Wild-type and Mutant AGAOs

Protein expression yielded approximately 105 - 110 g of wet *E. coli* cells. The D298A mutant behaved the same as WT during expression and purification. Table

4.1 shows a summary of the yields. The purity of the samples were ~99% as estimated from the SDS-PAGE gels.

Table 4.1 Protein yields for apo protein with optimized growth and purification conditions

Protein yields (mg/L)	Apo protein
WT	32.76
D298A	30.72

Biogenesis of LTQ-like Quinone in WT and D298A

The time course of cofactor formation in the presence and absence of *n*-butylamine hydrochloride was followed by UV/vis spectroscopy in WT- (Figure 4.1) and D298A-AGAO (Figure 4.2) protein samples. The apo-D298A was prepared by the standard procedure used to prepare apo-WT.[12,29] The apo-WT or D298A proteins were mixed with a solution of *n*-butylamine in buffer, briefly incubated, and further mixed with a Cu^{2+} solution in air at 30°C (final concentrations of 0.1 mM enzyme, 0.1 M *n*-butylamine hydrochloride, 0.15 M buffer, and 0.5 mM $CuSO_4$ or 0.1 mM enzyme, 50 mM buffer, and 0.2-0.5 mM $CuSO_4$). The biogenesis reactions of WT and D298A in the absence of *n*-butylamine at pH 6.8 are known to produce a TPQ cofactor with absorbencies of ~475 nm[35] and ~460 nm[46] respectively with no observed intermediates, as was seen in this study. However, the biogenesis of WT and D298A in the presence of *n*-butylamine produced a pink species with a broad visible absorbance centered at ~538 nm in WT and ~523 nm in D298A at pH 8.5. Cofactor biogenesis of D298A in the presence of methylamine was also monitored but resulted

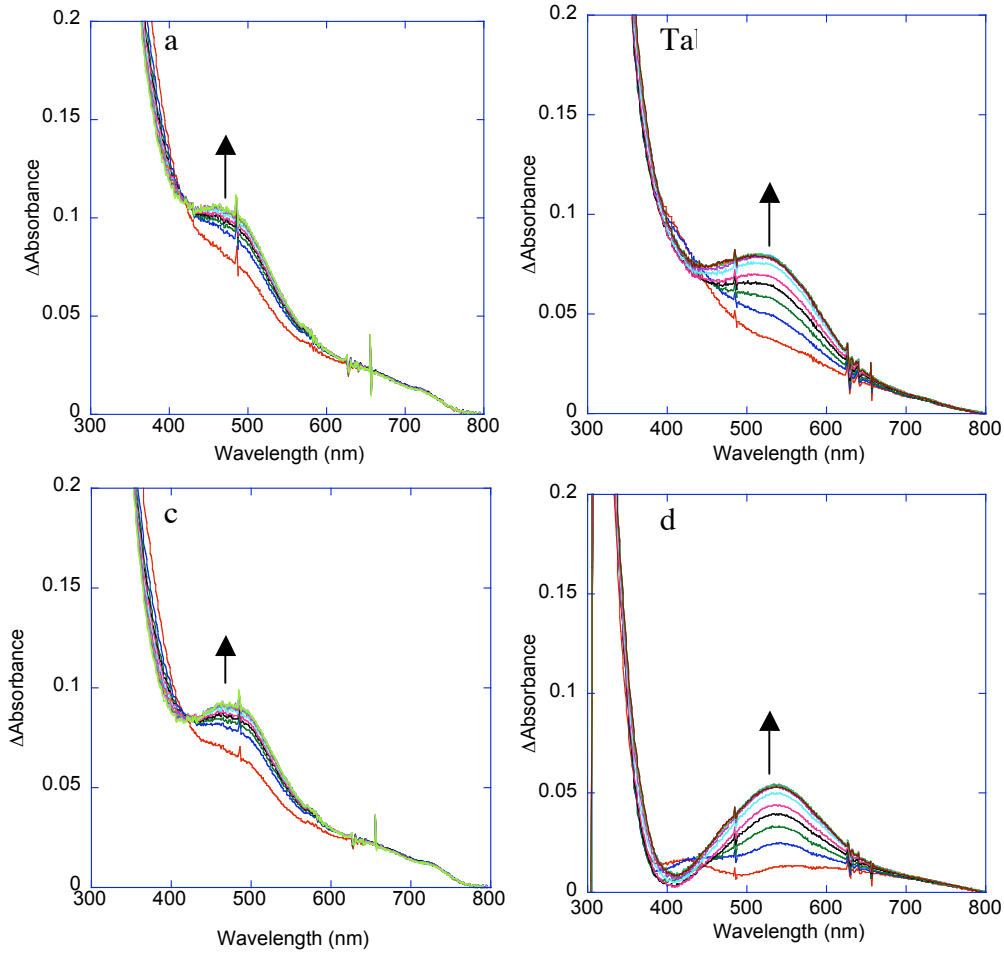

Figure 4.1 Biogenesis of WT in the presence and absence of *n*-butylamine. a) Biogenesis of 0.1 mM WT with 0.2 mM $CuSO_4$ in HEPBS at pH 8.5. b) Biogenesis of WT in the presence of 0.1 M *n*-butylamine hydrochloride with 0.5 mM $CuSO_4$ in HEPBS at pH 8.5. c) and d) are the difference spectra of a and b, respectively, minus the spectra taken in the absence of $CuSO_4$. —1 min, —2 min, —3 min, —4 min, —5 min, —7 min, —9 min, —11 min, —13 min, —15 min, —17 min, and —19 min

in absorbance spectra with a peak ~460 nm that was concluded to be TPQ. It is likely that the active site is not arranged to facilitate the reaction with methylamine. In the D298A *n*-butylamine sample, the peak, centered at 523 nm, shifted to ~500 nm as the reaction progressed from 10 min to 1 hr. The peak ~500 nm is very similar to that of

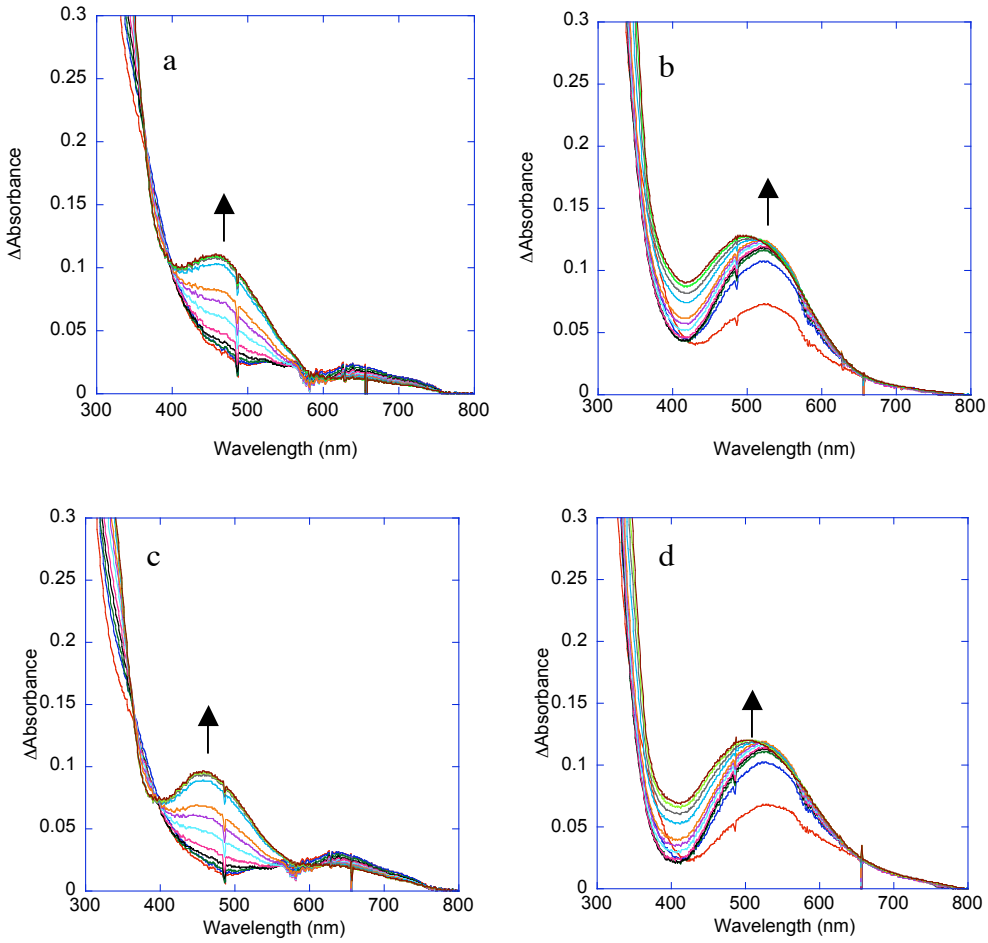

Figure 4.2 Biogenesis of D298A in the presence and absence of *n*-butylamine. a) Biogenesis of 0.1 mM D298A with 0.5 mM $CuSO_4$ in HEPBS at pH 8.5. b) Biogenesis of D298A in the presence of 0.1 M *n*-butylamine hydrochloride with 0.5 mM $CuSO_4$ in HEPBS at pH 8.5. .c) and d) are the difference spectra of a and b, respectively, minus the spectra taken in the absence of $CuSO_4$. —1 min, —2 min, —3 min, —4 min, —5 min, —7 min, —9 min, —11 min, —21 min, —31 min, —41 min, and —51 min

the LTQ model compound (Figure 2.9). The biogenesis of WT in the presence of *n*-butylamine was initially being studied as a control, but it appears that the same species is being formed in both WT and D298A. If this species is an LTQ-like quinone, the results support those found in the study of D298K in chapter 2, showing that the 1,4-addition of the ε-nitrogen of Lys to DPQ to form LTQ out competes the

natural hydration reaction to form TPQ. However, this study indicates that the free amine, and not just the bound Lys, is capable of undergoing the 1,4-addition reaction (Scheme 4.1). These results are also in agreement with the results observed in model studies of LTQ biogenesis, where DPQ can be trapped by secondary alkyl amines to form LTQ, but not by solvent water molecules to form TPQ.[1] Crystallographic studies may help to determine how the active sites in WT and D298A are arranged to accommodate *n*-butylamine, facilitate its reaction with DPQ, and lead to products with differing energies.

Absorbance changes at the initial λ_{max} for each species are plotted against time in Figure 4.3. The preliminary rates of biogenesis for WT and D298A with and without *n*-butylamine at pH 8.5 were each fitted to the sum of two single exponentials by the least-square method (Table 4.2). Compared to the rate of WT biogenesis, D298A biogenesis was ~4.4 x slower while D298A biogenized in the presence of

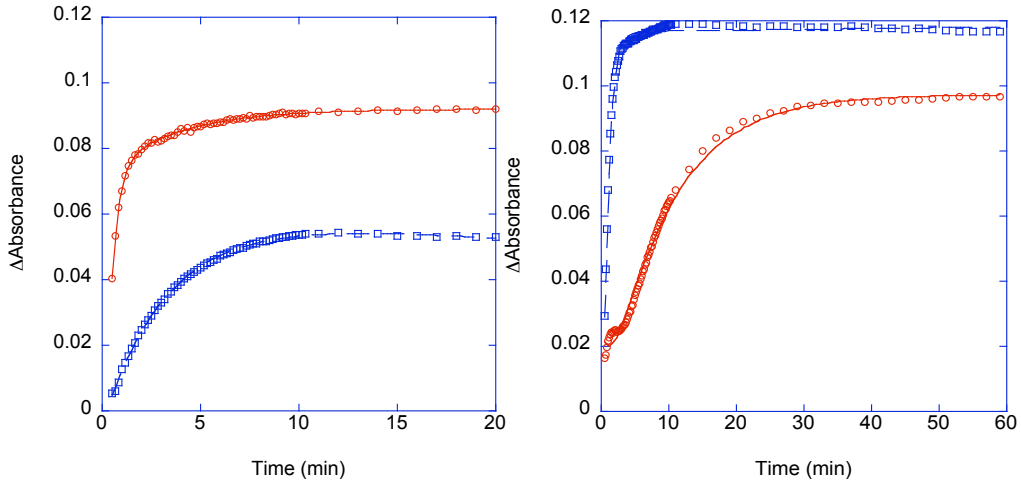

Figure 4.3 Preliminary rates of biogenesis for a) WT and b) D298A — with and — without *n*-butylamine at pH 8.5 fit to the sum of two exponentials by the least-square method

Table 4.2 Preliminary rates of cofactor biogenesis in the presence and absence of *n*-butylamine in WT- and D298A-AGAO

Sample	λ_{max}	Rate (min^{-1})
WT	475	2.66
WT with *n*-butylamine	538	0.295
D298A	458	0.613
D298A with *n*-butylamine	523	1.17

amine was ~2.3 x slower. The faster rate of biogenesis of D298A in the presence of amine compared to the biogenesis in the absence of amine supports the observation that the 1,4-addition of the amine to DPQ is more efficient than the addition of a copper associated water molecule. However, the rate of WT biogenesis in the presence of amine was ~9 x slower than the rate in the absence of amine, possibly indicating that the active site of the WT enzyme is not arranged to accommodate the amine in an appropriate place to react efficiently with DPQ.

In addition to the biogenesis reactions of D298A at pH 8.5, biogenesis reactions were also run at pH 9.0 and 10.0. Figure 4.4 shows the final, taken after 1

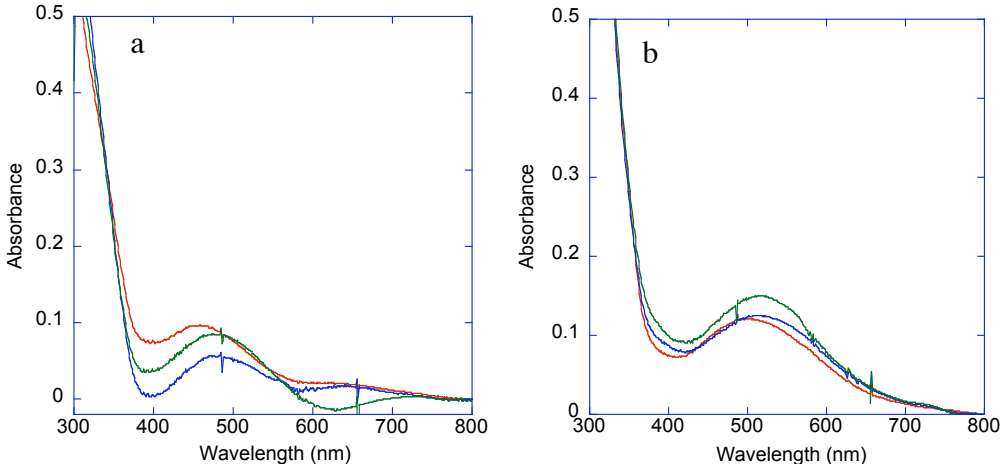

Figure 4.4 Final D298A biogenesis spectra at pH —8.5, —9.0 and —10.0 minus the initial apo spectra. a) Biogenesis in the absence of $BuNH_3^+$. b) Biogenesis in the presence of $BuNH_3^+$.

hr of D298A biogenesis with and without *n*-butylamine, minus the initial (apo) spectra at pH 8.5, 9.0 and 10.0. In the absence of *n*-butylamine, the final absorbance of cofactor formation in D298A shifts from ~460 nm at pH 8.5 to ~480 nm at pH 9.0 and 10.0. Similarly, the biogenesis reactions of D298A in the presence of *n*-butylamine resulted in peaks ~500 nm at pH 8.5 and 515 nm at pH 9.0 and 10.0. It is possible that at the higher pHs, the hydrogen bonding interaction between O4 of the quinone and Tyr284 is weaker and allows for a greater extent of electron density delocalization, leading to the red-shift observed in the absorbance spectra. In D298A, the crystal structure at 1.85 Å resolution shows that O4 of TPQ is 2.3 Å from Tyr284 as opposed to the 2.5 Å seen in WT at 1.8 Å resolution.[12,46] The ~30 nm blue-shift in the absorbance spectra of D298A to ~460 nm, has been attributed to this stronger hydrogen bonding interaction causing a localization of electron density at the O4 position of TPQ.[46] Additionally, in the D298A crystal structure, Y296 is rotated into the space created by the D298A mutation and a water molecule occupies the space created by the rotation of Tyr296. The water molecule is also hydrogen bonded to the O4 of TPQ and is likely contributing to the localization of electron density at that location.[46] The absorbance spectra of D298K also shows a ~30 nm blue-shift compared to WT.[4] In the crystal structure of D298K-AGAO, the location of Tyr296 is similar to its position in WT and an additional water molecule is not seen near O4 of LTI. The hydrogen bonding distance between LTI and Y284 is ~2.4 Å. However, disruption of the hydrogen bond between O4 of the quinone and Tyr284 by site-directed mutagenesis results in an absorbance spectram that is red-shifted ~50 nm,

supporting the observation that the localization or delocalization of electron density at O4 leads to differences in the electronic features of the quinone.[4]

In order to determine if the 500-515 nm absorbance is from a TPQ cofactor that was shifted due to the presence of *n*-butylamine, the D298A samples were dialyzed into pH 6.8 buffer. The UV/vis spectra of the samples biogenized in the absence of *n*-butylamine remained at ~460 and ~480 nm (Figure 4.5 a) while the spectra of the samples biogenized in the presence of *n*-butylamine shifted to ~480 and ~500 nm (Figure 4.5 b). If the *n*-butylamine samples contained a TPQ cofactor, the removal of *n*-butylamine should result in a shift in the spectra to ~460-480 nm as seen in the D298A samples biogenized in the absence of *n*-butylamine. However, this was not the case, indicating that the species with an absorbance of ~480-500 nm is a distinctly different species from TPQ and resembles that of LTQ in LOX and in model compounds at the higher pHs.[4,91]

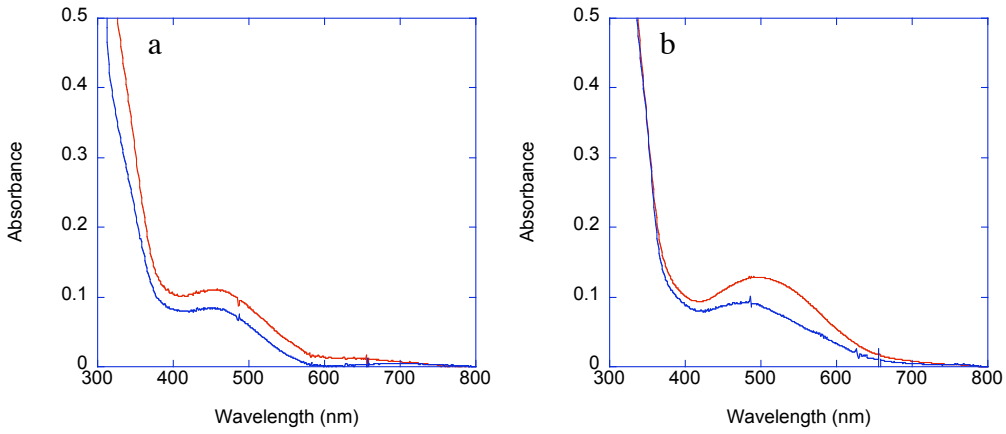

Figure 4.5 Final spectra of D298A biogenesis before — (pH 8.5) and after dialysis — (pH 6.8). a) In the absence of $BuNH_3^+$. b) In the presence of $BuNH_3^+$.

Enzyme samples biogenized in the presence of *n*-butylamine could be producing a mixture of TPQ and LTQ cofactors, particularly at a lower pH. The combination of LTQ and TPQ cofactors in the pH 8.5 samples may contribute to the difference in absorbance vs. pH 9 and 10 samples. As discussed in chapter 2, WT-AGAO reacts with hydrazines to produce hydrazone-azo derivatives in tautomeric equilibrium, but it exists primarily in the azo form.[12,29,56] D298A has also been known to react with hydrazines; however, the reaction occurred almost 200 x slower.[46] Additionally, LTQ containing proteins have also been shown to react with hydrazines to form, predominantly, the azo product.[3] The reactions between WT- and D298A-AGAO biogenized in the presence and absence of *n*-butyl amine with various hydrazines, including 2-hydrazinopyridine, 2-phenylethylhydrazine, and methylhydrazine, were monitored by UV/vis. WT-AGAO biogenized in the absence of *n*-butylamine was the only species that resulted in an absorbance corresponding to the hydrazone-azo derivative. Furthermore, prolonged incubation did not produce hydrazone-azo derivatives, even with D298A biogenized in the absence of *n*-butylamine that, in the literature, is reported to react slowly.[46] Although the samples did not react with the inhibitor, all of the samples were catalytically active with 2-

Table 4.3 Rates of catalysis with 2-phenylethylamine as a substrate.

Sample	Rate (mAbs/min(μM))
WT	17,110
WT with *n*-butylamine	417
D298A	96.4
D298A with *n*-butylamine	13.8

phenylethylamine as a substrate. Table 4.3 shows the rates of catalysis for each of the samples.

The D298A sample, previously biogenized in the presence of *n*-butylamine and after dialysis to removal excess amine, was incubated at 4°C, pH 8.5 for 1 month; this resulted in a spectrum with one peak centered ~470 nm and another with a large absorbance ~330 nm (Figure 4.6). As seen in chapter 2, the final absorbance spectrum of D298K had peaks centered ~450 nm and ~320 nm. The final spectrum in D298K was assigned to the LTI tautomer of LTQ. It is possible that in D298A biogenized in the presence of *n*-butylamine, the initial putative LTQ species is very slowly converting to the more stable LTI tautomer as seen in D298K.

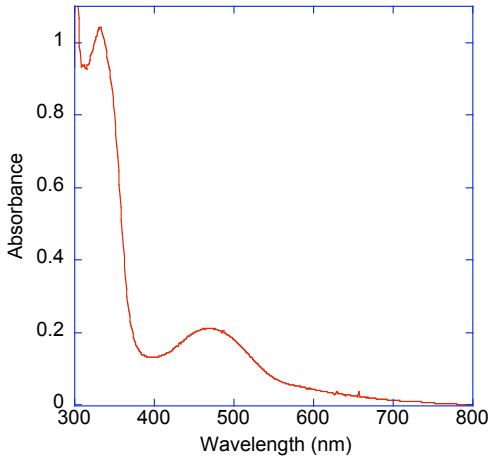

Figure 4.6 UV/vis spectrum of D298A biogenized in the presence of *n*-butylamine at pH 8.5 after one month of incubation at 4°C.

Attempts to determine the structure of the cofactors of WT and D298A derived from the reaction with *n*-butylamine have recently begun using mass spectroscopy and crystallography. Crystallography conditions have resulted in mainly

single needle shaped micro crystals that can be used as seed crystals in future crystal optimization experiments (Figure 4.7). The orange to red color of the crystals is consistent with the color of the protein in solution at pH 6.8, both initially and after one month. Holo-WT crystals formed under similar conditions also have a red color typical of the color of the protein in solution.[5] A continuation of these studies is required to determine the structure of the cofactor and its arrangement in the active site of the protein.

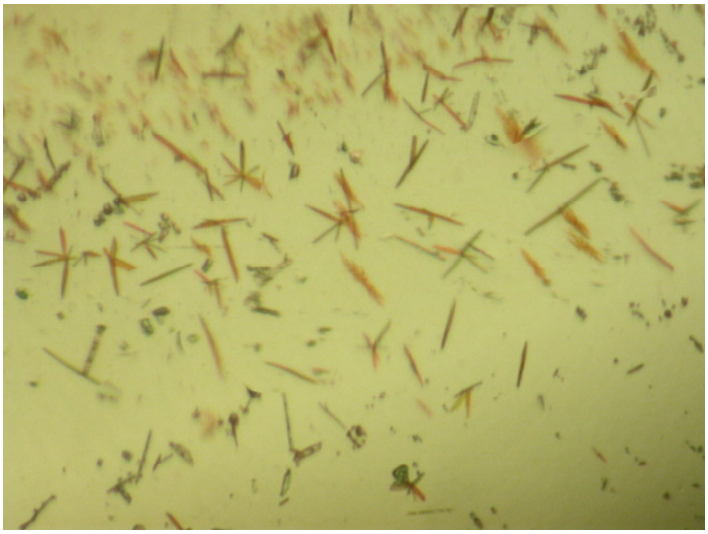

Figure 4.7 Photograph of microcrystals of D298A biogenized in the presence of *n*-butylamine

Conclusion

In WT- and D298A-AGAO, the formation of TPQ occurs directly from the Cu^{2+}-bound tyrosine precursor where no spectroscopic intermediates have been observed. In D298K-AGAO, the direct conversion of the Tyr to LTQ was observed by UV-vis spectroscopy. In the D298K mutant, the LTQ cofactor is formed through

the cross-linking of two amino acid residues, making it unable to rotate freely like the TPQ cofactor. In an attempt to generate an LTQ-like cofactor in AGAO that has an increased mobility, WT- and D298A-AGAO were biogenized in the presence of *n*-butylamine.

At pH 8.5 the biogenesis of WT and D298A cofactors in the absence of *n*-butylamine resulted in species having λ_{max} of 475 and 460 nm, respectively, in agreement with reports in the literature.[35,46] However, the biogenesis in the presence of *n*-butylamine hydrochloride resulted in peaks of 538 and 523 nm, respectively. It is likely that an LTQ-like cofactor is being formed in both WT and D298A proteins through the cross-linking of the free amine to the DPQ intermediate. This is further supported by the observation that peaks at 330 and 470 nm are seen after a one month incubation at 4°C, which correspond to the 320 and 450 nm peaks seen for the LTI cofactor in D298K (chapter 2). The rate of biogenesis of D298A in the presence of amine is faster than the rate in the absence of amine, but the opposite is true of WT. This indicates that the active site of D298A is arranged in a way to better facilitate the reaction between the amine and DPQ compared to WT.

In addition to the biogenesis of D298A at pH 8.5, the reactions were also run at pH 9.0 and 10.0 which resulted in peaks that were ~20 nm red-shifted from those at pH 8.5. It is possible that the hydrogen bonding interaction between O4 of the quinone and Tyr284 is weaker at the higher pHs and allows for a greater extent of electron density delocalization, leading to the red-shift observed in the absorbance spectra. Dialysis into pH 6.8 buffer resulted in a ~20 nm blue-shift of D298A samples

biogenized in the presence of *n*-butylamine, but not a ~50 nm shift, indicating that the species is not TPQ but a different species that spectroscopically resembles LTQ. The WT and D298A samples biogenized in the presence of amine and D298A biogenized in the absence of amine, did not react with the inhibitor; however, all of the samples exhibited catalytic activity that was 40- to 1000-fold less active than the wild-type. Crystallographic studies may provide structural reasons for the variations seen in the rates of catalysis.

Chapter 5: Mutagenesis Study on the LTQ Precursor Lysine Residue in LOX

Introduction

Lysyl oxidase (LOX) belongs to a family of copper-containing amine oxidases. It has been known to play a role in stabilizing the extracellular matrix by initiating the formation of intra-and intermolecular cross-links in collagen and elastin.[22,23] In humans, there are four *lox-like* (*loxl*) genes; each contains a ~ 630 bp sequence at the 3' end encoding the LOX catalytic domain.[23] Three of the *hloxl* genes (*hloxl2, hloxl3,* and *hloxl4*) contain four scavenger receptor cysteine rich (SRCR) domains.[108-113] SRCR proteins make up a family of cell-surface associated proteins that function mainly within the immune system.[114,115] SRCR domains are thought to be involved in protein-protein interactions, mediate cell adhesion and/or cell signaling.[116] The specific role of the SRCR domains on HLOXL2-4 has not been defined. Abnormal expression of LOX has been associated with several disorders including loose skin and joints and fibrotic diseases.[22,117,118] High levels of HLOXL2 (at the mRNA level) have been seen in the reproductive tissues.[108] Abnormally high expression levels of HLOX and HLOXL2 (at the mRNA level) have been observed in invasive breast cancer. The expression of LOXL2 has been highly up-regulated in metastatic but not nonmetastatic estrogen-dependent breast cancer cells (MCF7).[119] When LOXL2 was expressed in MCF7, the cells changed their phenotype to become invasive/metastatic and were surrounded by a high concentration of dense collagen fibers. However, MCF7 cells that do not express LOXL2 are not invasive, suggesting that LOXL2 enhances the malignancy and the fibrosis of tumors. The mechanism of

the up-regulation of LOXL2 expression seen in invasive and metastatic cell lines is currently unclear.[119-121] LOXL2 and LOXL3 have been proposed to oxidize two specific lysine residues (K98 and K137) on the transcription factor Snail, that controls epithelial-mesenchymal transitions (EMT).[122] Overexpression of LOXL2 and LOXL3 induces EMT to downregulate E-cadherin expression implicated in the mechanism of invasive and metastatic tumor progression. E-cadherin is an epithelial protein that mediates cell-cell interactions.[123] Down regulation of the E-cadherin gene decreases the strength of cellular adhesion and increases cell migration/invasion.[122] Recently, a study of LOXL2 expression by Hollosi and co-workers, has shown that LOXL2 expressed in malignantly transformed mammary cells demonstrated an altered localization and processing when compared to LOXL2 expressed in normal mammary epithelial cell lines.[121] Elucidating the mechanism by which HLOXL2 reacts with the Snail transcription factor may provide insight into its role in metastatic breast cancer.

Many studies have been performed to understand the mechanism of the biogenesis of TPQ.[5,9,14,29,30,55,64-74] It is widely accepted that TPQ is formed through a self-catalyzed mechanism requiring Cu^{2+} and O_2 with no help from other enzymes.[29,30] However, unlike the biogenesis mechanism of TPQ in CAO, little is known about the biogenesis of LTQ in LOX. It has been suggested that a 1,4-addition of an ε-amino side chain of a lysine to a DPQ intermediate could form the LTQ cofactor.[3] This suggestion has been supported by a model study on the biogenesis of LTQ.[1] The study showed that the addition of *n*-butylamine to 4-ethylphenol in the presence of

tyrosinase (to catalyze hydroxylation of the phenol and oxidation of the catechol) produces a mixture of products. This mixture was most likely formed due to the amine reacting with the *o*-quinone in 1,2-, 1,4-, and 1,6- additions. However, when *N*-methyl-*n*-butylamine is used instead, only the product of the 1,4-addition is observed, indicating a strong preference for 1,4-addition over 1,2- or 1,6-additions. In order for the 1,4-addition to happen selectively in the enzyme, it was proposed that the active site of LOX must be pre-organized.[1] Bollinger and co-workers reported that LTQ formation is also a self-catalyzed process using a recombinant LOXL1 from *Drosophila melanogaster*.[2] The study showed that denaturation with 6 M urea followed by the extensive dialysis of the apo-form of a recombinant protein secreted into the media of *Drosophila* S2 cells, with copper in air, leads to the formation of the LTQ cofactor. It was not clear why Cu^{2+} was not incorporated into the recombinant protein that was secreted into the media containing 0.5 mM Cu^{2+}. The recombinant HLOXL2 expression system produced in our lab (see materials and methods) yields active holo protein that does not require manipulation. Scheme 5.1 shows the proposed biogenesis mechanism of LTQ. Like the proposed biogenesis mechanism for the formation of TPQ, DPQ has been proposed as an intermediate in the formation of LTQ. In CAO, DPQ can be trapped with a lysine residue to form an LTQ like species in D298K suggesting DPQ as a common intermediate in both the biogenesis of TPQ in CAO and of LTQ in LOX. In CAO, the C2 oxygen of TPQ was derived from a solvent water molecule most likely involving the 1,4-addition of water to the C2 position of the DPQ intermediate.[66]

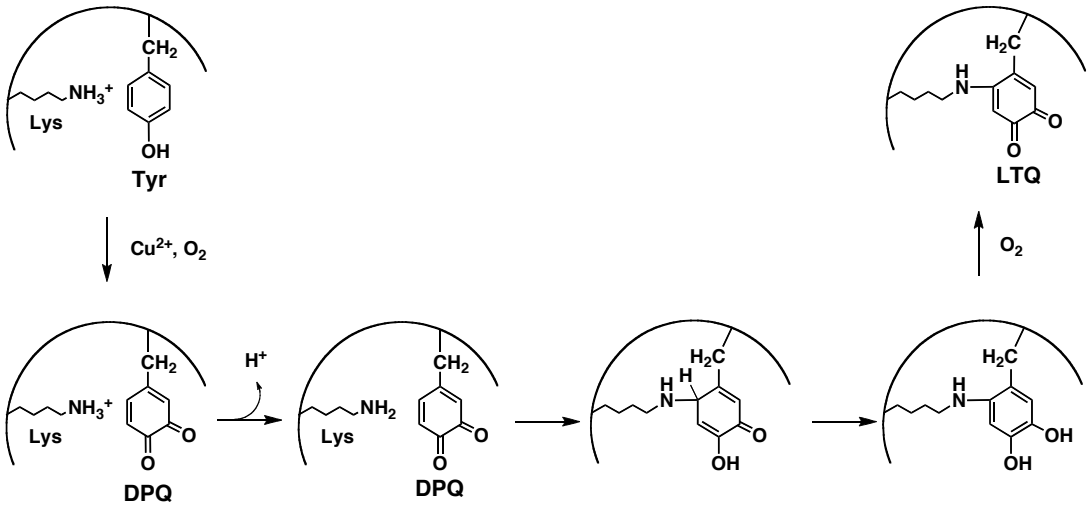

Scheme 5.1. Proposed mechanism for LTQ biogenesis.[1,3]

In order to identify the residues participating in the crosslink to form LTQ, a mutagenesis study was done on LOX from a rat aorta expressed in Chinese hamster ovary (CHO) cells.[3] Lys314 and Tyr349 were identified as the precursors for the LTQ cofactor from the sequence alignment with bovine aorta LOX where the structure of LTQ was assigned. Activity assays showed that both of the single mutants of these residues (K314A and Y349F), as well as the double mutant, were inactive. The study did not, however, fully characterize the mutants. An immunoblot assay, probing with rabbit antibodies of LOX, indicated that mutant protein concentrations ranged from 50 to 100% of wild type LOX. It is possible that the K314A mutant produced a TPQ-like quinone that was inactive. Additionally, Tyr349 may have undergone the initial steps of biogenesis but was trapped in the form of one of the intermediates, thus being unable to proceed in the biogenesis pathway. In order to examine these possibilities and to understand the mechanism of LTQ cofactor biogenesis, the corresponding

precursor lysine residue of the LTQ cofactor in the recombinant form of HLOXL2 expressed in S2 cells was mutated to an alanine. In addition to assessing the extent of biogenesis, the effect of the mutation on the enzyme activity was also examined.

In order to determine which Lys residue in HLOXL2 corresponds to Lys314 in rat aorta LOX, a sequence alignment was performed. Lys653 was identified as the corresponding precursor Tyr residue in HLOXL2. Figure 5.1 shows the results of the sequence alignment.

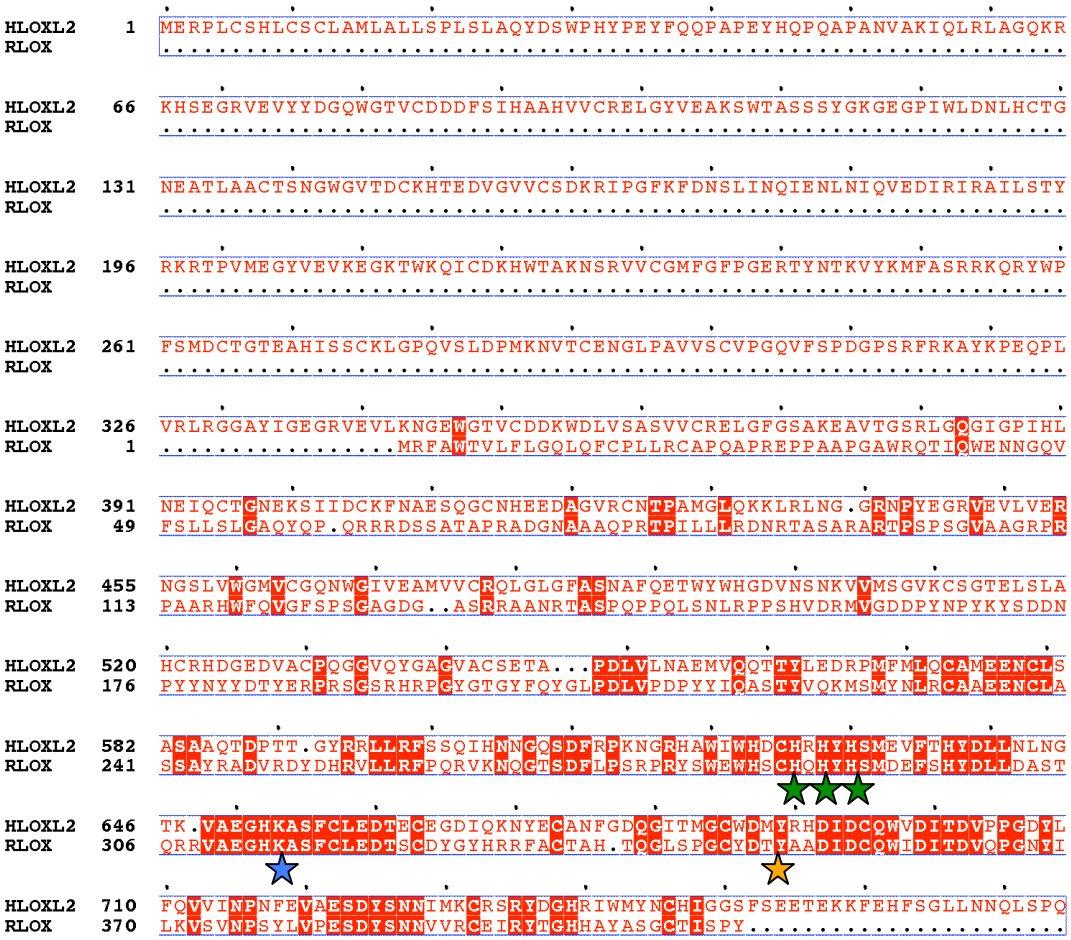

Figure 5.1 Sequence alignment between HLOXL2 and RLOX. K314 of LOX from a rat aorta corresponds to K653 in human LOXL2 protein. The alignment was done through the MultAlin website (http://bioinfo.genotoul.fr/multalin/multalin.html) and the results were exported to the ESPript 2.2 website (http://espript.ibcp.fr/ESPript/cgi-bin/ESPript.cgi) for graphic representation. The blue star indicates the lysine precursor. The orange star indicates the tyrosine precursor. The green stars indicate the proposed copper-binding site.

Materials and Methods

Materials

The site directed mutagenesis kit was purchased from Stratagene. The pMT/BiP/V5/His A vector was purchased from Invitrogen. The pASK-IBA3 vector

and the strep MBA-classic HRP conjugated antibody were purchased from IBA. PVDF membranes, PMSF, pepstatin A, leupeptin, Tris, sodium chloride, SDS, urea, sodium and potassium phosphates, and β-mercaptoethanol were purchased from Fisher Scientific. Antipain, serum free media and copper sulfate were purchased from Sigma Aldrich. Glycerol (85%) was purchased from Acros. Penicillin-streptomycin, Schneider's *Drosophila* Medium, fetal bovine serum, the biotinylated protein marker, the anti-biotin HRP linked antibody, LumiGlo reagents A and B for chemilluminescent detection and blasticidin were purchased from Invitrogen. Tween-20, and prestained low molecular weight protein marker were purchased from BioRad. Bovine serum albumin (BSA) was purchased from MP Biomedicals LLC. Proteinase K was purchased from Ambion. BioMix PCR enzyme was purchased from BioLine. Nonidet P-40 was purchased from AppliChem. The SuperFect reagent was purchased from Qiagen. All plasticware was purchased from MidSci. Synthetic oligonucleotides were purchased from Operon Biotechnologies, Inc. PCR was performed on a DNA Engine PTC-200 Peltier Thermal Cycler (BioRad). Plasmids were prepared using a QIAprep Spin Miniprep kit (Qiagen). DNA sequencing was performed at the UC Berkeley DNA sequencing facility. Western Blots were exposed to Classic Blue Autoradiography Film BX from MidSci and developed using an SRX-101A Konica Minolta processor.

Cloning

A cDNA containing the ORF of *hloxl2* was purchased from Origene. A 1.023

Kb cDNA coding one SRCR domain, and the LOX core domain of HLOXL2 (Δ1-3 *srcr hloxl2*) was amplified and cloned into pASK-IBA3 (IBA, Germany) between the BsaI restriction sites in order to incorporate the Strep tagII-coding sequence at the 3′ end. The Δ1-3 *srcr-hloxl2 + strep* was excised by PCR using a set of primers to engineer a SpeI (5′ end) and XhoI (3′ end) restriction enzyme sites and the SpeI/XhoI digested product was inserted into the pMT/Bip/V5-HisA vector between SpeI and XhoI restriction sites. The sequence was verified by DNA sequencing at UC Berkeley DNA sequencing facility. The resulting plasmid is termed, pMT/BiP/Δ1-3 *srcr hloxl2*/*strep* and contains a BiP excretion signal, the gene of interest, and a strep tag in a pMT vector.[124]

Site-directed Mutagenesis

The expression plasmid for K653A of Δ1-3 SRCR HLOXL2 was generated by site-directed mutagenesis using a QuikChange mutagenesis kit from Stratagene using pMT/BiP/Δ1-3 *srcr hloxl2*/*strep* as the parent vector. The DNA primers used for K653A mutagenesis were 5′-GGCAGAGGGCCACGCGGCCAGCTTCTGC-3′ (forward) and 5′-GCAGAAGCTGGCCGCGTGGCCCTCTGCC-3′ (reverse) (underlined nucleotides correspond to the sites of mutation). The gene of interest in the plasmid was sequenced in both directions and the point mutation was confirmed.

Transfection and Selection

The plasmid was co-transfected with the blasticidin selection vector, pCoBlast

(Invitrogen), into 3 mL of $2x10^6$ *Drosophila S*2 cells using the SuperFect transfection reagent (Qiagen) according to the SuperFect Transfection Reagent Handbook. For the selection, the transfected cells were maintained in a 5 mL of *Drosophila* complete medium containing Blastcidin for four weeks, according to the *Drosophila* Expression System manual, version F (Invitrogen). Dead cells were observed after ~10 days. S2 cells were grown at 27°C.

After three to four weeks of selection, cell lines were expanded to 5 mL T-flasks at 2 x 10^6 cells/mL. Cells were transferred at a concentration of 1 x 10^4 cells/mL, to an eppendorf tube and centrifuged at 1,000 rpm for 5 min. The supernatant was removed and the cells were resuspended in 200 μL of cell lysis solution containing 0.5% Tween-20, and 60 μg/mL proteinase K in water.[125] The mixture was incubated at 56°C for 4 hrs followed by 95°C for 30 min. The mixture was stored at 4°C. PCR was performed on the lysate using the BioMix PCR enzyme. The PCR primers used were 5'-TGTGTAAAGCCGCGTTTC-3' (forward) and 5'-CCGCTCGAGTTATTTTTCGAACTGCGGGT-3' (reverse). A DNA gel (1% agarose) was run to evaluate the integration of the gene of interest in the genomic DNA of the S2 cells. Aliquots of the PCR-verified clones (stable cells) were stored in liquid N_2.

Cell Expansion and Passaging

Stable cells were expanded/passaged when cells reached a density of 8 x 10^6 to 1 x 10^7 cells/mL. Cells were seeded at 2 x 10^6 cells/mL according to the *Drosophila* Expression System manual, version F (Invitrogen).

Protein Expression and Western Blotting

Protein was expressed by the addition of $CuSO_4$ (final concentration 0.6 mM) to a 15 mL T-flask containing cells at 4 x 10^6 cells/mL in serum free media. Cells and media (5 mL) were harvested 3-5 days post induction and centrifuged at 1,000 rpm for 8 min. Protease inhibitors (1 μL of 1,000x), PMSF, pepstatin A, leupeptin, and antipain, were added to 1 mL of media. Media and cells were frozen at -20°C until further use. Samples were thawed and 500 μL PBS buffer was used to resuspend cells. The mixture was centrifuged at 12,000 x g for 5 min and the supernatant was discarded. Protease inhibitors (0.1 μL of 1,000x) were added to the cells, and the cells were resuspended in 50 μL lysis buffer containing 50 mM Tris buffer, 150 mM NaCl, and 1% Nonidet P-40 at pH 7.8. The cells were incubated in lysis buffer for 10 min at 37°C. The lysis product was centrifuged at 12,000 x g for 5 min. The supernatant was set aside for Western blotting. The insoluble fraction was incubated overnight at 4°C in a 100 μL SDS solution containing 250 μL Tris pH 6.8, 30 % glycerol, 8 % β-mercaptoethanol, and 80 mg/mL SDS. The sample was centrifuged at 12,000 x g for 5 min and the supernatant was set aside for Western blotting. Urea (100 μL of 6 M) was added to the insoluble portion, and the sample was boiled for 5 min. SDS-PAGE

was run on samples of media (neat) separately from samples of lysis supernatant (5 μL in a total of 20 μL containing 1x sample buffer), SDS supernatant (neat), and the insoluble portion of the cells in 6 M urea (neat). A control of the wild-type Δ1-3 SRCR HLOXL2 (neat from media), biotinylated marker, and a pre-stained low molecular weight marker were run on each gel. Once the transfer to a PVDF membrane was complete, the membrane was washed 3 times with PBS buffer for 5 min each. The membrane was blocked for 1 hr with a 3% BSA solution containing 15 mL PBS, 0.75 mL Tween-20, and 0.45 g BSA. The membrane was then washed 3 times with PBST for 5 min each followed by incubation with 1° antibody (10 mL PBST, 2 μL anti-biotin antibody (Invitrogen) for detection of the biotin marker, and 3 μL pre-diluted strep MBA-classic HRP conjugated antibody (IBA) for protein detection) overnight. The membrane was washed two times with PBST and two times with PBS for 5 min each. This procedure was completed according to the strep MBA-classic HRP conjugated antibody directions from IBA. The membrane was incubated for 2 min in a chemilluminescent reagent (Invitrogen) before exposure to autoradiography film and development.

Results

Transfection and Selection of Stable Cell Lines

Co-transfection of plasmid containing the K653A mutant of Δ1-3 srcr *hloxl2* and plasmid containing pCoBlast selection marker was done in 12 wells from two 6 well plates making 12 independent cell lines. Half were transfected, followed in two

weeks by the other half. The addition of blasticidin to the media started the selection process. Cells that have both the blastcidin resistance and the gene of interest integrated into the genomic DNA survived during blastcidin selection. Dead cells were seen at ~10 days. Stable cell line selection occurred over a 4 week period. However, blasticidin continued to be added to all passaged or expanded populations in a volume of 5 mL or less.

Once stable cell lines were selected, PCR was performed to evaluate the integration of K653A mutant of Δ1-3 *srcr hloxl2* into the genomic DNA of the S2 cells. DNA gels of the PCR products reveal that the gene of 1.1 kb was incorporated into the genomic DNA in each of the 12 cell lines (Figure 5.2 shows the DNA gel for one of the cell lines).

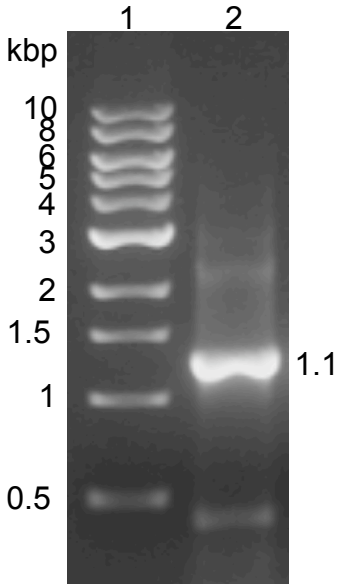

Figure 5.2 DNA gel of Δ1-3 *srcr hloxl2* K653A PCR product. Lane 1: marker; lane 2: PCR product

Protein Expression and Western Blotting

Protein production was induced by the addition of $CuSO_4$ (final concentration of 0.6 mM) to 15 mL of $4x10^6$ cells/mL. Cells and media were harvested after 3 days and separated by centrifugation. A western blot of the media showed no mutant protein present in the media (Figure 5.3 a). A monoclonal antibody specific for the Strep tagII was used for protein detection. A BiP signal at the 5' end of the gene should have directed the secretion of the expressed protein from the cell if it was folded like the wild-type. The absence of secreted protein in the media indicated that the protein was either not expressed, or it was being expressed but not secreted. To investigate this further, another 15 mL of cells were induced. The cells were harvested after 3 days and separated from the media. The cells were lysed in the presence of 1% Nonidet to help solubilize proteins. The soluble lysate was removed

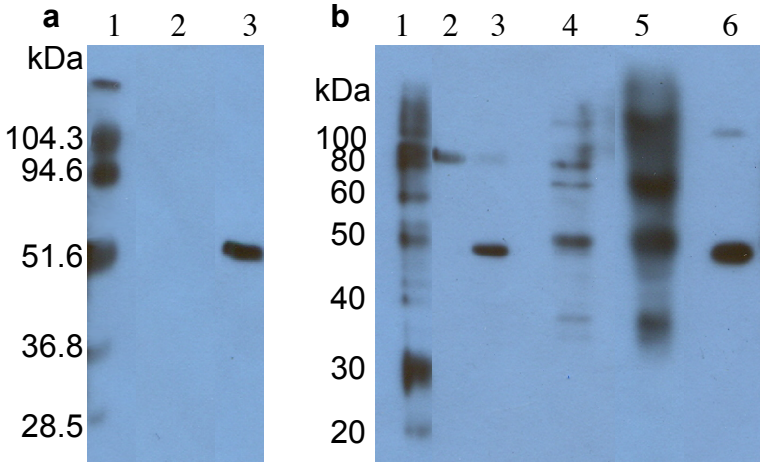

Figure 5.3 Western blot of Δ1-3 SRCR HLOXL2 expressed in S2 cells **a)** media fractions, lane 1: prestained SDS-PAGE marker; lane 2: K653A mutant; lane 3: WT, **b)** cytosolic fractions, lane 1: biotin marker; lane 2: low molecular weight marker; lane 3: soluble fraction; lane 4: 30% SDS extractable fraction; lane 5: insoluble fraction extracted with 6 M urea; lane 6: WT HLOXL2 control in media

after centrifugation and the insoluble portion of the cells were further incubated in a solution of SDS. Again the soluble portion of the SDS treated sample was removed after centrifugation and 6 M urea was added to the pellet. A Western blot was run on each of these fractions (Figure 5.3 b), and the HRP conjugated anti-strep antibody was used for protein detection. The results of the western blot indicate that the mutant protein was expressed in the cytosol but not secreted. Each of the fractions had a band that was similar in size to the wild-type Δ1-3 SRCR HLOXL2 that was secreted into the media. The protein in the cell appears to be mostly insoluble, likely in the form of an inclusion body. Most likely the protein was misfolded, the BiP signal was not exposed, and thus the protein was not secreted. A small amount of protein is soluble in Nonident-containing lysis buffer. Further investigation is required to determine if any solubilized protein can be purified from the cell and analyzed.

Wild-type Δ1-3 SRCR HLOXL2 expressed in the media should have the BiP signal cleaved off making the predicted molecular weight ~41 kDa; however, on the western blot, the molecular weight is observed ~48 kDa. Similarly, the K653A mutant of Δ1-3 SRCR HLOXL2 expressed in the cytosol likely retains the BiP signal making the predicted molecular weight ~42.6 kDa while the observed molecular weight is ~48 kDa. An SDS-PAGE gel of the purified wild-type Δ1-3 SRCR HLOXL2 indicates a molecular weight just above 45 kDa. The discrepancy in the apparent and predicted molecular weights of the proteins is unclear. The retention of the BiP signal would only account for a ~2 kDa increase in molecular weight, not the ~7 kDa increase that is observed. It is possible that the protein is glycosylated. Two

potential N-glycosylation sites have been identified in Δ1-3 SRCR HLOXL2;[111] however, the presence of glycosylation at these sites has not been identified. In order to check for glycosylation, the protein should be incubated with deglycosylase prior to SDS-PAGE. Additionally, the purified protein could be analyzed by mass spectroscopy to determine the exact mass of the protein.

The cytosolic expression of the K653 mutant of Δ1-3 SRCR HLOXL2 might explain the results found by Wang and co-workers.[3] A full-length *lox* from rat aorta was expressed in CHO cells and the processed LOX was secreted in the culture media. In comparison with the wild-type, the corresponding mutant, K314A, only showed negligible activity in the media. While the study reported that the WT protein was secreted to the media, it is unclear about the subcellular localization of mutant proteins. It is possible that the lack of activity observed in the media was due to the absence of protein, as seen in the current study.

Conclusion

Scheme 5.1 shows the proposed biogenesis mechanism of LTQ. In the proposed mechanisms of biogenesis for TPQ and LTQ, DPQ has been proposed as an intermediate. In CAO, DPQ can be trapped with a lysine residue to form an LTQ like species in D298K, suggesting DPQ as a common intermediate in both TPQ and LTQ biogenesis.

A mutagenesis study of LOX from a rat aorta expressed in CHO cells supported that Lys314 and Tyr349 are the precursors for the LTQ cofactor.[3]

Mutagenesis of these residues was performed followed by activity assays that showed both of the single mutants of these residues, as well as the double mutant, were inactive. The study did not, however, fully characterize the mutants. In an attempt to characterize the corresponding mutants of the recombinant HLOXL2, and to gain a better understanding of the mechanism of LTQ cofactor biogenesis, the corresponding Lys in HLOXL2 was mutated to an Ala (K653A).

In the present study, *Drosophila* S2 stable cells for the expression of the K653A mutant of Δ1-3 SRCR HLOXL2 were selected. The protein was expressed but was not secreted into the media despite the presence of a BiP secretion signal. The western blot results showed that the protein was expressed in the cytosol of the cell mostly as insoluble fractions, indicating that the protein was likely mis-folded into an inclusion body and the BiP signal was inaccessible, preventing protein secretion. The Lys653 residue is clearly involved in the proper folding of the protein in addition to being involved in the crosslink to form LTQ. Further studies will be needed to test for the proper folding of any solubilized protein from the cytosol and, if folded properly, to characterize the structure of the cofactor, to determine the enzymatic activity, and to gain a better understanding of the mechanism of LTQ cofactor biogenesis.

Chapter 6: Final Conclusions

Mutation of an active site residue in AGAO to a lysine, D298K, can effectively trap the DPQ intermediate and confirms the intermediacy of DPQ in TPQ biogenesis. This finding further supports the proposed intermediacy of DPQ in the biogenesis of LTQ. Additionally, the incorporation of the lysine residue in the Asp298 position of AGAO to trap DPQ, shows that the DPQ intermediate has mobility and can leave the active site copper and enter the wedge shaped cavity to react with Lys298.

Two distinct species are formed during cofactor biogenesis in D298K. The first, proposed to be an LTQ-like quinone, forms at ~ 500 nm at a similar rate as the formation of TPQ in WT AGAO. Therefore, it is likely that the initial steps of biogenesis, Tyr382 activation and oxidation to DPQ, are not affected by the mutation of D298K. The second species forms ~ 450 nm and has been proposed to be LTI, the tautomer of LTQ. The crystal structure of D298K suggests a hydrogen bonding interaction between the O4 of the quinone and Tyr284. This hydrogen bond has been shown to stabilize the quinone in the form of the LTI tautomer and disruption of the hydrogen bond by mutation results in an unstable protein with a λ_{max} of ~505 nm, like that of LTQ. The natural cofactor in LOX is LTQ with an absorbance of ~ 505 nm, suggesting that the corresponding carbonyl group of LTQ does not have such a hydrogen bonding interaction in the active site of LOX.

TPQ was not detected at any point during the biogenesis of D298K in the pH range studied (6.8 to 9.5). This indicates that amination can effectively out compete

hydration by a copper-associated water molecule, even though hydration occurs in the natural reaction. Changing the pH did have an affect on the λ_{max} of the LTQ-like species. As the pH increased from 6.8 to 9.5, the λ_{max} shifted from ~ 496 nm to ~ 518 nm, most likely corresponding to the amount of LTI present at the end of the first phase.

The pH profile of D298K biogenesis showed a pH-dependence on rate for both the 505 and 450 nm species. The pH-dependency for the rate of the LTQ-like species showed a bell-shaped curve with pK_as of 7.93 ± 0.10 and 9.62 ± 0.13, respectively with a maximum rate at ~ pH 8.8. The residue responsible for the pK_a of 7.93 ± 0.10 is deprotonated when the rate is the fastest and was assigned to the precursor tyrosine (Y382). The residue responsible for the pK_a of 9.62 ± 0.13 is protonated when the rate is the fastest and was assigned to Tyr284. It is likely that Tyr284 is responsible for holding DPQ in the wedge shaped cavity, through a hydrogen bond, to react with Lys298.

The pH-dependency for the rate of conversion of the LTQ-like species to LTI occurred with a pK_a of 7.68 ± 0.086 that was also assigned to Tyr284. Tyr284 is known to hydrogen bond to LTQ/LTI to stabilize the LTI tautomer. Therefore, deprotonation of this residue may be influencing the thermodynamic equilibrium.

In the initial minute of cofactor biogenesis of both WT- and D298K-AGAO, a ~ 370 nm absorbance was observed. This species is proposed to be a charge transfer species where the formation is not O_2-dependent. The species is likely formed off the reaction pathway, as this species was not observed to convert to cofactor in an

isosbestic manner. However, it is likely that the formation of this species involves Cu^{2+} in the active site of the protein, due to the observation that it was not formed in the Zn^{2+}-substituted enzyme.

The LTQ-like species formed in D298K is trapped in the flipped, inactive conformation because the cross-link is formed between two amino acid residues. In an attempt to generate an LTQ-like cofactor in AGAO that has an increased mobility and is potentially in the active conformation, WT- and D298A-AGAO were biogenized in the presence of *n*-butylamine hydrochloride. Typical peaks for the biogenesis in the absence of amine to form the TPQ cofactor in WT and D298A are 475 and 460 nm, respectively. However, when biogenesis occurred in the presence of *n*-butylamine, peaks at 538 and 523 nm were observed for WT and D298A, respectively; TPQ was not detected. This most likely indicates the formation of an LTQ-like cofactor. After incubation at 4°C for one month, peaks were observed at 330 and 470 nm, which correspond to the peaks at 320 and 450 nm observed for LTI in D298K. Other than the WT-sample biogenized in the absence of amine, the samples did not react with inhibitors but all of the samples showed catalytic activity that was 40- to 1000- fold less than WT.

As with the biogenesis of TPQ in CAO, DPQ has also been proposed as a biogenic intermediate in the formation of LTQ in LOX. The formation of an LTQ-like cofactor in AGAO supports this proposal but is not conclusive. An attempt to generate a TPQ cofactor in LOX was made to evaluate this proposal. In addition to the possibility of forming TPQ, it is possible that the reaction would be incomplete

and DPQ would be observed directly. The mutation of Lys653 to Ala in a recombinant form of HLOXL2, resulted in the formation of a mis-folded protein that was expressed mainly as an inclusion body in *Drosophila* S2 cells. Although the conclusive identification of DPQ as an intermediate on the pathway to form LTQ was not confirmed, this result shows that Lys653 is important to the proper folding of the protein as well as the formation of LTQ.

References

(1) Mure, M.; Wang, S. X.; Klinman, J. P. *Journal of the American Chemical Society* **2003**, *125*, 6113-6125.
(2) Bollinger, J. A.; Brown, D. E.; Dooley, D. M. *Biochemistry* **2005**, *44*, 11708-11714.
(3) Wang, S. X.; Mure, M.; Medzihradszky, K. F.; Burlingame, A. L.; Brown, D. E.; Dooley, D. M.; Smith, A. J.; Kagan, H. M.; Klinman, J. P. *Science* **1996**, *273*, 1078-1084.
(4) Moore, R. H.; Spies, M. A.; Culpepper, M. B.; Murakawa, T.; Hirota, S.; Okajima, T.; Tanizawa, K.; Mure, M. *Journal of the American Chemical Society* **2007**, *129*, 11524-11534.
(5) Kim, M.; Okajima, T.; Kishishita, S.; Yoshimura, M.; Kawamori, A.; Tanizawa, K.; Yamaguchi, H. *Nature Structural Biology* **2002**, *9*, 591-596.
(6) Cooper, R. A.; Knowles, P. F.; Brown, D. E.; McGuirl, M. A.; Dooley, D. M. *Biochemical Journal* **1992**, *288*, 337-340.
(7) Mure, M. *Accounts of Chemical Research* **2004**, *37*, 131-139.
(8) Carter, S. R.; McGuirl, M. A.; Brown, D. E.; Dooley, D. M. *Journal of Inorganic Biochemistry* **1994**, *56*, 127-141.
(9) Wilce, M. C.; Dooley, D. M.; Freeman, H. C.; Guss, J. M.; Matsunami, H.; McIntire, W. S.; Ruggiero, C. E.; Tanizawa, K.; Yamaguchi, H. *Biochemistry* **1997**, *36*, 16116-33.
(10) Elmore, B. O.; Bollinger, J. A.; Dooley, D. M. *Journal of Biological Inorganic Chemistry* **2002**, *7*, 565-579.
(11) McGuirl, M. A.; McCahon, C. D.; McKeown, K. A.; Dooley, D. M. *Plant Physiology* **1994**, *106*, 1205-1211.
(12) Kishishita, S.; Okajima, T.; Kim, M.; Yamaguchi, H.; Hirota, S.; Suzuki, S.; Kuroda, S.; Tanizawa, K.; Mure, M. *Journal of the American Chemical Society* **2003**, *125*, 1041-1055.
(13) Green, J.; Haywood, G. W.; Large, P. J. *Biochemical Journal* **1983**, *211*, 481-493.
(14) DuBois, J. L.; Klinman, J. P. *Biochemistry* **2005**, *44*, 11381-11388.
(15) Murray, J. M.; Saysell, C. G.; Wilmot, C. M.; Tambyrajah, W. S.; Jaeger, J.; Knowles, P. F.; Phillips, S. E. V.; McPherson, M. J. *Biochemistry* **1999**, *38*, 8217-8227.
(16) Rea, G.; Laurenzi, M.; Tranquilli, E.; D'Ovidio, R.; Federico, R.; Angelini, R. *FEBS Letters* **1998**, *437*, 177-182.
(17) Seiler, N. *Amino Acids* **2004**, *26*, 217-233.
(18) Masinia, E.; Vannaccia, A.; Gianninia, L.; Befanib, O.; Nistric, S.; Mateescud, M. A.; Mannaionia, P. F.; Mondovìc, B.; Federico, R. *European Journal of Pharmacology* **2004**, *502*, 253-264.
(19) Bono, P.; Salmi, M.; Smith, D. J.; Jalkanen, S. *The Journal of Immunology* **1998**, *160*, 5563-5571.

(20) Bono, P.; Salmi, M.; Smith, D. J.; Leppänen, I.; Horelli-Kuitunen, N.; Palotie, A.; Jalkanen, S. *The Journal of Immunology* **1998**, *161*, 2953-2960.
(21) Smith, D. J.; Salmi, M.; Bono, P.; Hellman, J.; Leu, T.; Jalkanen, S. *Journal of Experimental Medicine* **1998**, *188*, 17-27.
(22) SmithMungo, L. I.; Kagan, H. M. *Matrix Biology* **1998**, *16*, 387-398.
(23) Csiszar, K. *Prog Nucleic Acid Res Mol Biol* **2001**, *70*, 1-32.
(24) Payne, S. L.; Fogelgren, B.; Hess, A. R.; Seftor, E. A.; Wiley, E. L.; Fong, S. F. T.; Csiszar, K.; Hendrix, M. J. C.; Kirschmann, D. A. *Cancer Research* **2005**, *65*, 11429-11436.
(25) Davidson, V. L. *Biochemistry* **2007**, *46*, 5283-5292.
(26) Janes, S. M.; Mu, D.; Wemmer, D.; Smith, A. J.; Kaur, S.; Maltby, D.; Burlingame, A. L.; Klinman, J. P. *Science* **1990**, *248*, 981-7.
(27) Westerling, J.; Frank, J.; Duine, J. A. *Biochemical and Biophysical Research Communications* **1979**, *87*, 719-724.
(28) Salisbury, S. A.; Forrest, H. S.; Cruse, W. B. T.; Kennard, O. *Nature* **1979**, *280*, 843-844.
(29) Matsuzaki, R.; Fukui, T.; Sato, H.; Ozaki, Y.; Tanizawa, K. *Febs Letters* **1994**, *351*, 360-364.
(30) Cai, D. Y.; Klinman, J. P. *Journal of Biological Chemistry* **1994**, *269*, 32039-32042.
(31) van der Palen, C. J. N. M.; Reijnders, W. N. M.; de Vries, S.; Duine, J. A.; van Spanning, R. J. M. *Antonie Van Leeuwenhoek* **1997**, *72*, 219-228.
(32) van der Palen, C. J. N. M.; Slotboom, D.-J.; Jongejan, L.; Reijnders, W. N. M.; Harms, N.; Duine, J. A.; van Spanning, R. J. M. *European Journal of Biochemistry* **1995**, *230*, 860-871.
(33) Datta, S.; Mori, Y.; Takagi, K.; Kawaguchi, K.; Chen, Z. W.; Okajima, T.; Kuroda, S.; Ikeda, T.; Kano, K.; Tanizawa, K.; Mathews, F. S. *Proceedings of the National Academy of Sciences of the United States of America* **2001**, *98*, 14268-14273.
(34) Sofia, H. J.; Chen, G.; Hetzler, B. G.; Reyes-Spindola, J. F.; Miller, N. E. *Nucleic Acids Research* **2001**, *29*, 1097-1106.
(35) Mure, M.; Mills, S. A.; Klinman, J. P. *Biochemistry* **2002**, *41*, 9269-9278.
(36) Kumar, V.; Dooley, D. M.; Freeman, H. C.; Guss, J. M.; Harvey, I.; McGuirl, M. A.; Wilce, M. C.; Zubak, V. M. *Structure* **1996**, *4*, 943-955.
(37) Duff, A. P.; Cohen, A. E.; Ellis, P. J.; Kuchar, J. A.; Langley, D. B.; Shepard, E. M.; Dooley, D. M.; Freeman, H. C.; Guss, J. M. *Biochemistry* **2003**, *42*, 15148-15157.
(38) Li, R.; Klinman, J. P.; Mathews, F. S. *Structure* **1998**, *6*, 293-307.
(39) Nymalm, Y.; Kidron, H.; Söderholm, A.; Viitanen, L.; Kaukonen, K.; Pihlavisto, M.; Smith, D.; Veromaa, T.; Airenne, T. T.; Johnson, M. S.; Salminen, T. A. *Acta Crystallographica Section D* **2003**, *59*, 1288-1290.
(40) Lunelli, M.; Di Paoloa, M. L.; Biadene, M.; Calderone, V.; Battistutta, R.; Scarpa, M.; Rigo, A.; Zanotti, G. *Journal of Molecular Biology* **2005**, *346*, 991-1004.

(41) Parsons, M.; Convery, M.; Wilmot, C.; Yadav, K.; Blakeley, V.; Corner, A.; Phillips, S.; McPherson, M.; Knowles, P. *Structure* **1995**, *3*, 1171-1184.
(42) Brazeau, B. J.; Johnson, B. J.; Wilmot, C. M. *Archives of Biochemistry and Biophysics* **2004**, *428*, 22-31.
(43) Salminen, T.; Smith, D.; Jalkanen, S.; Johnson, M. *Protein Engineering* **1998**, *11*, 1195-1204.
(44) Shepard, E. M.; Smith, J.; Elmore, B. O.; Kuchar, J. A.; Sayre, L. M.; Dooley, D. M. *European Journal of Biochemistry* **2002**, *269*, 3645-3658.
(45) Airene, T. T.; Nymalm, Y.; Kidron, H.; Smith, D. J.; Pihlavisto, M.; Salmi, M.; Jalkanen, S.; Johnson, M. S.; Salminen, T. A. *Protein Science* **2005**, *14*, 1964-1974.
(46) Chiu, Y.-C.; Okajima, T.; Murakawa, T.; Uchida, M.; Taki, M.; Hirota, S.; Kim, M.; Yamaguchi, H.; Kawano, Y.; Kamiya, N.; Kuroda, S. i.; Hayashi, H.; Yamamoto, Y.; Tanizawa, K. *Biochemistry* **2006**, *45*, 4105-4120.
(47) Duff, A. P.; Trambaiolo, D. M.; Cohen, A. E.; Ellis, P. J.; Juda, G. A.; Shepard, E. M.; Langley, D. B.; Dooley, D. M.; Freeman, H. C.; Guss, J. M. *Journal of Molecular Biology* **2004**, *344*, 599-607.
(48) Johnson, B. J.; Cohen, J.; Welford, R. W.; Pearson, A. R.; Schulten, K.; Klinman, J. P.; Wilmot, C. M. *Journal of Biological Chemistry* **2007**, *282*, 17767-17776.
(49) Mure, M.; Klinman, J. P. *Journal of the American Chemical Society* **1993**, *115*, 7117-7127.
(50) Mure, M.; Klinman, J. P. *Journal of the American Chemical Society* **1995**, *117*, 8698-8706.
(51) Mure, M.; Klinman, J. P. *Journal of the American Chemical Society* **1995**, *117*, 8707-8718.
(52) Nakamura, N.; Moënne-Loccoz, P.; Tanizawa, K.; Mure, M.; Suzuki, S.; Klinman, J. P.; Sanders-Loehr, J. *Biochemistry* **1997**, *36*, 11479-11486.
(53) Wilmot, C. M.; Murray, J. M.; Alton, G.; Parsons, M. R.; Convery, M. A.; Blakeley, V.; Corner, A. S.; Palcic, M. M.; Knowles, P. F.; McPherson, M. J.; Phillips, S. E. V. *Biochemistry* **1997**, *36*, 1608-1620.
(54) Plastino, J.; Green, E. L.; Sanders-Loehr, J.; Klinman, J. P. *Biochemistry* **1999**, *38*, 8204-8216.
(55) Hevel, J. M.; Mills, S. A.; Klinman, J. P. *Biochemistry* **1999**, *38*, 3683-3693.
(56) Mure, M.; Brown, D. E.; Saysell, C.; Rogers, M. S.; Wilmot, C. M.; Kurtis, C. R.; McPherson, M. J.; Phillips, S. E. V.; Knowles, P. F.; Dooley, D. M. *Biochemistry* **2005**, *44*, 1568-1582.
(57) Schwartz, B.; Green, E. L.; Sanders-Loehr, J.; Klinman, J. P. *Biochemistry* **1998**, *37*, 16591-16600.
(58) Su, Q.; Klinman, J. P. *Biochemistry* **1998**, *37*, 12513-12525.
(59) Mills, S. A.; Goto, Y.; Su, Q.; Plastino, J.; Klinman, J. P. *Biochemistry* **2002**, *41*, 10577-10584.
(60) Hirota, S.; Iwamoto, T.; Kishishita, S. i.; Okajima, T.; Yamauchi, O.; Tanizawa, K. *Biochemistry* **2001**, *40*, 15789-15796.

(61) Medda, R.; Padiglia, A.; Bellelli, A.; Sarti, P.; Santanch e, S.; Finazzi Agro, A.; Floris, G. *Biochemical Journal* **1998**, *332*, 431-437.
(62) Padiglia, A.; Medda, R.; Pedersen, J. Z.; Agrò, A. F.; Lorrai, A.; Murgia, B.; Floris, G. *Journal of Biological Inorganic Chemistry* **1999**, *4*, 608-613.
(63) Turowski, P. N.; McGuirl, M. A.; Dooley, D. M. *Journal of Biological Chemistry* **1993**, *268*, 17680-17682.
(64) Ruggiero, C. E.; Smith, J. A.; Tanizawa, K.; Dooley, D. M. *Biochemistry* **1997**, *36*, 1953-1959.
(65) Ruggiero, C. E.; Dooley, D. M. *Biochemistry* **1999**, *38*, 2892-2898.
(66) Nakamura, N.; Matsuzaki, R.; Choi, Y. H.; Tanizawa, K.; Sanders-Loehr, J. *J. Biol. Chem.* **1996**, *271*, 4718-24.
(67) Matsunami, H.; Okajima, T.; Hirota, S.; Yamaguchi, H.; Hori, H.; Mure, M.; Kuroda, S.; Tanizawa, K. *Biochemistry* **2004**, *43*, 2178-2187.
(68) Okajima, T.; Kishishita, S.; Chiu, Y.-C.; Murakawa, T.; Kim, M.; Yamaguchi, H.; Hirota, S.; Kuroda, S.; Tanizawa, K. *Biochemistry* **2005**, *44*, 12041-12048.
(69) Schwartz, B.; Dove, J. E.; Klinman, J. P. *Biochemistry* **2000**, *39*, 3699-3707.
(70) Dove, J. E.; Schwartz, B.; Williams, N. K.; Klinman, J. P. *Biochemistry* **2000**, *39*, 3690-3698.
(71) Schwartz, B.; Olgin, A. K.; Klinman, J. P. *Biochemistry* **2001**, *40*, 2954-2963.
(72) DuBois, J. L.; Klinman, J. P. *Archives of Biochemistry and Biophysics* **2005**, *433*, 255-265.
(73) Samuels, N. M.; Klinman, J. P. *Biochemistry* **2005**, *44*, 14308-14317.
(74) DuBois, J. L.; Klinman, J. P. *Biochemistry* **2006**, *45*, 3178-3188.
(75) DuBois, J. L.; Klinman, J. P. *Methods in Enzymol.* **2004**, *378*, 17-31.
(76) Chen, Z.; Schwartz, B.; Williams, N. K.; Li, R.; Klinman, J. P.; Mathews, F. S. *Biochemistry* **2000**, *39*, 9709-17.
(77) Mills, S. A.; Klinman, J. P. *Journal of the American Chemical Society* **2000**, *122*, 9897-9904.
(78) Choi, Y.-H.; Matsuzaki, R.; Suzuki, S.; Tanizawa, K. *Journal of Biological Chemistry* **1996**, *271*, 22598-22603.
(79) Waite, J. H. *Comparative Biochemistry and Physiology B-Comparative Biochemistry* **1990**, *97*, 19-29.
(80) Burzio, L. A.; Waite, J. H. *Biochemistry* **2000**, *39*, 11147-11153.
(81) Christensen, A. M.; Schaefer, J.; Kramer, K. J.; Morgan, T. D.; Hopkins, T. L. *Journal of the American Chemical Society* **1991**, *113*, 6799-6802.
(82) Nkpa, N. N.; Chedekel, M. R. *Journal of Organic Chemistry* **1981**, *46*, 213-215.
(83) Deibel, R. B.; Chedekel, M. R. *Journal of the American Chemical Society* **1982**, *104*, 7306-7309.
(84) Benathan, M.; Labidi, F. *Archives of Dermatological Research* **1996**, *288*, 697-702.
(85) Wakamatsu, K.; Kageshita, T.; Furue, M.; Hatta, N.; Kiyohara, Y.; Nakayama, J.; Ono, T.; Saida, T.; Takata, M.; Tsuchida, T.; Uhara, H.; Yamamoto, A.; Yamazaki, N.; Naito, A.; Ito, S. *Melanoma Research* **2002**, *12*, 245-253.

(86) Shimizu, E.; Ohta, K.; Takayama, S.; Kitagaki, Y.; Tanizawa, K.; Yorifuji, T. *Biosci. Biotech. Biochem.* **1997**, *61*, 501-505.
(87) Szutowicz, A.; Kobes, R. D.; Orsulak, P. J. *Analytical Biochemistry* **1984**, *138*, 86-94.
(88) Paz, M. A.; Fluckiger, R.; Boak, A.; Kagan, H. M.; Gallop, P. M. *J. Biol. Chem.* **1991**, *266*, 689-692.
(89) Tang, C.; Klinman, J. P. *J. Biol. Chem.* **2001**, *276*, 30575-30578.
(90) Janes, S. M.; Palcic, M. M.; Scaman, C. H.; Smith, A. J.; Brown, D. E.; Dooley, D. M.; Mure, M.; Klinman, J. P. *Biochemistry* **1992**, *31*, 12147-12154.
(91) Wang, S. X.; Nakamura, N.; Mure, M.; Klinman, J. P.; Sanders-Loehr, J. *J Biol Chem* **1997**, *272*, 28841-4.
(92) Culpepper, M. B.; Mure, M. **Manuscript in preparation.**
(93) Leopold, A. C.; Plummer, T. H. *Plant Physiology* **1961**, *36*, 589-591.
(94) Tan, T. C.; Chen, Y. *International Journal of Chemical Kinetics* **1992**, *24*, 1023-1034.
(95) Ling, K.-Q.; Sayre, L. M. *J. Am. Chem. Soc.* **2006**, 4777-4784.
(96) Atkins, W. M.; Wang, R. W.; Bird, A. W.; Newton, D. J.; Lu, A. Y. *Journal of Biological Chemistry* **1993**, *268*, 19188-19191.
(97) Grimshaw, C. E.; Bohren, K. M.; Lai, C.-J.; Gabbay, K. H. *Biochemistry* **1995**, *34*, 14374-14384.
(98) Sorkin, D. L.; Duong, D. K.; Miller, A.-F. *Biochemistry* **1997**, *36*, 8202-8208.
(99) Thompson, A.; Land, E. J.; Chedekel, M. R.; Subbarao, K. V.; Truscott, T. G. *Biochimica et Biophysica Acta (BBA) - General Subjects* **1985**, *843*, 49-57.
(100) G_sowska, B.; Wojtasek, H.; Hurek, J.; Dr_g, M.; Nowak, K.; Kafarski, P. *European Journal of Biochemistry* **2002**, *269*, 4098-4104.
(101) Murray, J. M.; Kurtis, C. R.; Tambyrajah, W.; Saysell, C. G.; Wilmot, C. M.; Parsons, M. R.; Phillips, S. E. V.; Knowles, P. F.; McPherson, M. J. *Biochemistry* **2001**, *40*, 12808-12818.
(102) Contakes, S. M.; Juda, G. A.; Langley, D. B.; Halpern-Manners, N. W.; Duff, A. P.; Dunn, A. R.; Gray, H. B.; Dooley, D. M.; Guss, J. M.; Freeman, H. C. *Proceedings of the National Academy of Sciences* **2005**, *102*, 13451-13456.
(103) Moenneloccoz, P.; Nakamura, N.; Steinebach, V.; Duine, J. A.; Mure, M.; Klinman, J. P.; Sandersloehr, J. *Biochemistry* **1995**, *34*, 7020-7026.
(104) Farnum, M.; Palcic, M.; Klinman, J. P. *Biochemistry* **1986**, *25*, 1898-1904.
(105) Albert, A.; Serjant, E. P. In *The determination of ionization constants*; 3rd ed.; Chapman and Hall: New York, 1984, p 136-175.
(106) Bordwell, F. G.; McCallum, R. J.; Olmstead, W. N. *Journal of Organic Chemistry* **1984**, *49*, 1424-1427.
(107) Langley, D. B.; Duff, A. P.; Freeman, H. C.; Guss, J. M. *Acta Crystallographica Section F* **2006**, *62*, 1052-1057.
(108) Saux, C. J.-L.; Tronecker, H.; Bogic, L.; Bryant-Greenwood, G. D.; Boyd, C. D.; Csiszar, K. *Journal of Biological Chemistry* **1999**, *274*, 12939-12944.
(109) Mäki, J. M.; Tikkanen, H.; Kivirikko, K. I. *Matrix Biology* **2001**, *20*, 493-496.

(110) Huang, Y.; Dai, J.; Tang, R.; Zhao, W.; Zhou, Z.; Wang, W.; Ying, K.; Xie, Y.; Mao, Y. *Matrix Biology* **2001**, *20*, 153-157.
(111) Saito, H.; Papaconstantinou, J.; Sato, H.; Goldstein, S. *Journal of Biological Chemistry* **1997**, *272*, 8157-8160.
(112) Kim, Y.; Boyd, C. D.; Csiszar, K. *Journal of Biological Chemistry* **1995**, *270*, 7176-7182.
(113) Kenyon, K.; Modi, W. S.; Contente, S.; Friedman, R. M. *Journal of Biological Chemistry* **1993**, *268*, 18435-18437.
(114) Resnick, D.; Pearson, A.; Krieger, M. *Trends in Biochemical Sciences* **1994**, *19*, 5-8.
(115) Aruffo, A.; Bowen, M. A.; Patel, D. D.; Haynes, B. F.; Starling, G. C.; Gebe, J. A.; Bajorath, J. *Immunology Today* **1997**, *18*, 498-504.
(116) Bodian, D. L.; Skonier, J. E.; Bowen, M. A.; Neubauer, M.; Siadak, A. W.; Aruffo, A.; Bajorath, J. *Biochemistry* **1997**, *36*, 2637-2641.
(117) Kagan, H. M. *Pathology Research and Practice* **1994**, *190*, 910-919.
(118) Streichenberger, N.; Peyrol, S.; Philit, F.; Loire, R.; Sommer, P.; Cordier, J. F. *Virchows Archiv-an International Journal of Pathology* **2001**, *439*, 78-84.
(119) Akiri, G.; Sabo, E.; Dafni, H.; Vadasz, Z.; Kartvelishvily, Y.; Gan, N.; Kessler, O.; Cohen, T.; Resnick, M.; Neeman, M.; Neufeld, G. *Cancer Research* **2003**, *63*, 1657-1666.
(120) Kirschmann, D. A.; Seftor, E. A.; Fong, S. F. T.; Nieva, D. R. C.; Sullivan, C. M.; Edwards, E. M.; Sommer, P.; Csiszar, K.; Hendrix, M. J. C. *Cancer Research* **2002**, *62*, 4478-4483.
(121) Hollosi, P.; Yakushiji, J. K.; Fong, K. S. K.; Csiszar, K.; Fong, S. F. T. *International Journal of Cancer* **2009**.
(122) Peinado, H.; Cruz, M. d. C. I.-d. l.; Olmeda, D.; Csiszar, K.; Fong, K. S. K.; Vega, S.; Nieto, M. A.; Cano, A.; Portillo, F. *European Molecular Biology Organization Journal* **2005**, *24*, 3446-3458.
(123) Shook, D.; Keller, R. *Mechanisms of Development* **2003**, *120*, 1351-1383.
(124) Mure, M. In *unpublished work*.
(125) Lee, C.-G.; Reichman, T. W.; Baik, T.; Mathews, M. B. *Journal of Biological Chemistry* **2004**, *279*, 47740-47745.